DOI:10.5281/zenodo.23469199.

CURRENT DEVELOPMENTS AND THEMATIC REVIEWS IN SCIENCE AND MATHEMATICS

Editor
Prof. Mustafa Dede, PhD.

Current Developments and Thematic Reviews in Science and Mathematics

Editor

Prof. Mustafa Dede, PhD.

Publisher
Platanus Publishing®

Editor in Chief

Prof. Mustafa Dede, PhD.

Cover & Interior Design
Platanus Publishing®

The First Edition
October, 2026

ISBN

978-625-91314-7-4

©copyright
All rights reserved. No part of this publication may be reproduced or transmitted in any form or by any means, electronic or mechanical, including photocopy, or any information storage or retrieval system, without permission from the publisher.

Platanus Publishing®
Address: Natoyolu Cad. Fahri Korutürk Mah. 157/B, 06480, Mamak, Ankara, Turkey.

Phone: +90 312 390 1 118
web: www.platanuspublishing.com
e-mail: platanuskitap@gmail.com



Platanus Publishing®

CONTENTS

CHAPTER 1 5

Stress Physiology in Plants
Emrah Şirin

CHAPTER 2 17

Atmospheric Microplastics: A Thematic Review on Sources, Environmental Impacts, Analytical Research Techniques, and Biomonitoring Approaches
Gülşah Çobanoğlu
Ezgi Özen
Handan Kurtulmuş Sancak

CHAPTER 3 45

The Therapeutic Potential of Venoms Across The Animal Kingdom with a Focus on Insects
Sadi Arda Köse
Aylin Er
Pınar Güner

CHAPTER 4 65

Plant Aging and Death Process – Senescence
Yüksel Keleş

CHAPTER 5 89

Investigation of Tert-Butanol/Water Mixture Using Two Types of TD-NMR Devices
Cengiz Okay

CHAPTER 6 97

Optimal Boundary Control of Vibration Problems: Modeling, Regularization, and The Adjoint Method
Hakkı Güngör

CHAPTER 7 111

Drug Resistance in Breast Cancer: Subtype-Specific Mechanisms and Strategies to Overcome Treatment Failure
İdil Çetin
Mehmet Topçul

CHAPTER 8 135

Generalized Tribonacci Three-Parameter Generalized Octonions and Their Hamilton Matrix Sequences

Göksal Bilgici

CHAPTER 1

Stress Physiology in Plants

***Emrah Şirin*[1]**

[1] Doç. Dr., Selçuk Üniversitesi Fen Fakültesi Biyoloji Bölümü
ORCID: 0000-0003-3408-7186

The meaning and importance of stress

The term "stress" is used for plants just as it is used for humans and animals. In other words, plants also undergo stress and suffer damage just like humans and animals. A wide variety of biotic and abiotic environmental factors in nature cause stress in plants. Abiotic factors can be grouped as physical and chemical environmental factors. What is stress? What is meant when plants are said to be under stress? The changes that occur in plants under the influence of biotic and abiotic stress factors are expressed as stress. Stress adversely affects plant growth and development by leading to significant physiological and metabolic changes, and it can cause a loss in product quality and quantity, as well as the death of the plant and plant organs (Kacar et al., 2017).

When are plants not under stress in nature? Plants are not under stress when environmental conditions do not cause damage to them, and when no negative effect occurs on their growth, development, or the quality and quantity of the product. Conditions that do not create stress are expressed as *Optimum Environmental Conditions*, and in this case, the adaptation of plants to the environment is complete. Starting from zero, stress factors cause a reduction in growth and development at moderate and highest levels, leading to a loss in the quality and quantity of the product.

The damage caused by stress factors varies depending on the degree of genetic adaptation of the plant to the environment (Dubey, 1994). This phenomenon is the primary factor determining the optimum growth of different plants in different regions.

Biotic and abiotic stress factors adversely affect the nutrition of humans and animals by causing significant crop losses in various plants. Under optimum conditions, while the average crop loss due to the effect of biotic and abiotic stress factors varies between 65% and 87% compared to the potential yield obtainable from various plants, the average loss caused by abiotic factors alone varies between 51% and 82%. With the development and introduction of stress-resistant plant varieties through biotechnological applications, the solution to the nutritional problem in our universe will become much easier (Kacar et al., 2017).

Stress physiology

It is not always possible to understand that plants are under stress. Most stress factors in the environment can cause damage to plants without giving a clear diagnosis. In addition, plants gain resistance against stress factors through metabolic changes and try to minimize the damage. The mechanism of *stress resistance* operates in two ways in plants. Plants either prevent the activity of stress factors through the *avoidance mechanisms* they develop, or they resist stress factors through *tolerance mechanisms* and sustain their lives.

Plants gain resistance to abiotic stress factors through *acclimation*, in other words, by being habituated to climatic conditions. For example, temperate climate plants become more resistant to cold through the mechanisms they develop after experiencing a short-term cold shock, that is, after being acclimated (Kacar et al., 2017).

Different plant genotypes growing under different environmental conditions struggle against stress factors through morphological, physiological, and metabolic changes. For example, in most hot climate (desert) plants, while the cutin layer thickens, the surface/volume ratio decreases, stomata are located as deep as possible and close during the day, leaves curl, hairs form on the leaf, and the plant positions itself to reflect solar radiation maximally. Plant roots grow as deep as possible, and the plant adapts to the environmental conditions in which it develops through the necessary changes.

Water stress (Drought stress)

Water stress, which is synonymous with drought stress, occurs when the amount of water lost in the form of vapor within a certain period in plants (transpiration) is greater than the amount of water absorbed from the environment. In most green plants, 85-90% of the fresh weight is water (Kacar et al., 2017).

As explained previously, water absorbed from the soil through the roots of higher plants is transported to the shoot organs of the plant according to osmotic rules. If the amount of water lost through transpiration is greater than the amount of water absorbed, a competition starts between plant organs to obtain water due to the negative pressure (tension) formed inside the conduction vessels (xylem).

Osmotic potential varies depending on the amount of substance dissolved in water in the form of molecules or ions. Turgor potential, on the other hand, occurs as a result of water molecules present independently in the cell colliding with membrane surfaces and cell walls. Turgor pressure (TP) in the cell must always be positive. When turgor pressure drops, the phenomenon of wilting occurs in the plant. For this reason, turgor potential is the fundamental element of water potential in plants undergoing water stress or drought stress (Kacar et al., 2017).

Soil pores formed between particles and aggregates of different sizes are filled with air and water. As water is lost through drainage and evaporation, and as water is absorbed by plant roots, the amount of water present in liquid form in the soil decreases. If this continues, the water around the soil particles is held by them with an increasingly greater force.

Depending on the decrease in soil water potential and the water being held with an increasingly greater force by soil particles, the water absorption capacity of plant roots also decreases. As a result of this, the plant cannot absorb sufficient water required from the soil with its roots, and wilting begins in the plant. The

continuation of the inability to absorb water leads to permanent wilting in the plant. At this time, the amount of water in the soil is at the Permanent Wilting Point (PWP). At the permanent wilting point, the water potential of the soil varies between -1 and -2 MPa (megapascal = 10 bar). While the amount of water in the soil where plants show normal development is -0.03 MPa, the amount of water at the permanent wilting point is 1.5 MPa (absolute value).

Water stress occurs when the amount of available water for the plant in the soil decreases and water loss continues as a result of transpiration and evaporation under the influence of atmospheric conditions. Stress can be daily or long-term. Long duration of water stress and failure to achieve sufficient water uptake can lead to death in plants (Kacar et al., 2017).

Plants that adapt to different conditions with different water contents through morphological and physiological changes and sustain their lives have been classified under different names. For example, *Hydrophytes* are plants that grow in areas where water is abundant and always available. *Mesophytes* are plants that grow in conditions where the amount of available water is at a moderate level. *Xerophytes* are plants that grow in arid and desert conditions where water is scarce for most of the year. *Halophytes*, on the other hand, constitute plants that grow in saline conditions.

Water stress significantly affects growth as well as product quality and quantity in plants. In case of stress, the loss of turgor adversely affects cell growth, causing cells to remain small. The decrease in cell growth also leads to a decrease in cell wall synthesis. While protein and chlorophyll synthesis are adversely affected, seeds lose their germination capacity, and photosynthesis and respiration are also negatively affected. The negative effect on cell growth causes the leaves of plants to shrink, thereby leading to a decrease in photosynthetic products (Pugnaire et al., 1994).

Water stress has a critical effect especially during the fruit and grain formation stage. Due to the absence of a sufficient level of water, the decrease in water potential in xylem conduction vessels adversely affects the transport of photosynthetic products. As a result of this, fruits remain small and grain filling in cereals cannot be fully realized. Respiration in plant leaves decreases significantly. Collier and Cummins (1996) determined that this phenomenon results from the inability of the plant to meet its energy requirement due to insufficient transport of photosynthetic products (Kacar et al., 2017).

Water stress also exerts a significant effect on enzyme activity and enzyme amount in plants (Walton, 1980; Salisbury and Marinos, 1985; Plaut, 1995). The amount of abscisic acid (ABA) increases 40-fold in leaves, while this increase is less in other organs, including the root. Abscisic acid (ABA) prevents the closure of stomata and the loss of water through transpiration. By reducing development

in the shoot organs of the plant, it also ensures that water is used in the root system, thereby causing the root to elongate deeply.

As seen from the figure, ABA accumulating in the western wheatgrass plant under water stress stopped development in the above-ground organs while causing the root system to elongate deeply. In the plant not subjected to water stress, development in the above-ground and underground organs is balanced (Fitter and Hay, 1981).

Due to the alteration of the internal structures of chloroplasts under water stress, the decrease in the amount and functions of chlorophyll causes photosynthesis to be adversely affected (Paljakoff-Mayber, 1981; Havaux et al., 1988). It has been determined that nitrate reductase enzyme activity decreases in the leaves of plants under water stress. According to Shaner and Boyer (1976), this phenomenon resulted from the decrease of nitrate transport within the xylem (Kacar et al., 2017).

Salt stress

Soil salinity, which is one of the most important stress factors, adversely affects growth, development, and the quality and quantity of the product in plants. This phenomenon is observed in cultivated plants grown in different countries of the world, especially in arid and semi-arid regions (Kalaji and Pietkiewicz, 1993). In rainy regions, salts are leached and mix with groundwater and are then transported to the seas by rivers. For this reason, salinization does not practically occur in rainy regions. River deltas and low-lying lands close to the sea, where soils remain under the influence of seawater, are exceptions to this.

In arid and semi-arid regions, leaching of salts is negligibly low due to the scarcity of rainfall. In these regions, where water loss due to evaporation is high, salts accumulate in the soil and on the soil surface. Irrigation to be carried out without providing good drainage is another factor that causes an increase in salinity. Salts present in irrigation water and water table rise to the soil surface over time, leading to an increase in salinity. Salt accumulation also occurs when water permeability is low and the groundwater level is high. The high level of the groundwater is generally related to topography. In closed basins where drainage pathways are not well formed, water seeping from the surrounding high land accumulates in low places, raising the groundwater level. The upward movement of saline groundwater and the loss of surface water by evaporation prepare the ground for the formation of saline soils (Kacar et al., 2017).

Salt stress generally arises in plants due to two reasons. While the increase in osmotic potential as a result of the excess of dissolved salts in the root zone constitutes one of the important reasons, the high concentration of toxic ions constitutes the other reason. While some plants create counter-mechanisms against stress conditions, some adapt to the conditions. However, most cultivated

plants sensitive to salt show wilting. In advanced stages, their lives terminate or they suffer significant crop loss. Under saline conditions, the amount of ions that are not absolutely necessary for plants is greater than the amount of ions that are absolutely necessary. The uptake of absolutely necessary ions leads to a gradual increase in the amount of ions that are not absolutely necessary in the medium. Research conducted on plants growing under these conditions has made it possible to know the mechanisms developed against salt stress.

As a result of this, ecologists have named plants as *Halophytes* and *Glycophytes* according to their state of resistance to salt stress. Halophytes growing in saline soils with high salt concentration are also called *Facultative Halophytes* or *Obligate Halophytes*. In addition, halophytes are named according to their growth status at salinity levels. For example, while plants growing under extremely saline conditions are called *Euhalophytes*, those growing under moderately saline conditions are called *Oligohalophytes*. In contrast, plants that cannot sustain their lives at high salt concentrations are called *Glycophytes* or *Nonhalophytes* (Kacar et al., 2017).

Temperature stress

Temperature is one of the most critical environmental factors regulating plant distribution, growth, and agricultural productivity across the globe. Temperature stress occurs when environmental temperatures rise significantly above or fall below the optimum temperature range required for the normal physiological functions of a specific plant species. Temperature stress is broadly categorized into two major types:

Heat stress

High temperature stress disrupts the cellular homeostasis and severely hampers the growth and development of plants. The degree of damage depends heavily on the intensity (the maximum temperature level), duration of exposure, and the rate of temperature increase (Kacar et al., 2017).

Physiological and Metabolic Effects of Heat Stress:

Membrane Fluidity and Structural Integrity: High temperatures increase the fluidity of the lipid bilayer of cellular membranes. Excessive fluidity leads to a structural transition, causing chemical leakage of essential ions, organic solutes, and metabolites out of the cell.

Inactivation and Denaturation of Enzymes: Enzymes are protein molecules that strictly require a specific three-dimensional conformation to perform catalytic functions. Heat stress breaks the weak bonds stabilizing this structure, leading to denaturation.

Inhibition of Photosynthesis: Photosynthesis is highly sensitive to heat stress. The primary site of heat injury within the chloroplast is the Photosystem II (PSII)

complex and its oxygen-evolving complex. Furthermore, the activity of the enzyme RuBisCO (Ribulose-1,5-bisphosphate carboxylase/oxygenase) decreases significantly under elevated temperatures due to the direct inactivation of RuBisCO activase (Kacar et al., 2017).

Induction of Oxidative Stress: Heat stress accelerates the accumulation of Reactive Oxygen Species (ROS) such as superoxide radicals and hydrogen peroxide, leading to cellular oxidative damage, lipid peroxidation, and rapid chlorophyll degradation.

Mechanisms of Heat Tolerance in Plants:

Plants have evolved various physiological and molecular mechanisms to avoid or tolerate high temperature stress:

Heat Shock Proteins (HSPs): Under sudden temperature increases, plants rapidly synthesize a specific class of highly conserved proteins known as Heat Shock Proteins (HSPs). HSPs function as molecular chaperones. They bind to other cellular proteins, preventing their aggregation and denaturation under heat stress, and actively help re-fold damaged proteins.

Antioxidant Defense System: Tolerant genotypes significantly increase the expression and activity of antioxidant enzymes such as Superoxide Dismutase (SOD), Catalase (CAT), and Peroxidase (POD) to effectively scavenge harmful ROS molecules (Kacar et al., 2017).

Transpirational Cooling: Provided that sufficient water is available in the soil, plants can lower their leaf surface temperature by several degrees through increased transpiration rates.

Cold Stress (Chilling stress)

This type of stress is particularly damaging to tropical and subtropical crops (such as maize, rice, tomato, and cotton) that completely lack innate low-temperature tolerance mechanisms.

Physiological Changes Under Chilling Stress:

Membrane Phase Transition: Unlike heat stress which increases fluidity, chilling stress causes cellular membranes to transition from a flexible, fluid liquid-crystalline state to a rigid, solid-gel state. This rigidification severely impairs the function of membrane-bound transport proteins and channels (Kacar et al., 2017).

Restricted Water and Nutrient Uptake: The rigidification of root cell membranes combined with the increased viscosity of water at low temperatures drastically reduces root hydraulic conductivity. Consequently, plants suffer from a temporary "physiological drought" even if the soil profile contains adequate water.

Metabolic Imbalance: Low temperatures slow down metabolic reactions unevenly. While some enzymatic pathways are restricted, others continue at a normal pace, leading to the toxic accumulation of metabolic intermediates and the rapid generation of ROS.

Freezing stress

The primary site of freezing injury is not the cold temperature itself, but the mechanical and osmotic stress caused by ice formation.

Mechanisms of Ice Formation:

Extracellular Freezing: In most cases, ice crystal formation initiates in the extracellular spaces (apoplast) because the solute concentration is lower there than inside the cell (protoplast). As extracellular ice grows, it withdraws water from the inside of the cell due to vapor pressure differences. This leads to severe cellular dehydration (Kacar et al., 2017).

Intracellular Freezing: If the temperature drops very rapidly, ice crystals can form directly inside the cytoplasm or vacuole (symplast). Intracellular ice crystals mechanically rupture cell membranes and organelles, which always results in instantaneous cell death.

Light and ultraviolet (UV) stress

Light Stress (Photoinhibition)

While light is the primary energy source for photosynthesis, excessive light intensities can cause severe stress in plants, a phenomenon known as **photoinhibition**. When the amount of light energy absorbed by chlorophyll molecules exceeds the chemical capacity of the photosynthetic apparatus to utilize it, the excess energy induces the formation of singlet oxygen and other ROS. This damages the D1 protein of the Photosystem II (PSII) reaction center, shutting down photosynthetic activity (Kacar et al., 2017).

To protect themselves from excess light, plants utilize the xanthophyll cycle, which safely dissipates excess light energy as thermal heat (non-photochemical quenching).

Ultraviolet (UV) stress

Ultraviolet radiation, particularly UV-A (320-400 nm), UV-B (280–320 nm) and UV-C (200–280 nm), possesses high energy that can directly damage plant macromolecules. UV radiation induces DNA mutations (such as pyrimidine dimers), degrades photosynthetic pigments, and disrupts protein structures (Kacar et al., 2017).

Plants defend themselves against UV stress by accumulating UV-absorbing compounds, primarily **flavonoids and phenolic compounds**, within the epidermal cell layers. These compounds act as an internal sunscreen, reflecting

or absorbing harmful UV wavelengths while allowing visible light to pass through to the photosynthetic tissues.

Flooding (Excess Water) stress

Flooding, waterlogging, or submergence stress occurs when agricultural soils become completely saturated with water. The primary consequence of flooding is hypoxia (low oxygen availability) or anoxia (complete absence of oxygen) in the root zone. Because oxygen diffuses roughly 10,000 times slower in water than in air, plant roots rapidly deplete the remaining dissolved oxygen for respiration (Kacar et al., 2017).

Metabolic Transitions Under Flooding:

Switch to Anaerobic Respiration: In the absence of oxygen, the mitochondrial electron transport chain stops. Roots are forced to switch from aerobic respiration to alcoholic fermentation or lactic acid fermentation to maintain ATP production.

Energy Crisis: Fermentation produces only 2 ATP molecules per molecule of glucose compared to the 36–38 ATP molecules produced via aerobic respiration. This causes a severe energy crisis, limiting root growth and nutrient uptake (Kacar et al., 2017).

Anatomical Adaptations: Flood-tolerant plants develop specialized anatomical structures such as aerenchyma (gas-filled tissue with large intercellular spaces) that allows oxygen to diffuse from the above-ground shoots down to the submerged roots. Some species also form adventitious roots near the water surface.

Oxidative stress

Oxidative stress is a secondary stress condition that almost always accompanies all other primary biotic and abiotic stresses (drought, salinity, heavy metals, extreme temperatures, pathogens, etc.). It is defined as a disruption in the balance between the production of **Reactive Oxygen Species (ROS)** and the cellular antioxidant defense mechanisms (Kacar et al., 2017).

Cellular damage caused by ROS:

Lipid Peroxidation: ROS directly attack polyunsaturated fatty acids in cellular and organelle membranes, converting them into lipid peroxides. This degrades membrane fluid dynamics and creates structural leaks.

Protein Oxidation: ROS oxidize amino acid side chains, leading to protein fragmentation, cross-linking, and complete enzyme inactivation (Kacar et al., 2017).

DNA Damage: ROS induce base modifications, strand breaks, and cross-links in both nuclear and organellar DNA, leading to mutations or programmed cell death.

Plants manage oxidative stress through a sophisticated network of enzymatic antioxidants (SOD, CAT, APX, GR) and non-enzymatic antioxidants (ascorbate, glutathione, tocopherols, and carotenoids) that rapidly neutralize ROS before they can cause catastrophic cellular damage (Kacar et al., 2017).

REFERENCES

Collier, D. E. and W. R. Cummins (1996). The rate of development of water deficits effects *Saxifraga cernua* leaf respiration. Physiol. Plant. 96: 291-297.

Dubey, R. S. (1994). Handbook of Plant and Crop Stress, (M. Pessarakli, ed.) p. 277. Marcel Dekker, New York.

Fitter, A. H. and R. K. M. Hay (1981). *Environmental physiology of plants*. Academic Press, New York.

Havaux, M., M. Ernez and R. Lannoye (1988). J. Plant Physiol. 133-555.

Kacar, B., Katkat, A. V., and Öztürk, Ş. (2017). Stres fizyolojisi in Bitki fizyolojisi. Nobel Akademik Yayıncılık, Ankara, p. 485-537 (in Turkish).

Kalaji, M. H. and S. Pietkiewicz (1993). Acta Physiol. Plant. 15: 89-93.

Plaut, Z. (1995). Handbook of Plant and Crop Physiology, (M. Pessarakli, ed.) p. 587. Marcel Dekker, New York.

Paljakoff-Mayber, A. (1981). Physiology and Biochemistry of Drought Resistance in Plants. p. 389 (L.G. Paleg and D. Aspinall eds.). Academic Press. Australia.

Pugnaire, F. L., L. S. Endolz and J. Pardos (1994). Handbook of Plant and Crop Stress (M. Pessarakli, ed.). p. 247, Marcel Dekker, New York.

Salisbury, F. B., and N. G. Marinos (1985). The ecological role of plant growth substances. p. 707-708. In: Encyclopedia of Plant Physiology. Vol. II. (R.P. Pharis and D.M. Reid. eds.) Springer-Verlag, Berlin.

Shaner, D. L. and J. S. Boyer (1976). Nitrate reductase activity in maize (*Zea mays* L.) leaves. I. Regulation by nitrate flux. Plant Physiol. 58: 499-504.

Walton, D. C. (1980). Biochemistry and physiology of abscisic acid. Annual Review of Plant Physiology. 31: 453-489.

CHAPTER 2

Atmospheric Microplastics: A Thematic Review on Sources, Environmental Impacts, Analytical Research Techniques, and Biomonitoring Approaches

Gülşah Çobanoğlu[1]
Ezgi Özen[2]
Handan Kurtulmuş Sancak[3]

[1] Prof. Dr., Department of Biology/Botany, Faculty of Science, Marmara University, Istanbul, Türkiye, ORCID 0000-0002-3549-2872
[2] Department of Biology, Institute of Pure and Applied Sciences, Marmara University, Istanbul, Türkiye, ORCID: 0000-0001-7262-6780
[3] Department of Plant and Animal Production, Balıkesir University Edremit Vocational School, Türkiye, ORCID: 0000-0003-3531-8548

Introduction

Over the past few decades, global plastic production levels have steadily increased, particularly for single-use plastics (139 million metric tons worldwide in 2021 alone). If necessary measures are not taken, global plastic production is projected to triple by 2060 (Paddison, 2023). Plastic waste has been found in ocean gyres all over the world, covering all coastal ecosystems. Plastic pollution has become a global problem, and the environmental concerns it causes have attracted significant attention in scientific research. The most striking recent study was the discovery of rocks made of plastic on an island in Brazil, demonstrating that plastic waste can even alter ecosystems (Queiroz, 2023). Furthermore, it causes serious harm to the health of most living things, including humans. Animals become entangled in large plastic waste, causing acute and chronic injuries or death. Plastics have been reported to harm over 270 different wildlife species, including mammals, reptiles, birds, and fish (Du et al., 2021). It has been shown that some animals can die from digestive blockages after ingesting large amounts of plastic, or that toxins from ingested plastic can negatively impact their reproductive and immune systems (WWF, 2019).

Plastics contain numerous complex chemical compounds; more than 4,000 chemicals have been identified in connection with plastic packaging alone. Furthermore, it has been reported that over 80% of plastic chemicals leach into water, increasing the potential for exposure to living organisms (Zimmermann et al., 2021). Once plastic waste enters the environment, it loses its mechanical integrity and breaks down spontaneously or through chemical and physical degradation processes including photooxidation and abrasion, forming microplastic particles (Gambino et al., 2023) or nanoplastic particles smaller than 100 nm (Niccolai et al., 2023). Microplastics are generally defined as plastic pieces smaller than 5 mm or between 1 micrometer and 5 millimeters (Wright et al., 2020). Nanoplastics are polymer-containing particles smaller than 1 μm, generally within the 1–1000 nm range, originating from the manufacture or degradation of plastic materials (Gigault et al., 2018).

Plastic particles and microplastics, along with additives, pose a significant chemical threat. Microplastics can act as vectors for other pollutants (toxic metals, etc.) and pathogens in the environment. In sedimentary environments, pathogenic bacteria associated with microplastics have been reported to be primarily Gammaproteobacteria and Pseudomonadota (particularly *Pseudomonas aeruginosa* and *Acinetobacter baumannii*) (Shu et al., 2025). Due to their lipophilic properties, microplastics can contain various persistent organic pollutants such as dichlorodiphenyltrichloroethane (DDT), polycyclic aromatic hydrocarbons (PAHs), and hormone disruptors on their surfaces (Jimenez-Skrzypek et al., 2021; Silva et al., 2022).

Due to the complex interactions of microplastics with the environment, assessing their presence, quantifying them, and studying their impacts on the environment represents a new, very challenging and interdisciplinary issue that requires different skills from physical, chemical, and environmental fields. Therefore, developing and improving methods for identification, detection, mapping, and quantification to assess the presence of microplastics in different environments is of paramount importance (Avella et al., 2019). Research has shown that microplastics not only end up in water but also enter various terrestrial environments, including the atmosphere, on a global scale, causing soil, water, and air pollution (Shao et al., 2022; Krystek et al., 2025). Initially regarded as primarily a marine pollution issue, recent research has revealed that micro- and even nanoplastics are pervasive throughout ecosystems, affecting freshwater, soil, and air, as well as thousands of species, including humans. The first study on the transport of microplastics in the atmosphere was conducted by Dris et al., (2015), who stated that the fibers found in freshwater mainly originate from atmospheric deposition. The effect of the Asian summer monsoon on the transport of atmospheric microplastics between marine and terrestrial ecosystems in China has been investigated, and it has been determined that due to the backward trajectory and wind field, microplastics transported in the air over the ocean are carried back to the continent from Vietnam, the Philippines, and Malaysia towards southeastern China, and only a portion of them enter the marine ecosystem (Wang et al., 2021). As a result, the transport and deposition of microplastics are related to meteorological factors such as rain, snow, temperature, humidity, air pressure and wind speed (Shao et al., 2022). Therefore, atmospheric microplastic pollution can be considered separately from a research perspective, but its interactions with different ecosystems must be taken into account.

Our study addresses the subject through its lesser-known aspect: “atmospheric microplastics”. This chapter aims to guide future research by compiling information from recent studies—based on existing literature—that highlight the environmental pollution and human health risks posed by airborne microplastics. It comprehensively summarizes current knowledge on atmospheric microplastics, focusing on their formation, sources, physicochemical properties, environmental interactions, effects on living organisms, microscopic and chemical detection and analytical techniques, biological monitoring methods, and potential strategies for reducing microplastic pollution. Particular emphasis is placed on approaches developed for the biomonitoring of microplastics as air pollutants using lichens and mosses. This work brings together comprehensive and up-to-date publications on the environmental damage caused by microplastics, a significant problem today.

Origin, Sources and Physicochemical Properties of Atmospheric Microplastics

Atmospheric microplastics primarily originate from anthropogenic activities such as textile fiber abrasion, traffic-related wear, industrial processes, and the fragmentation of larger plastic debris. Due to their small size and distinct physicochemical properties, they can remain suspended for extended periods, enabling long-range transport and deposition in diverse ecosystems. The main sources of atmospheric microplastic pollution originate from plastic particles such as synthetic textiles, plastic granules, city dust, and road signs, which are produced, used, and discarded into the environment as waste in various sectors as a result of human and industrial activities (Veerasingam et al., 2021). Microplastics can be divided into two groups based on how they are formed from their source. Primary microplastics are those intentionally produced at microscopic dimensions for a specific purpose, for example, as components of industrial, pharmaceutical or cosmetic products (paints, adhesive coatings, microbeads) (Van Wezel et al., 2016). Secondary microplastics are formed by the fragmentation of larger plastic particles through the long-term physical, chemical and biological degradation process (Oleksiuk et al., 2022; Shao et al., 2022). Plastic waste undergoes biotic degradation (carried out by microorganisms) and abiotic degradation (photodegradation due to exposure to UV radiation or abrasion) in the environment. Large plastics and primary microplastics in seawater can be degraded into small fragments, resulting in an increasing number of secondary microplastics and nanoplastics (Geng et al., 2021). All physicochemical properties of microplastics, such as size, color, shape, polymer type, morphology, and mobility, affect living organisms (Chouchene et al., 2023). The abiotic and biotic degradation rate of plastic waste depends on the chemical structure of the plastic, the hydrophilicity of its surfaces, and environmental conditions (Vieira et al., 2021). Microplastics in various environments vary in shape, size, and polymer composition depending on the sources, degradation and erosion processes, and residence times (Zhang et al., 2025).

The chemical structure of microplastics consists of carbon and hydrogen atoms linked together in polymer chains. The dominant polymer components found in airborne microplastics include polyethylene (PE), polypropylene (PP), polyvinyl chloride (PVC), polystyrene (PS), polyethylene terephthalate (PET), polyester (PES), polyamide (PA), polyurethane (PUR), and resins (Figure 1). Other chemicals such as phthalates, polybrominated diphenyl ethers (PBDEs), and tetra bromo bisphenol A (TBBPA) are also commonly found in microplastics, and many of these chemical additives leach from plastics after they enter the environment (Zhang et al., 2025). PE is used in the manufacturing of containers and bags, while PET is a significant raw material widely used to produce fabrics in the textile industry. As for nylon, it is used in industrial areas such as wheels, textiles and ropes (Zhao et al., 2023).

There are many different types of microplastics that vary in size, shape, color, composition, and chemical properties. Some common shape categories they fall into include fibers, pellets, pieces, films, foams, particles, ellipses, lines, and flakes. Their sizes vary greatly depending on the region and point of degradation. The different compositions of various polymers determine the unique physicochemical properties of microplastics, such as crystallinity, density, molecular weight distribution, and surface chemistry. Crystallinity is important because of its effect on density. The higher the crystallinity, the harder the polymer (Silva et al., 2022). Due to their small size and large surface area, microplastics can accumulate persistent organic pollutants (POPs) such as organochlorine pesticides (OCPs), polycyclic aromatic hydrocarbons (PAHs), polychlorinated biphenyls (PCBs) (Jimenez-Skrzypek et al., 2021), and heavy metals such as lead (Pb) (Zhu et al., 2023) (Figure 1). These toxic substances associate with microplastics through various types of bonds, including hydrogen bonding, hydrophobic interactions, electrostatic interactions, halogen bonding, and van der Waals forces (Ivleva et al., 2021).

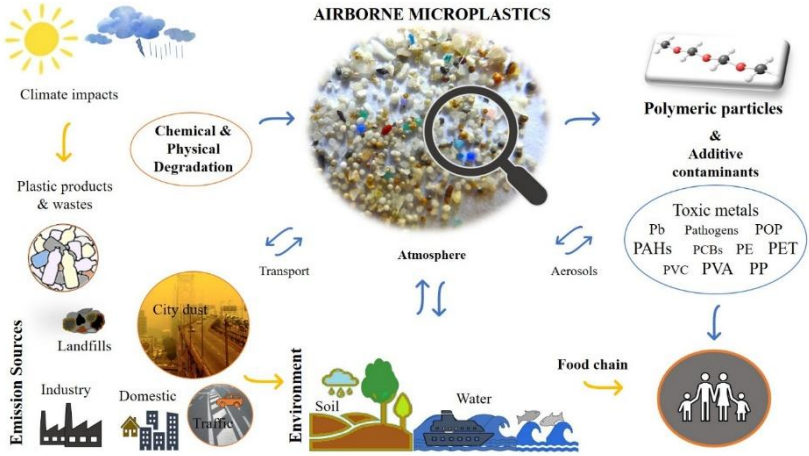


Figure 1. Sources, formation, and circulation of atmospheric microplastics in the environment.

Primary microplastics are released into the environment in their manufactured form, while secondary microplastics are formed as a result of the abrasion and degradation of larger plastics that have previously entered the environment. The release of secondary microplastics into the environment occurs through three mechanisms: natural degradation of microplastics under the influence of atmospheric conditions and microbial activity, decomposition of macroplastics into microplastics by direct action of organisms, and resuspension of microplastic particles in soil or sediment. Plastic waste undergoes biotic

degradation (carried out by microorganisms) and abiotic degradation (photodegradation due to exposure to UV radiation or abrasion) in the environment. Today, microplastic particles are ubiquitous. They are found in both marine and terrestrial ecosystems. Their presence has been demonstrated in salt water, surface water bodies, wastewater, and groundwater (Oleksiuk et al., 2022).

EPA (Environmental Protection Agency) has reported the results of the assessment regarding the factors affecting the formation of microplastics (Lassen et al., 2022; USEPA, 2015):

a) Plastics remain intact for many years,
b) Plastic consumption is increasing worldwide,
c) Plastics mixed into water are distributed between continents,
d) Plastics decompose and turn into micro or nano plastics,
e) Microplastics are found at all levels in aquatic food chains,
f) There is not enough information about nano particles.

The study by Swinnerton et al., (2024) investigated the emission and physicochemical properties of microplastics formed during the shredding of waste, new polyethylene terephthalate, polypropylene and high-density polyethylene, which are regularly used in mechanical recycling. It has been found that the number concentrations of both submicron and micron-sized respirable particles are 3–2910 times higher during decomposition periods, exposing workers to high concentrations of microplastics in the air. The technology commonly used in the repair of sewer pipes has been identified as one of the sources of airborne microplastic emissions in urban areas. Plastic particles may contain potentially toxic additives for organisms incorporated into polymers during their production to extend their lifespan and give them better resistance to heat, oxidation, and degradation mechanisms. The complex structure of microplastics is characterized by at least five dimensions that must be considered in the chemical analysis of these small particles (Ivleva, 2021):

- Wide size range, i.e., from 1 μm to 1 mm (and up to 5 mm for large microplastics),
- Different types of polymers with various chemical compositions (including traditional and biopolymers with different structures and densities),
- Different shapes (spheres, irregular particles, fibers, films, foams),
- Various additives (antioxidants, light stabilizers, plasticizers, flame retardants, pigments, etc.), weathering products, and adsorbed pollutants (persistent organic pollutants, antibiotics, heavy metals, etc.),

- Different accumulation status (primary and secondary microplastics, biofouling), surface charge, and hydrophobicity.

Interaction of Airborne Microplastics with Environmental Quality and Living Organisms

Studies on general food and water resources have highlighted the transfer of microplastics from the ocean to humans via the food chain. Microplastics reach humans through the consumption of animals that have ingested microplastics from the environment (e.g., fish that have ingested plastic waste or drunk contaminated water), as well as through plastic contamination during the production and packaging of seafood and other industrial foods (Cox et al., 2019). Plastics used worldwide remain undegraded in nature for years, and those that do decompose eventually mix with the soil and are found at all stages of the food chain. It is reported that micro-nano plastics, which are widespread in the environment, can be taken up by plants, animals, and humans through air, soil, water, and food (Krystek et al., 2025). Furthermore, it has been reported to affect microorganisms by reshaping the structure and function of microbial communities and altering their dispersal pathways (Zhao et al., 2023). The presence of microplastics in tap water, bottled water and even in the air we breathe is gradually increasing the risk of human exposure (Zhang et al., 2020). However, data on the effects of direct microplastic contamination at the cellular and tissue levels are still quite limited, and more accurate data are needed through reliable standardized tests (Gouin et al., 2022; Lee at al., 2024). In recent years, people have become increasingly aware of exposure to microplastics through food (Pekmezekmek, 2022). According to research conducted in waters, it is estimated that the amount of microplastics in water will exceed the biomass of fish in 2050 (Eerkes-Medrano et al., 2015). Daily used PET bottles release high levels of microplastics into the environment in nylon containers (Schymanski et al., 2018). After microplastics was detected in seafood, honey, milk, table salt, drinking water and air, the effects of microplastic on human health have recently become the focus of attention (Cox et al., 2019; Gambino et al., 2023). It has been stated that microplastics can disrupt human endocrine systems and cause developmental and reproductive problems in infants (Sripada et al., 2022).

One of the primary ways living organisms are exposed to atmospheric microplastics is through airborne particles. Due to their small size and low density, these airborne microplastics can be carried by wind and transferred between aquatic and terrestrial environments (Carriera et al., 2024). Studies have shown that inhaling and ingesting airborne microplastics can lead to their accumulation in tissues and organs, negatively impacting human health. This can affect many organisms, from plankton to mammals. Recent studies on agricultural plants such as wheat show that microplastics can disrupt nutrient cycling, reduce growth rate, and inhibit seed germination. Reported adverse

effects include decreased leaf size, chlorophyll content, and photosynthetic efficiency; impaired photosynthesis and stomatal conductivity; stomatal blockage; increased peroxidase; and decreased root hydraulic conductivity (Lee at al., 2024).

Potential risks to human health from microplastics through inhalation and skin contact include inflammation, oxidative stress, and cellular dysfunction, as well as increased levels of alanine aminotransferase in the blood, an indicator of liver inflammation. They can cause respiratory problems and worsen pre-existing lung conditions; exposure to chemicals found on microplastic surfaces inhaled through the skin can negatively impact individuals' respiratory health and overall well-being. Microplastics found in personal care products and textiles can come into direct contact with human skin. While the effects of direct skin exposure are an ongoing area of research, absorption of chemicals associated with microplastics can have detrimental effects on skin health, including irritation and allergic reactions. Furthermore, they have been reported to reduce embryo formation, decrease sperm quality, trigger ovarian cancer, cause liver damage and inflammation, and lead to kidney damage. The long-term effects of the interaction between microplastics and human health require more detailed investigation (Lee at al., 2024). In Buenos Aires (Argentina), meso (> 5 mm) and microplastic (< 5 mm) particle content was detected in the dried thalli of *Usnea amblyoclada* sold in herbalist shops and in the teas prepared from these lichens (Gollo et al., 2023). All studies show that nano and microplastics are spreading more and more into the environment, and that the exposure of living organisms will increase over the years (Krystek et al., 2025). Although the prevailing view is that there will be no effects on humans, such as illness or death, or long-term exposure, it is not a result to be underestimated that more than 140,000 marine animals have died each year since the 1990s due to aquatic organisms defined as bioindicators in nature, ingesting plastics or being surrounded by plastics (Pekmezekmek, 2022). Sustainable solutions are being developed through applications using naturally-derived coagulants in water treatment methods to remove microplastics and nanoparticles from aquatic environments (Hanif et al., 2026).

Based on their structural properties, microplastics act as carriers of toxic chemicals and other pollutants, leading to environmental pollution and consequently threatening ecosystems (Campanale et al., 2020). A study in China investigated microplastics in the atmosphere of a coastal city in terms of their numerical concentrations, chemical types, shapes, and sizes, comparing the effects of land and sea transportation and the difference between day and night Liu et al., (2025). Their findings showed that the majority of microplastics originating from land transportation were rubber (20.2%), while those from sea transportation were phenol-formaldehyde resin (18%), and that the numerical concentration of microplastics in the air was higher during the day than at night.

Some sources indicate that humans are exposed to microplastics transported from the atmosphere both outdoors and indoors. A modeling study (Soltani et al., 2021) examining the microplastic content of indoor dust samples taken from homes in Sydney (Australia), reported that 99% of the accumulated dust consisted of microplastic fibers, the majority of which were natural (42%), 18% processed natural-based fibers, and 39% petrochemical-based fibers. Higher amounts of polyethylene, polyester, polyamide, polyacrylic, and polystyrene fibers were found in homes with carpet as the main floor covering, while polyvinyl fibers were the most dominant petrochemical fiber type in areas without carpet. This revealed the role of floor materials or coverings in determining the microplastic composition and accumulation rate. The mean inhaled microplastic weight and number were reported as 0.2±0.07 mg/kg body weight and 12891±4472 fibers/year, respectively. The highest respiratory intake rates were observed in the under-0.5 year age group, with 0.31 mg/kg body weight per year. Another comparative study examining microplastics in indoor and outdoor air environments in New Jersey, United States, detected polystyrene (PS), polyethylene terephthalate (PET), polyethylene (PE), polyvinyl chloride (PVC), and polypropylene (PP) microplastic fibers, films, and particles in offices, hallways, classrooms, and detached houses. While PVC particles predominated in outdoor air samples, PE particles or fibers were identified as the primary microplastic in indoor air samples (Yao et al., 2022).

Solutions are being sought to reduce urban atmospheric microplastics, which are known to originate mainly from industrial activities, traffic emissions, waste disposal sites, agricultural processes, and marine aerosolization (Lee et al., 2024). In urban areas, precipitation carries airborne microplastics and accompanying pollutants into stormwater drains, causing them to mix with water and spread pollution to distant areas (Bhardwaj et al., 2024). It has been noted that urban trees (especially evergreen species) have the capacity to reduce atmospheric microplastic pollution through passive capture and retention processes. Therefore, urban green spaces are becoming increasingly important as one of the solutions sought through a nature-based approach to reducing airborne microplastics (Bhattacharjee et al., 2025).

Methods and Approaches Applied in Atmospheric Microplastic Research

Atmospheric microplastics are widespread global pollutants that threaten biota and ecosystem functioning. Recent advences in instrumentatal and analytical techniques have enabled the application of a diverse range of methods for the identification and monitoring microplastics in the air. Sampling, visualization, and chemical identification techniques are now routinely integrated to characterize microplastics in atmospheric samples, including dust and particulate matter fractions such as $PM_{2.5}$ and PM_{10} (Solórzano et al., 2025). Airborne microplastics are identified using both “visual” and “chemical”

analytical approaches. Visualization methods (microscopy-based) assess particle features such as size, shape, and morphology, while chemical techniques determine polymer composition and confirm plastic identity (Han et al., 2024). Analytical methods used to determine the presence, quantity, and chemistry of atmospheric microplastics can be carried out more efficiently and complementarily with biological methods. Biomonitoring encompasses techniques based on the spatial and temporal monitoring of microplastics and often associated additives through a biological indicator organism that accumulates airborne pollutants (Loppi et al., 2021; Capozzi et al., 2024; Taurozzi et al., 2024; Basile et al., 2025). Microplastics identified with this approach are characterized by visual and chemical analyses. Within the scope of this compilation, the methods and techniques in question are addressed individually in the subsequent sections.

In recent years, ecotoxicological studies have increasingly focused on their potential impacts, including those arising from plastic additives and adsorbed hazardous compounds. However, the environmental relevance of many studies remains limited due to inadequate particle characterization and the use of unrealistic test conditions, which compromise robust risk assessment. New, cost-effective approaches that can support mechanisms to improve the efficiency of analytical methodologies applied for the identification, quantification, and characterization of micro(nano)plastics are still being developed (Silva et al., 2022).

Analytical techniques/methods for examining microplastics

Studies aimed at detecting, identifying, and characterizing microplastics in the air primarily rely on analyses that provide "visual" and "quantitative" data (Figure 2). Microscopic techniques are used to visualize and morphologically (in terms of shape, number, and size) identify atmospheric microplastics. Analytical methods are applied to characterize their chemical composition.

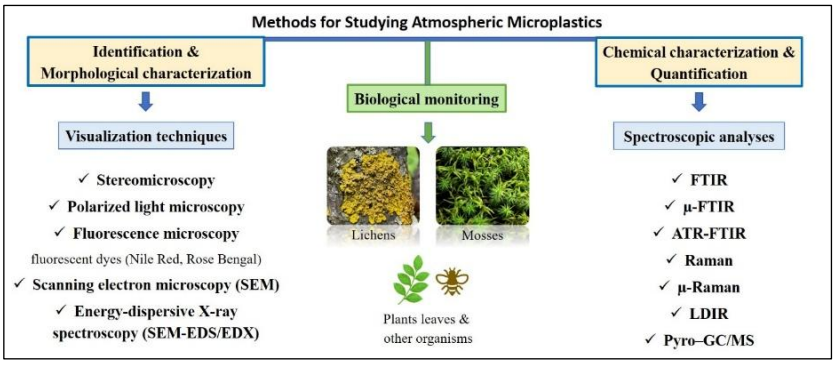


Figure 2. Diagram of analytical techniques and biomonitoring methods.

Visualization methods

Microscopic inspection provides visual confirmation and morphological characterization of microplastics collected from the air (Silva et al., 2022; Solórzano et al., 2025). These visualization methods are essential for qualitative descriptions of particle shape (fibers, fragments) and approximate size distributions (Han et al., 2024). Common imaging techniques are listed below:

- **Optical microscopy**; used for initial screening and counting of larger microplastic particles.
- **Polarized light microscopy**; this inexpensive and fast method causes characteristic color changes in samples under polarized light. This allows for easy identification of microplastics and the acquisition of images (Abbasi et al., 2017).
- **Fluorescence microscopy**; often requires the use of fluorescent dyes (e.g., Nile Red, Rose Bengal) to enhance visibility and distinguish microplastics from non-plastic particles. Fluorescent staining is a rapid and cost-effective pre-screening tool, particularly when combined with automated image analysis.
- **Scanning electron microscopy (SEM)**; yields high-magnification imaging of particle surface morphology and structure; when combined with energy-dispersive X-ray spectroscopy (SEM-EDS/EDX), it can provide elemental context (e.g., carbon-rich particles) that supports polymer identification.

Analytical methods

Several analytical methods are employed in studies aimed at characterizing the chemistry of microplastic samples. One of the key components of these methods is the "**digestion of organic matter**" applied during the sample preparation process using the wet peroxide oxidation method (H_2O_2 solution). The aim here is to reduce variable matrix compositions that could adversely affect data interpretation, without having a negative impact on microplastics (Bargagli and Rota, 2026; Dumont et al., 2025).

Another simple method used in many studies is the "**hot needle test**" (or "hot spot test" to include instruments other than needles). Its basic principle is the reaction of the suspected plastic to a hot spot, and this is particularly limited to verifying polymers that exhibit melting (Beckingham et al., 2023).

Common analytical methods are listed below:

Fourier transform infrared spectroscopy (FTIR); is one of the most widely used chemical identification techniques for microplastics. It detects characteristic vibrational signatures of polymer bonds, allowing reliable polymer type

determination (e.g., polyethylene, polypropylene, PET). FTIR is effective across a broad range of particle sizes and is often combined with microscopic imaging (μ-FTIR) for spatially resolved analysis. Recent advancements include direct μ-FTIR imaging of microplastics collected on filters, enabling better quantification of airborne microplastic characteristics in indoor environments (Li et al., 2025; Solórzano et al., 2025). In recently study, Niida et al (2026) developed a derivative-based approach to quantify the photo-oxidative degradation of airborne PET microplastics using μFTIR-ATR imaging.

Raman spectroscopy; complements FTIR by providing vibrational spectra based on inelastically scattered light. It is particularly useful for identifying microplasitcs at smaller size ranges and can reveal structural details not easily resolved with FTIR. Raman methods, including mapping techniques, are increasingly applied to assess polymer identity and particle composition with high spectral specificity (Umurhan et al., 2025). Because Raman can be less sensitive to water interference and has a higher spatial resolution than conventional FTIR, it is useful for characterizing microplastics in complex environmental matrices, including airborne dust and PM fractions.

Pyrolysis–GC/MS; is a destructive thermal method that breaks down plastic polymers into characteristic pyrolytic fragments, which are then separated and identified by GC/MS. This approach provides quantitative mass-based data on polymer types and is increasingly applied to airborne microplastic research, including $PM_{2.5}$ and PM_{10} samples. Recent studies demonstrate that Py-GC/MS, especially when combined with thermal desorption or two-shot approaches, enhances sensitivity to small microplastics and nanoplastics that may be below optical detection thresholds (Bazzazpour et al., 2025; Dumont et al., 2025).

Laser direct infrared imaging (LDIR); is one of the analytical methods used to study the physico-chemical properties of atmospheric microplastics Liu et al., (2025). The highly sensitive LDIR instrument provides infrared spectra of microplastic samples in a short time, allowing for their detection and quantitative determination of trace components by comparing them with a plastic library (particle size range, 20-500 μm).

Compared to FTIR, LDIR is described as a non-destructive and rapid analytical method that does not require chemical or physical processing of samples. Microplastic samples can be analyzed without damage or alteration to their chemical properties. Compared to μ-FTIR, LDIR has a smaller margin of error, eliminating the need for visual selection of suspected microplastic particles before testing (Liu et al., 2025).

Biological Monitoring Methods for Airborne Microplastics

Biomonitoring is defined as a technique using an animal, plant or fungal species that provides information about the quality of the environment in which

it is located (Baroudi et al., 2020). In other words, refers to processes and activities that enable the characterization and monitoring of environmental quality using native biological species (Harner et al., 2003). An organism used to indicate the quality of an environmental setting and the health of a population, community, or ecosystem is referred to as a bioindicator (Parmar et al., 2016). A bioindicator is an organism that provides qualitative information about the environmental pollution. On the other hand, a biomonitor is an organism that contains information about quantitative aspects of the quality of the environment (Markert et al., 2003). The same organism can, in some cases, serve as both a biological indicator and a biological tracer, and is used in biological air quality monitoring in both urban and rural environments (Boamponsem et al., 2010). "Biological monitoring" refers to the planned use of organisms to determine environmental quality. Bioindication and biomonitoring are relatively quick and convenient methods that provide long-term information about the degree of pollution or degradation of ecosystems. Depending on the conditions of the study area, native or transplanted samples can be used. Lichen or moss transplant samples are exposed to pollutants for a specific period using the "bag technique", and then the accumulation levels are analyzed.

Recent studies were searched in the "PubMed", "Elsevier", "Web of Science" and "Google scholar" databases using the keywords "biomonitoring" and "airborne microplastics" from 2020 to the present. Outdoor biological monitoring studies of atmospheric microplastics conducted in different geographical regions of the world are presented in Table 1. It includes detailed information on biological monitoring organisms, microplastic identification and measurement methods, and the determined polymer content.

Table 1. Current airborne microplastic biomonitoring studies, in chronological order backwards from the present (2020-2026)

Bioindicator Organism(s)		MP/Polymer Type	Visual/Chemical Analysis	Location	Reference
Moss *Pleurozium schreberi*	T	Fibres, PET, PP, PE, PVC	SM, µFTIR	Ontario, Canada	Jafarova and Aherne, (2026)
Lichen (fruticose) *Evernia prunastri*	N, T	Fragments, Fibers, PET, PP, PS, PVC, PO, ABS, acrylic rubber, PES, PE	SM, FTIR	Pisa, Tuscany, Central Italy	Basile et al., (2025)
Lichen (fruticose) *Ramalina celastri*	T	Fragments, Fibers	SM, Hot needle test	Luján, Argentina	Gollo et al., (2025)
Mosses *Brachitecium rutabulum, Eurynchium striatulum, Eurynchium striatum, Homalothecium sericeum, Hylocomium*	N	Fibers, Filaments, PET, PAA, PA, PE, COPE	SM, µ-FTIR	Tuscany, Central Italy	Jafarova et al., (2025)

splendens, Hypnum cupressiforme, Isothecium alopecuroides, Pseudoscleropodium purum					
Lichen (fruticose) *Ramalina celastri*	T	Microfibers	SM, UV-FM μFTIR	Luján, Buenos Aires, Argentin	Nistal et al., (2025)
Plant leaves *Pittosporum tobira*	N	Microfibers, PET	SM, SEM-EDS Raman	Naples, Italy	Capozzi et al., (2024)
Honeybees *Apis mellifera* pollens	N	Fibers, Fragments, Films, PET, PP, PE, PAN, PA	SM, μ-FTIR	Denmark	Cortés-Corrales et al., (2024)
Lichen (foliose) *Xanthoria parietina*	N	MPs with amine, aldehyde, alkene, carboxylic acid, methyl, methylene, NO_2, SO_2	FM/Nile red staining, FTIR	İstanbul, Türkiye	Çobanoğlu and Özen, (2024)
Moss *Grimmia crinita*	N	Fibers, Fragments, Films, PET, Nylon, PP	SM, μ-Raman	South-west Iran	Khodabakhsh loo et al., (2024)
Lichens (crustose, fruticose) *Acarospora bullata, Acarospora cervina, Anaptychia bryorum, Candelariella rhodax*					
Lichen (fruticose) *Anaptychia ciliaris*	N	Microfibers, PET, PUR, PA, PVC	SM/Rose Bengal staining, FTIR μ-Raman	Yozgat, Türkiye	Kocakaya et al., (2024)
Plant (leaf dust) *Polyalthia longifolia*	N	PE, PET, PP, PS, PVC, PTEs	GC-MS	Dhaka, Savar Bangladesh	Parvez et al., (2024)
Plants (leaf surface) *Ficus benghalensis, Polyalthia longifolia, Mangifera indica*	N	Beads, Fibers, Films, Fragments	SM, FM/Nile red staining, biochemical tests	Sambalbur, India	Sahu et al., (2024)
Lichens (foliose, fruticose) *Cladonia, Xanthoria*	N	Fibers, Fragments, PP, PET, PS, PES	SM, μFTIR-ATR microscope	Castelporzian, Arcinazzo, Rome, Italy	Taurozzi et al., (2024)
Moss *Hypnum cupressiforme*	N	Mcrofibers, PET, PP, PS, PVC	SM, FTIR-microscope	Campania, southern Italy	Capozzi et al., (2023a)
Moss *Hypnum cupressiforme*	T	Microfibers, PET, PVC, PE, PP	SM, Raman-microscope	Campania, southern Italy	Capozzi et al., (2023b)
Lichen (fruticose) *Pseudevernia furfuracea*					
Moss *Pseudoscleropodium purum*	N	Fibers, Fragments	SM	Central Italy	Jafarova et al., (2023a)
Lichen (fruticose) *Evernia prunastri,*					

Plant (leaflets) *Robinia pseudoacacia*	N	Microfibres, Rubber, PA, PES,	SM, µ-FTIR microscope	Siena, Italy	Jafarova et al., (2023b)
Lichen (fruticose) *Evernia prunastri*	T	Fibers, Fragments	SM, FM/Rose Bengal staining	Milan, Italy	Jafarova et al., (2022)
Lichen (foliose) *Flavoparmelia caperata*	N	Fibres, Fragments, PES, PE	SM/Rose Bengal staining, µ-Raman	Tuscany, Central Italy	Loppi et al., (2021)
Moss *Hylocomium splendens*	N	Microfibers	SM, FM/Rose Bengal staining, Raman	Lake catchments, Ireland	Roblin and Aherne, (2020)

ABS acrylonitrile butadiene styrene, *COPE* copolyester; *PA* polyamide, *PAA* polyacrylic acid, *PAN* polyacrylonitrile, *PE* polyethylene, *PES* polyester, *PET* polyethylene terephthalate, *PO* polyolefins, *PP* polypropylene, *PS* polystyrene, *PTEs* potentially toxic elements, *PUR* polyurethane, *PVC* polyvinyl chloride; NO_2 nitrogen dioxide, SO_2 sulphur dioxide, *SM* stereomicroscopy, *FM* fluorescence microscopy, *N* native sample, *T* transplant sample.

When all these new airborne microplastic biomonitoring studies are evaluated (Table 1), the following points can be drawn:

- Passive biological monitoring studies of human-induced airborne microplastic pollution conducted so far have shown that biological agents such as lichens and mosses, certain plants, pollens, and honeybees can be effectively used in urban and natural ecosystems.
- The morphology and ecological characteristics of biological monitoring organisms can influence the type (chemical and physical properties) and quantity of atmospheric microplastics they capture and accumulate.
- "Native" or "transplant" samples (lichens and mosses) can be preferred for monitoring airborne microplastisc depending on the ecosystem of the study area.
- Among epiphytic lichens, *Evernia prunastri, Xanthoria parietina*, and *Ramalina* spp., and among mosses, *Hypnum cupressiforme* and *Hylocomium splendens* are the most commonly used biological monitoring organisms.
- The selection of biomonitoring organisms and sampling method has a significant impact on determining the level of microplastic pollution in the air.
- Combined methods are preferred for the visual identification (morphological, quantitative) and chemical content of microplastics. Microscope-based visual techniques for imaging and counting, and measurement-based techniques for the identification of polymers and chemicals are used together in the same studies.

Lichens and mosses, which have been considered the best biological indicators of air pollutants such as toxic gases, trace metals, heavy metals, and

persistent organic pollutants since the late 1900s (Nimis et al., 2002), are similarly highlighted in new research as potentially serving the same function in terms of biomonitoring of atmospheric microplastics. However, currently, there are very few studies on lichen-based MP biomonitoring worldwide.

The first study using moss (*Hylocomium splendens*) as a biological indicator of human-generated microfiber release into the atmosphere was carried out by Roblin and Aherne, (2020) in Ireland. The first study to use an epiphytic foliose lichen (*Flavoparmelia caperata*) for the same purpose was conducted by Loppi et al., (2021) around a landfill in central Italy.

Unlike other persistent atmospheric pollutants, as Bargagli and Rota, (2026) also note, there are currently no standardized protocols or monitoring devices for airborne microplastics. Establishing and maintaining such atmospheric pollutant monitoring systems in urban and industrial settings would be both costly and limited to a small number of fixed points. Therefore, developing reliable, cost-effective, and readily implementable biological monitoring approaches to assess spatial and temporal trends in microplastic accumulation would be more advantageous. When widely available, these biological monitoring methods could also complement short-term or instantaneous measurements obtained from air sampling devices.

In selecting biomonitoring organisms, it is necessary to consider morphological and structural differences that vary depending on the species and habitat, as these can play a role in the retention and accumulation of pollutants (Garty, 2001). For example, morphological distinctions in lichens, show differences in surface area and roughness in thallus types belonging to crustose, foliose, or filamentous species, which can affect the amount of MP particles they will accumulate. Similarly, epiphytic (on tree trunks and branches) lichens, are preferred because they are less contaminated by pollutants settling on the ground compared to soil and rock lichens, and therefore better reflect the level of atmospheric MP pollution. Sampling protocols generally recommend collecting or transplanting lichen samples at a height > 1 m from the ground. Bargagli and Rota, (2026) argued that the higher MP concentrations in epigeic mosses compared to epiphytic lichens collected from the same location (native or transplanted samples) were based on morphological and physiological characteristics supporting MP accumulation in mosses. However, the fact that mosses are collected from the ground, as opposed to lichens which are usually sampled from the high trunks and branches of trees, may also have increased the amount of MPs deposited in mosses from the atmosphere.

Lichens and mosses, known for their high potential for trapping pollutants from the atmosphere, are widely used as outdoor biomonitors of atmospheric pollution, including toxic elements and, in recent years, microplastics (Çobanoğlu Özyiğitoğlu, 2020). Although very few studies have been conducted on indoor

air quality and its effects (Rizzi et al., 2023), biological monitoring based on lichens and mosses can also provide important data on indoor MP concentrations (Grifoni et al., 2025). However, for now, information on indoor microplastics is still very limited.

The answer to the question of whether biological monitoring of MP accumulation in organisms reflects the actual concentration in the air is unclear. However, most moss and lichen biomonitoring studies assume the gradual biological accumulation of microplastics, and estimates of MP concentrations in average annual atmospheric deposition can provide valuable information.

Comparative studies suggest that moss-bags are more effective at trapping and deposition of the smallest anthropogenic microfibers compared to lichens in the same area. Monitoring studies in urban areas and around landfills have reported that epiphytic lichens accumulate high concentrations of microplastics. However, it is argued that the interaction between lichen thalli and microplastics is not sufficiently understood, and therefore the levels of anthropogenic fibers and plastic fragments captured and retained by lichens do not fully reflect their levels in atmospheric accumulation (Bargagli and Rota, 2026). Mosses, on the other hand, are believed to accumulate much higher concentrations of microplastics due to their biological structure, and therefore, their use in both active and passive biological monitoring research is recommended.

Conclusions and Recommendations

Today, the increasing population and the resulting single-yield increase have caused microplastic rows to be at the top of the list of environmental problems. Plastic materials pose a threat to the environment, no matter how easy they are to use. MPs that join the food chain are found in the structure of almost all living things. Airborne microplastics have emerged as a distinct and increasingly important component of global plastic pollution, functioning as an efficient medium for the redistribution of plastic particles across environmental compartments. Unlike localized plastic contamination, airborne microplastics enable transboundary transport driven by meteorological processes, leading to their deposition in remote terrestrial and aquatic ecosystems. The diversity in particle size, morphology, polymer composition, and surface chemistry strongly influences their transport behavior and interaction with co-occurring chemical pollutants. Microplastics are widespread and ubiquitous in all terrestrial ecosystems via atmospheric transport, and their concentrations in bulk or wet atmospheric deposition can generally be detected in samples collected away from urban and industrial areas.

General conclusions regarding atmospheric microplastics can be summarized as follows:

- Microplastics are ubiquitous because they are small and lightweight.

- They are found at almost every stage of the food chain.
- Determining the fine details of microplastic dimensions is difficult. Therefore, it needs to be developed through new nanoplastic research.
- Methodologies related to microplastic detection and their interaction with the environment should continue to be developed using analytical and biological approaches.

Evidence compiled in this review demonstrates that atmospheric microplastics are capable of concentrating hazardous substances and facilitating their entry into biological systems through inhalation and environmental deposition. Despite growing detection frequencies, the toxicological implications of chronic exposure particularly involving nanoplastics remain insufficiently characterized, underscoring the need for deeper mechanistic understanding. Furthermore, inconsistencies in sampling strategies and analytical workflows continue to hinder the establishment of reliable global datasets.

To advance research in this field, future studies should focus on the standardization of atmospheric microplastic monitoring, including unified protocols for sample collection, pretreatment, and polymer identification. Experimental investigations addressing dose response relationships, bioavailability, and cellular level impacts of inhaled micro and nanoplastics are critically required. The integration of biomonitoring organisms with high resolution analytical techniques may enhance the detection sensitivity and ecological relevance of atmospheric microplastic assessments. From a regulatory perspective, mitigation efforts should emphasize source control, particularly targeting emissions from synthetic textiles, traffic related abrasion, and industrial activities. Incorporating atmospheric microplastics into air quality regulations and environmental risk assessment frameworks will be essential for developing effective strategies to reduce their environmental and public health impacts.

References

Abbasi, S., Keshavarzi, B., Moore, F., et al. (2017). Investigation of micro rubbers, microplastics and heavy metals in street dust: a study in Bushehr city, Iran. *Environ Earth Sci,* 76, 798. https://doi.org/10.1007/s12665-017-7137-0

Avella, M., Avolio, R., Cocca, M., Di Pace, E., Errico, M.E. & Gentile, G. (2019). Focus point on microplastic pollution: Assessment, effects and mitigation strategies. *European Physical Journal Plus*, 134, 1–2. https://doi.org/10.1140/epjp/i2019-12452-2

Bargagli, R. & Rota, E. (2026). Potential role of mosses in evaluating airborne microplastic deposition in terrestrial ecosystems. *Journal of Xenobiotics*, 16:1, 21. https://doi.org/10.3390/jox16010021

Baroudi, F., Al Alam, J., Fajloun, Z. & Millet, M. (2020). Snail as sentinel organism for monitoring environmental pollution: A review. *Ecological Indicators*, 113, 106240. https://doi.org/10.1016/j.ecolind.2020.106240

Basile, C.S., Jafarova, M., Aherne, J., Wyonch, J., Castiglione, M.R., Spanò, C. & Paoli, L. (2025). Greenspaces can reduce the level of airborne microplastic contamination in urban environments: Evidence from a lichen biomonitoring study. *Environmental Research*, 122334. https://doi.org/10.1016/j.envres.2025.122334

Bazzazpour, S., Yousefi, M., Mohseni-Bandpei, A., Hopke, P.K., Torabbeigi, M., Kermani, M. & Shahsavani, A. (2025). Insights into the simultaneous analysis of airborne microplastic and microrubber particles by off-line pyrolysis GC/MS. *Journal of Aerosol Science*, 106732. https://doi.org/10.1016/j.jaerosci.2025.106732

Beckingham, B., Apintiloaiei, A., Moore, C. & Brandes, J. (2023). Hot or not: systematic review and laboratory evaluation of the hot needle test for microplastic identification. *Microplastics and Nanoplastics*, 3(8). https://doi.org/10.1186/s43591-023-00056-4

Bhardwaj, L.K., Rath, P., Yadav, P. & Gupta, U. (2024). Microplastic contamination, an emerging threat to the freshwater environment: a systematic review. *Environmental Systems Research*, 13(8). https://doi.org/10.1186/s40068-024-00338-7

Bhattacharjee, S., Ghosh, P.K., Podder, A., Mandal, B. & Mukherjee, A. (2025). Urban trees as natural interceptors for aerial microplastics: Mechanisms, influencing factors, and selection of tree types for mitigation. *Science of the Total Environment*, 992, 179950. https://doi.org/10.1016/j.scitotenv.2025.179950

Boamponsem, L.K., Adam, J.I., Dampare, S.B., Nyarko, B.J.B. & Essumang, D.K. (2010). Assessment of atmospheric heavy metal deposition in the Tarkwa

gold mining area of Ghana using epiphytic lichens. *Nuclear Instruments and Methods in Physics Research Section B: Beam Interactions with Materials and Atoms*, 268(9),1492–1501. https://doi.org/10.1016/j.nimb.2010.01.007

Campanale, C., Massarelli, C., Savino, I., Locaputo, V. & Uricchio, V.F. (2020). A detailed review study on potential effects of microplastics and additives of concern on human health. *International Journal of Environmental Research and Public Health*, 17(4),1212. https://doi.org/10.3390/ijerph17041212

Capozzi, F., Granata, A., Gaglione, A., Gargiulo, T., Rallo, A., Marino, F. & Giordano, S. (2024). Sequential extraction of anthropogenic microfibers from the leaves of *Pittosporum tobira*. *Chemosphere*, 367, 143628. https://doi.org/10.1016/j.chemosphere.2024.143628

Capozzi, F., Sorrentino, M.C., Cascone, E., Iuliano, M., De Tommaso, G., Granata, A., Giordano, S. & Spagnuolo, V. (2023a). Biomonitoring of airborne microplastic deposition in semi-natural and rural sites using the moss *Hypnum cupressiforme*. *Plants*, 12, 977. https://doi.org/10.3390/plants12050977

Capozzi, F., Sorrentino, M.C., Granata, A., Vergara, A., Alberico, M., Rossi, M., Spagnuolo, V. & Giordano, S. (2023b). Optimizing moss and lichen transplants as biomonitors of airborne anthropogenic microfibers. *Biology,* 12, 1278. https://doi.org/10.3390/biology12101278

Carriera, F., Di Fiore, C. & Avino, P. (2024). Occurrence of microplastics in the atmosphere: An overview on sources, analytical challenges, and human health effects. *Atmosphere*, 15(7), 863. https://doi.org/10.3390/atmos15070863

Chouchene, F., Masmoudi, F., Baaziz, A., Maatouk & F., Ghedira, H. (2023). Clinical status and assessment of caries on first permanent molars in a group of 6- to 13-year-old Tunisian school children. *Clinical and Experimental Dental Research,* 9(1), 240–248. https://doi.org/10.1002/cre2.676

Cortés-Corrales, L., Flores, J.J., Rosa, A., Van der Steen, J.J., Vejsnæs, F., Roessink, I. & Fernández-Alba, A.R. (2024). Evaluation of microplastic pollution using bee colonies: An exploration of various sampling methodologies. *Environmental Pollution*, 350, 124046. https://doi.org/10.1016/j.envpol.2024.124046

Cox, K.D., Covernton, G.A., Davies, H.L., Dower, J.F., Juanes, F. & Dudas, S.E. (2019). Human consumption of microplastics. *Environmental Science & Technology*, 53(12), 7068–7074. https://doi.org/10.1021/acs.est.9b01517

Çobanoğlu, G. & Özen, E. (2024). Detection of atmospheric microplastics accumulated in *Xanthoria parietina*: A lichen biomonitoring study on the Asian side of Istanbul. *International Journal of Environmental Research,* 18(4), 65. https://doi.org/10.1007/s41742-024-00596-4

Çobanoğlu Özyiğitoğlu, G. (2020). Use of Lichens in Biological Monitoring of Air Quality. In V. Shukla Dr. N. Kumar (Eds.) *Environmental Concerns and Sustainable Development* - Volume 1: Air, Water and Energy Resources. Springer Nature Singapore, pp. 61–95. https://doi.org/10.1007/978-981-13-5889-0_3

Dris, R., Gasperi, J., Rocher, V., Saad, M., Renault, N. & Tassin, B. (2015). Microplastic contamination in an urban area: A case study in Greater Paris. *Environmental Chemistry*, 12, 592–599. https://doi.org/10.1071/EN14167

Du, J., Zhou, Q., Li, H., Xu, S., Wang, C., Fu, L. & Tang, J. (2021). Environmental distribution, transport and ecotoxicity of microplastics: A review. *Journal of Applied Toxicology*, 41(1), 52–64. https://doi.org/10.1002/jat.4034

Dumont, G., Rodrigues, A., Velimirovic, M., Lievens, S., Jordens, J., Focant, J.F. & Stefanuto, P.H. (2025). Microplastic and nanoplastic analysis: From pyrolysis gas chromatography–mass spectrometry to pyrolysis two-dimensional gas chromatography–mass spectrometry—A critical review. *Journal of Separation Science*, 48(10), e70287. https://doi.org/10.1002/jssc.70287

Eerkes-Medrano, D., Thompson, R.C. & Aldridge, D.C. (2015). Microplastics in freshwater systems: A review of the emerging threats, identification of knowledge gaps and prioritisation of research needs. *Water Research*, 75, 63–82. https://doi.org/10.1016/j.watres.2015.02.012

Gambino, I., Malitesta, C., Bagordo, F., Grassi, T., Panico, A., Fraissinet, S. & De Benedetto, G.E. (2023). Characterization of microplastics in water bottled in different packaging by Raman spectroscopy. *Environmental Science: Water Research & Technology*, 9(12), 3391–3397. https://doi.org/10.1039/D3EW00197K

Garty, J. (2001). Biomonitoring atmospheric heavy metals with lichens: theory and application. *Critical Reviews in Plant Sciences*, 20(4), 309–371. https://doi.org/10.1080/20013591099254

Geng, G., Zheng, Y., Zhang, Q., Xue, T., Zhao, H., Tong, D. & Davis, S.J. (2021). Drivers of PM2.5 air pollution deaths in China 2002–2017. *Nature Geoscience*, 14(9), 645–650. https://doi.org/10.1038/s41561-021-00792-3

Gigault, J., ter Halle, A., Baudrimont, M., Pascal, P. Y., Gauffre, F., Phi, T. L., El Hadri, H., Grassl, B. & Reynaud, S. (2018). Current opinion: What is a nanoplastic?. *Environmental Pollution*, 235, 1030-1034. https://doi.org/10.1016/j.envpol.2018.01.024

Gollo, M.S., Rodríguez, J.M., Pighín, A.F., Villagra, E., Ferro, J. & Gomez, J.J. (2023). Micro y mesoplásticos en la infusión “té de la piedra” [Micro and mesoplastics in “stone tea” infusion]. Glalia. *Revista Electrónica del Grupo Latinoamericano de Liquenólogos*, 9(1), 35–44.

Gollo, M.S., Villagra, E.L.B. & Gomez, J.J. (2025). Atmospheric microplastic accumulation in *Ramalina celastri* (Sprengel) Krog & Swinscow Thalli: a transplant study across different levels of urbanization. *Folia Oecologica*, 52(1), 62–69. https://doi.org/10.2478/foecol-2025-0007

Gouin, T., Ellis-Hutchings, R., Hampton, L.M.T., Lemieux, L.C. & Wright, S.L. (2022). Screening and prioritization of nano- and microplastic particle toxicity studies for evaluating human health risks: Development and application of a toxicity study assessment tool. *Microplastics and Nanoplastics*, 2, 2. https://doi.org/10.1186/s43591-021-00023-x

Grifoni, L., Jafarova, M., La Colla, N.S., Aherne, J., Raulli, A. & Loppi, S. (2025). Comparison of Lichen and Moss Transplants for Monitoring the Deposition of Airborne Microfibers. *Sustainability*, 17 537. https://doi.org/10.3390/su17020537

Han, I., Lee, C., Belchez, C., Shipper, A.G. & Wiens, K.E. (2024). Microplastics in urban ambient air: A rapid review of active sampling and analytical methods for human risk assessment. *Environments*, 11(11), 256. https://doi.org/10.3390/environments11110256

Hanif, M.A., Ibrahim, N., Azhari, A.W., Dahalan, F.A., Hasan, M., Lutpi, N.A., Othman, N. & Isa, M.H. (2026). Natural-based coagulants/flocculants for microplastics and nanoplastics removal via coagulation–flocculation: a systematic review. *International Journal of Environmental Science and Technology*, 23(4), 313. https://doi.org/10.1007/s13762-026-07100-9

Harner, T., Su, K., Genualdi, S., Karpowicz, J., Ahrens, L., Mihele, C. & Narayan, J. (2013). Calibration and application of PUF disk passive air samplers for tracking polycyclic aromatic compounds (PACs). *Atmospheric Environment*, 75, 123–128. https://doi.org/10.1016/j.atmosenv.2013.04.012

Ivleva, N.P. (2021). Chemical analysis of microplastics and nanoplastics: Challenges, advanced methods, and perspectives. *Chemical Reviews*, 121(19), 11886–11936. https://doi.org/10.1021/acs.chemrev.1c00178

Jafarova, M. & Aherne, J. (2026). In search of an optimal moss transplant biomonitor for airborne microplastics: Moss cubes. *Environmental Pollution*, 388, 127391. https://doi.org/10.1016/j.envpol.2025.127391

Jafarova, M., Aherne, J. & Loppi, S. (2025). Regional sources drive atmospheric microplastic deposition at rural background sites. *Environmental Research*, 285, 122663. https://doi.org/10.1016/j.envres.2025.122663

Jafarova, M., Contardo, T., Aherne, J. & Loppi, S. (2022). Lichen biomonitoring of airborne microplastics in Milan (N Italy). *Biology*, 11(12), 1815. https://doi.org/10.3390/biology11121815

Jafarova, M., Grifoni, L., Aherne, J. & Loppi, S. (2023a). Comparison of lichens and mosses as biomonitors of airborne microplastics. *Atmosphere*, 14(6), 1007. https://doi.org/10.3390/atmos14061007

Jafarova, M., Grifoni, L., Renzi, M., Bentivoglio, T., Anselmi, S., Winkler, A. & Loppi, S. (2023b). *Robinia pseudoacacia* L. (black locust) leaflets as biomonitors of airborne microplastics. *Biology*, 12(12), 1456. https://doi.org/10.3390/biology12121456

Jimenez-Skrzypek, G., Hernandez-Sanchez, C., Ortega-Zamora, C., González-Sálamo, J., González-Curbelo, M.Á. & Hernandez-Borges, J. (2021). Microplastic-adsorbed organic contaminants: Analytical methods and occurrence. *TrAC Trends in Analytical Chemistry*, 136, 116186. https://doi.org/10.1016/j.trac.2021.116186

Khodabakhshloo, N., Abbasi, S., Oleszczuk, P., & Turner, A. (2024). Biomonitoring of airborne microplastics and microrubbers in Shiraz, Iran, using lichens and moss. *Environmental Geochemistry and Health*, 46(7), 244. https://doi.org/10.1007/s10653-024-01977-6

Kocakaya, Z., Yılmaz, E., Duman, F., Kocakaya, M. & Pekdemir, S. (2024). Biomonitoring of Yozgat Çamlık National Park's anthropogenic microfiber pollution: A comprehensive analysis of lichen-supported air quality assessment and microplastic composition insights. *Kastamonu University Journal of Forestry Faculty*, 25(3), 306-322 https://doi.org/10.21203/rs.3.rs-4163112/v1

Krystek, P., Koelmans, A.A., Quik, J., Swart, E., Krause, S., Legler, J., Aardema, H. & Vethaak, D. (2025). Micro- and nanoplastics in soil: New insights, knowledge gaps and challenges. *Chemosphere*, 373, 144117. https://doi.org/10.1016/j.chemosphere.2025.144117

Lassen, C., Hansen, S.F., Magnusson, K., Hartmann, N.B., Jensen, P.R. & Nielsen, T.G. (2022). Microplastics: Occurrence, effects and sources of releases to the environment in Denmark (Environmental Project No. 1993). *Danish Environmental Protection Agency*.

Lee, J.Y., Chia, R.W., Veerasingam, S., Uddin, S., Jeon, W.H., Moon, H.S. & Lee, J. (2024). A comprehensive review of urban microplastic pollution sources, environment and human health impacts, and regulatory efforts. *Science of the Total Environment*, 946, 174297. https://doi.org/10.1016/j.scitotenv.2024.174297

Li, R., Wontor, K., Olubusoye, B.S., Brewer, J.S. & Cizdziel, J.V. (2025). Direct μ-FTIR analysis of microplastics deposited on silicon in indoor air environments. *npj Emerging Contaminants*, 1(1), 11. https://doi.org/10.1038/s44454-025-00009-x

Liu, P., Shao, L., Guo, Z., Zhang, Y., Cao, Y., Ma, X. & Morawska, L. (2025). Physicochemical characteristics of airborne microplastics of a typical coastal city in the Yangtze River Delta Region, China. *Journal of Environmental Sciences*, 148, 602–613. https://doi.org/10.1016/j.jes.2023.09.027

Loppi, S., Roblin, B., Paoli, L. & Aherne, J. (2021). Accumulation of airborne microplastics in lichens from a landfill dumping site (Italy). *Scientific Reports*, 11(1), 4564. https://doi.org/10.1038/s41598-021-84251-4

Markert, B.A., Breure, A.M. & Zechmeister, H.G. (Eds.). (2003). *Bioindicators and biomonitors*, (Vol. 6), Elsevier.

Niccolai, E., Colzi, I., Amedei, A. (2023). Adverse effects of micro- and nanoplastics on humans and the environment. *International Journal of Molecular Sciences*, 24, 15822. https://doi.org/10.3390/ijms242115822

Niida, Y., Fujii, Y., Inatsugi, Y. & Takenaka, N. (2026). Quantifying UV-driven aging of sub-10 μm airborne microplastics with high-resolution μFTIR-ATR imaging. *Atmosphere*, 17(2), 146 https://doi.org/10.3390/atmos17020146

Nimis, P.L., Scheidegger, C. & Wolseley, P. (2002). Monitoring with lichens—Monitoring lichens. *Springer Science-*, Business Media Dordrecht.

Nistal, A., Coviella, C. & Gomez, J. (2025). Methodological predicament: Distinguishing between the accumulated and deposited microplastics in lichen thalli. *Environmental Monitoring and Contaminants Research*, 5, 76–82. https://doi.org/10.5985/emcr.20240030

Oleksiuk, K., Krupa-Kotara, K., Wypych-Ślusarska, A., Głogowska-Ligus, J., Spychała, A. & Słowiński, J. (2022). Microplastic food and water: Current knowledge and awareness of consumers. *Nutrients*, 14(22), 4857. https://doi.org/10.3390/nu14224857

Paddison, L. (2023). The world can cut plastic pollution by 80% by 2040, the UN says. Here's how. *CNN*, 16 May 2023 https://www.cnn.com/2023/05/16/world/plastic-pollution-unep-climate-intl/index.html

Parmar, T.K., Rawtani, D. & Agrawal, Y.K. (2016). Bioindicators: the natural indicator of environmental pollution. *Frontiers in Life Science*, 9(2), 110–118. https://doi.org/10.1080/21553769.2016.1162753

Parvez, M.S., Czédli, H., Hoque, M.I., Rahman, M.M., Anwar, A., Uddin, A.H.M.M. & Simon, E. (2024). Accumulation of microplastics and potentially toxic elements in plant leaves along an urbanization gradient in Bangladesh. *Toxics*, 12(12), 848. https://doi.org/10.3390/toxics12120848

Pekmezekmek, A. (2022). Mikroplastiklerin canlılara etkileri. *Arşiv Kaynak Tarama Dergisi*, 31(2), 94–98. https://doi.org/10.17827/aktd.1058792

Queiroz, S. (2023). Brazilian researchers find 'terrifying' plastic rocks on remote island. *Reuters* https://www.reuters.com/lifestyle/science/brazilianresearchers-find-terrifying-plastic-rocks-remote-island-2023-03-15

Rizzi, G., Modenesi, P. & Giordani, P. (2023). Lichens and mosses as indoor air pollution biomonitors: A comprehensive review. *Biology*, 12(9), 1248. https://doi.org/10.3390/toxics12120848

Roblin, B. & Aherne, J. (2020). Moss as a biomonitor for the atmospheric deposition of anthropogenic microfibres. *Science of the Total Environment*, 715, 136973. https://doi.org/10.1016/j.scitotenv.2020.136973

Sahu, C., Dash, P.K. & Basti, S. (2024). Accumulation of airborne microplastics and its impact on pollution tolerance ability of plants in an urban setup in India. *Air Quality, Atmosphere & Health*, 1–13. https://doi.org/10.1007/s11869-024-01639-7

Schymanski, D., Goldbeck, C., Humpf, H.U. & Fürst, P. (2018). Analysis of microplastics in water by micro-Raman spectroscopy: Release of plastic particles from different packaging into mineral water. *Water Research*, 129, 154-162. https://doi.org/10.1016/j.watres.2017.11.011

Shao, L., Li, Y., Jones, T., Santosh, M., Liu, P., Zhang, M. & BéruBé, K. (2022). Airborne microplastics: A review of current perspectives and environmental implications. *Journal of Cleaner Production*, 347, 131048. https://doi.org/10.1016/j.jclepro.2022.131048

Shu, J., Hou, S., Cao, H., Liu, X., Cai, W., Zeng, Y. & Chen, Z. (2025). Spread performance and underlying mechanisms of pathogenic bacteria and antibiotic resistance genes adhered on microplastics in the sediments of different urban water bodies. *Environmental Pollution*, 126758. https://doi.org/10.1016/j.envpol.2025.126758

Silva, A.L.P., Silva, S.A., Duarte, A., Barceló, D. & Rocha-Santos, T. (2022). Analytical methodologies used for screening micro(nano)plastics in (eco)toxicity tests. *Green Analytical Chemistry*, 3, 100037. https://doi.org/10.1016/j.greeac.2022.100037

Solórzano, L.A., Gavilanes, D., Cadena, F., Irusta, L., González, A. & Aldas, M. (2025). A review of the sampling, analysis, and identification techniques of microplastics in the air: Insights into PM2.5 and PM10. *Polymers*, 17(22), 3045. https://doi.org/10.3390/polym17223045

Soltani, N.S., Taylor, M.P., & Wilson, S.P. (2021). Quantification and exposure assessment of microplastics in Australian indoor house dust. *Environmental Pollution*, 283, 117064. https://doi.org/10.1016/j.envpol.2021.117064

Sripada, K., Wierzbicka, A., Abass, K., Grimalt, J.O., Erbe, A., Röllin, H.B., Weihe, P., Díaz, G.J., Singh, R.R., Visnes, T., Rautio, A., Odland, J.Ø. & Wagner,

M. (2022). A children's health perspective on nano- and microplastics. *Environmental Health Perspectives*, 130(1), 015001. https://doi.org/10.1289/EHP9086

Swinnerton, S., Su, J. & Tsai, C.S. (2024). The emission and physicochemical properties of airborne microplastics and nanoplastics generated during the mechanical recycling of plastic via shredding. *Scientific Reports*, 14(1), 24755. https://doi.org/10.1038/s41598-024-73775-0

Taurozzi, D., Gallitelli, L., Cesarini, G., Romano, S., Orsini, M. & Scalici, M. (2024). Passive biomonitoring of airborne microplastics using lichens: A comparison between urban, natural and protected environments. *Environment International*, 187, 108707. https://doi.org/10.1016/j.envint.2024.108707

Umurhan, Y., Songsart-Power, M., Limbu, T.B. & Phan, T. (2025). Applications of Raman spectroscopy for microplastic detection and characterization: A comprehensive spectral reference. *Environmental Science and Pollution Research*, 025, 1–48. https://doi.org/10.1007/s11356-025-37224-3

United States Environmental Protection Agency (2015). Summary of expert discussion forum on possible human health risks from microplastics in the marine environment. https://www.epa.gov

Van Wezel, A., Caris, I. & Kools, S.A. (2016). Release of primary microplastics from consumer products to wastewater in the Netherlands. *Environmental Toxicology and Chemistry*, 35(7), 1627–1631. https://doi.org/10.1002/etc.3316

Veerasingam, S., Ranjani, M., Venkatachalapathy, R., Bagaev, A., Mukhanov, V., Litvinyuk, D., Mugilarasan, M., Gurumoorthi, K., Guganathan, L., Aboobacker, V.M. & Vethamony, P. (2021). Contributions of Fourier transform infrared spectroscopy in microplastic pollution research: A review. *Critical Reviews in Environmental Science and Technology*, 51(22), 2681–2743. https://doi.org/10.1080/10643389.2020.1807450

Vieira, Y., Lima, E.C., Foletto, E.L. & Dotto, G.L. (2021). Microplastics physicochemical properties, specific adsorption modeling and their interaction with pharmaceuticals and other emerging contaminants. *Science of the Total Environment*, 753, 141981. https://doi.org/10.1016/j.scitotenv.2020.141981

Yao, Y., Glamoclija, M., Murphy, A. E. & Gao, Y. (2022). Characterization of microplastics in indoor and ambient air in northern New Jersey. *Environmental Research*, 207, 112142. https://doi.org/10.1016/j.envres.2021.112142

Wang, X., Liu, K., Zhu, L., Li, C., Song, Z. & Li, D. (2021). Efficient transport of atmospheric microplastics onto the continent via the East Asian summer

monsoon. *Journal of Hazardous Materials*, 414(12)5477. https://doi.org/10.1016/j.jhazmat.2021.125477

Wright, S.L., Ulke, J., Font, A., Chan, K.L.A. & Kelly, F.J. (2020). Atmospheric microplastic deposition in an urban environment and an evaluation of transport. *Environment International*, 136, 105411. https://doi.org/10.1016/j.envint.2019.105411

WWF (2019). Solving plastic pollution through accountability. *WWF International*. (Accessed: March 30, 2026). http://d2ouvy59p0dg6k.cloudfront.net/downloads/solving_plastic_pollution_through_accountability_eng_singles.pdf

Zhang, Q., Xu, E.G., Li, J., Chen, Q., Ma, L., Zeng, E.Y. & Shi, H. (2020). A review of microplastics in table salt, drinking water, and air: Direct human exposure. *Environmental Science & Technology*, 54(7), 3740–3751. https://pubs.acs.org/doi/10.1021/acs.est.9b04535?goto=supporting-info

Zhang, Y., Slade, J. H., Ault, A.P. & Chan, A.W. (2025). An atmospheric chemistry perspective on airborne micro- and nanoplastic particles. *Environmental Science & Technology*, 59(16), 7810–7819. https://doi.org/10.1021/acs.est.5c03264

Zhao, X., Zhou, Y., Liang, C., Song, J., Yu, S., Liao, G. & Wu, C. (2023). Airborne microplastics: Occurrence, sources, fate, risks and mitigation. *Science of the Total Environment*, 858, 159943. https://doi.org/10.1016/j.scitotenv.2022.159943

Zhu, G., Yue, K., Ni, X., Yuan, C. & Wu, F. (2023). The types of microplastics, heavy metals, and adsorption environments control the microplastic adsorption capacity of heavy metals. *Environmental Science and Pollution Research*, 30(33), 80807–80816. https://doi.org/10.1007/s11356-023-28131-6

Zimmermann, L., Bartosova, Z., Braun, K., Oehlmann, J., Völker, C. & Wagner, M. (2021). Plastic products leach chemicals that induce in vitro toxicity under realistic use conditions. *Environmental Science & Technology*, 55(17), 11814–11823. https://doi.org/10.1021/acs.est.1c01103

CHAPTER 3

The Therapeutic Potential of Venoms Across The Animal Kingdom with a Focus on Insects

Sadi Arda Köse[1]
Aylin Er[2]
Pınar Güner[3]

[1] Balıkesir University, Faculty of Arts and Sciences, Department of Biology, Balikesir, Türkiye, ORCID: 0009-0008-5188-9678
[2] Prof. Dr., Balıkesir University, Faculty of Arts and Sciences, Department of Biology, Balikesir, Türkiye, ORCID: 0000-0002-8108-8950
[3] Asst. Prof., Balıkesir University, Faculty of Arts and Sciences, Department of Biology, Balikesir, Türkiye, ORCID: 0000-0001-6922-7009

1. Introduction

For much of human history, the lethality and danger of venomous animals had been the primary focus. However, the challenge of turning these natural toxins into valuable resources has become highly meaningful in today's scientific era. Animal venoms have evolved primarily for predation and defense, representing exceptionally rich natural reservoirs of bioactive molecules with a broad range of molecular targets. Recent research has revealed that these compounds offer significant therapeutic benefits for human health (Bose et al., 2026; Utkin et al., 2017). Consequently, the study of venoms provides critical insights into diverse biological disciplines, such as pharmacology, immunology, and structural biology (Casewell et al., 2012). As highly complex and species-specific mixtures of proteins, peptides, and other compounds, their varied pharmacological activities and diverse structures make them highly valuable for developing novel therapeutics and research tools (Román et al., 2022; Anal et al., 2025).

Building on this wide range of potential, peptides and proteins derived from animal venoms show many different biological activities, including analgesic, anticoagulant, antihypertensive, anticancer, antimicrobial, and neuroprotective effects (Kim et al., 2025). In this context, insect venoms are receiving increasing attention for their potential therapeutic applications. For example, recent studies have shown that certain toxins isolated from bee venom have strong potential as anti-tumor agents (Rady et al., 2017). To better understand and use this molecular diversity, modern venom research increasingly relies on "venomics." By combining genomics, transcriptomics, and proteomics, venomics provides valuable tools for studying the composition and variation of venoms, as well as the structural complexity of toxins across different species (Modahl et al., 2019).

Despite their great molecular diversity, insect venoms are still less studied in pharmacological research than those of other venomous animals. With recent advances in technology, this review aims to summarize the therapeutic potential of venoms across the animal kingdom, with a particular focus on how modern research on insect venoms is contributing to the development of new treatments for various human diseases.

2. Animal Venoms in Modern Medicine

Animal venoms and poisons are complex mixtures of proteins, peptides, and neurotransmitters. They serve as powerful tools for hunting and self-defense by causing serious harm to the body's normal functions (De Castro Figueiredo Bordon et al., 2020). Because of this, these chemical mixtures represent a large and mostly untapped source for new drug development. Different evolutionary groups from invertebrates like bees, spiders, and jellyfish to vertebrates like snakes have developed these venom systems over time. Through this process, they have produced rich collections of highly powerful compounds that target specific receptors, making them especially suitable for drug research and

development (Escoubas & King, 2009). Venom systems have evolved independently more than 100 times across at least eight different animal groups, which is a striking example of convergent evolution (Figure 1). In these various species, protein and peptide-based toxins developed from harmless ancestral molecules. Many unrelated lineages separately came to use similar molecular structures for delivering venom (Schendel et al., 2019).

The main active components of animal venoms are proteins and peptides, which are usually held stable by multiple disulfide bridges. The amount of this cross linking differs greatly between animal groups. For example, cone snail toxins generally have 10 to 40 cysteine residues, while scorpion and snake toxins have 40 to 80. These differences, shaped over long periods of natural selection and coevolution, have created an amazing variety of peptide structures among venoms from different lineages (Figure 2) (Chen et al., 2018).

So far, 11 drugs derived from toxins have made it to the market. Most of these come from snake venoms (captopril, enalapril, tirofiban, eptifibatide, batroxobin, and cobratide). Others come from lizards (exenatide and lixisenatide), leeches (bivalirudin and desirudin), and cone snails (ziconotide). As for how they are made, batroxobin and cobratide are purified directly as natural compounds, and desirudin is made using recombinant techniques, while the rest of the approved drugs are made through artificial synthesis (De Castro Figueiredo Bordon et al., 2020).

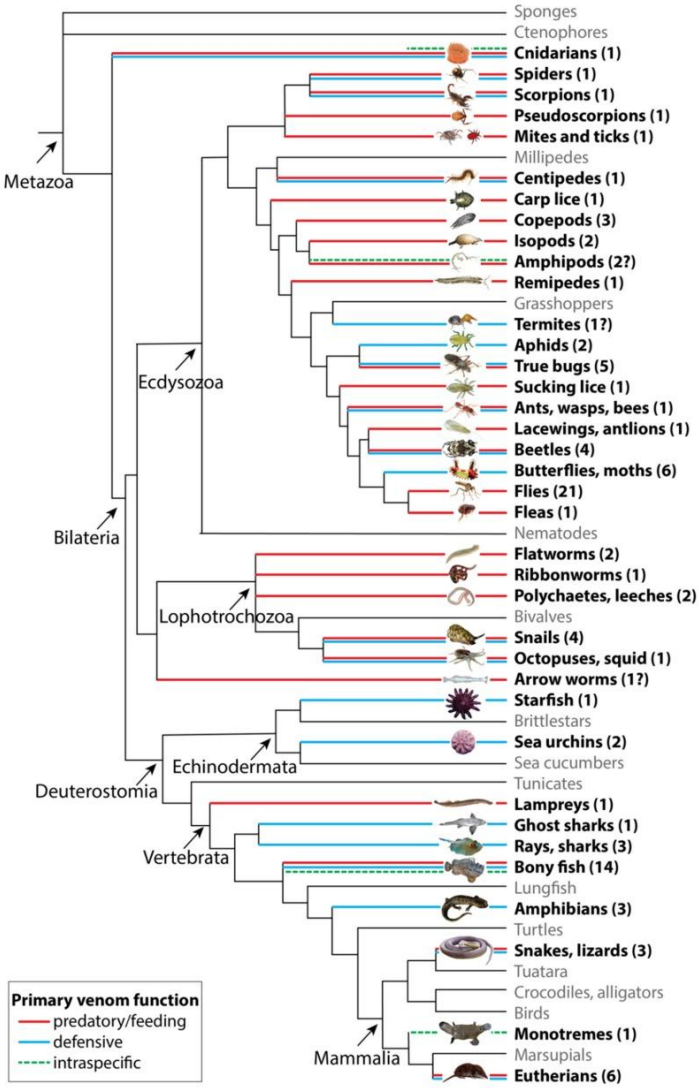


Figure 1. Taxonomic diversity and the main primary functions of venom. Adapted from Schendel et al. (2019).

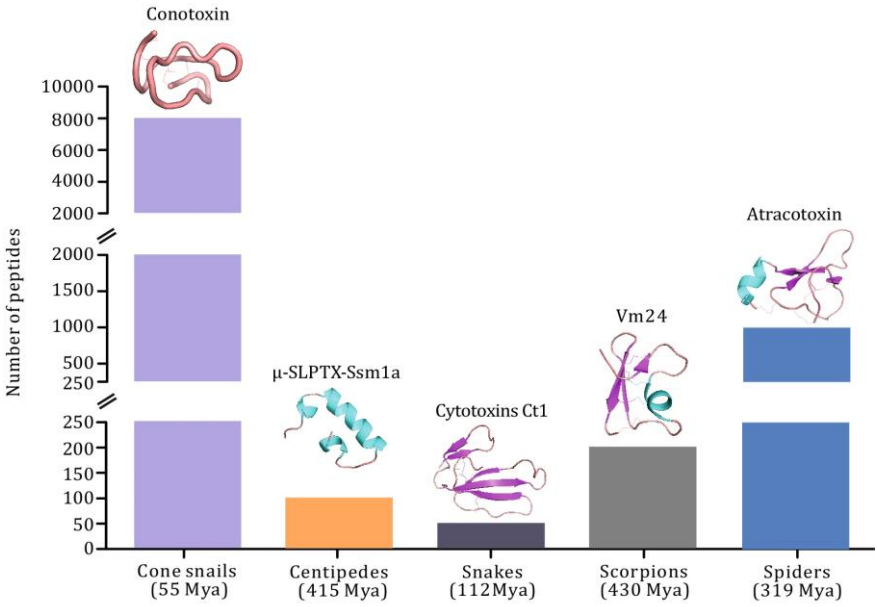


Figure 2. Estimated number of venom peptides and representative three-dimensional structural models across major venomous lineages. Adapted from Chen et al. (2018).

2.1. Snake Venoms

Approved in 1981, Captopril represents a landmark achievement in venom-based drug discovery as the first angiotensin-converting enzyme (ACE) inhibitor. Rather than being extracted directly from the animal, Captopril is a synthetically manufactured therapeutic whose chemical design was modeled after a bradykinin-potentiating peptide originally discovered in the venom of the Brazilian pit viper, *Bothrops jararaca* (Messadi, 2023). Each snake species has its own unique venom, with different amounts of toxic and non-toxic compounds. The makeup of the venom changes within and between species depending on age, where they live, sex, and environment (Waheed et al., 2017). However, besides their deadly and harmful effects, people have known since ancient times that venoms can also heal. This is why the snake became a symbol of pharmacy and medicine (Oliveira et al., 2022). Snake venoms show a wide range of biological activities. These activities are important for studying the pharmacological and medical potential of snake venoms. Today, thanks to technological developments and the steady progress of science, researchers have managed to turn these life-threatening toxins into life-saving therapeutic agents. For a long time, components of snake venom have shown great promise in developing lead compounds for new drugs. New drugs are constantly being developed, from treatments for blood clotting disorders and bleeding to anti-cancer agents (Waheed et al., 2017). Currently, six drugs based on snake venom have been approved by the FDA and are used in procedures and conditions such as plastic

and abdominal surgery, high blood pressure, heart attacks, and strokes (Figure 3) (El-Aziz et al., 2019).

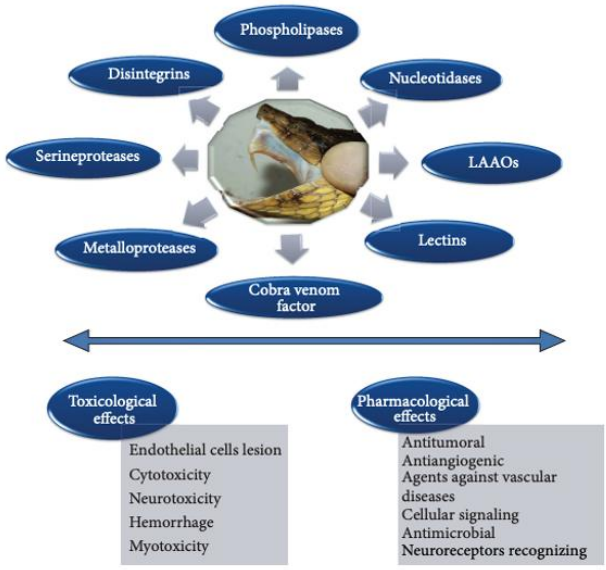


Figure 3. Broad spectrum of activity and applications of snake venom properties. Adapted from Calderon et al. (2014).

Snake venoms are usually a complex mix of proteins that carry out enzymatic activity, typically made up of 20 to 100 components (Oliveira et al., 2022), with molecular weights ranging from 6 to 100 kD. Along with these proteins, smaller polypeptides are also present, and these are the actual deadly compounds (Gold et al., 2002). The makeup of venom varies a lot between species and can even differ within the same species. Other factors like environmental conditions, age, sex, or the type of prey available can also affect venom composition (Oliveira et al., 2022). Snake venom is rich in components and contains many biologically active molecules, with peptides and proteins making up more than 95% of the venom's dry weight. The remaining 5% is made up of lipids, carbohydrates, and biogenic amines. These proteins carry out various jobs that help with capturing and then digesting prey (Bedraoui et al., 2024). The four main protein families found in viper (*Viperidae*) venoms are as follows (Tasoulis & Isbister, 2022): Snake venom phospholipase A2 (PLA2), Snake venom metalloproteinase (SVMP), Three finger toxins (3FTx), Snake venom serine proteinase (SVSP). Besides these, the enzymes found in the general composition include hyaluronidase, 5' nucleotidase, phosphodiesterase, and collagenase (Wiezel et al., 2015) (Sanz et al., 2008). The secondary protein families that make up the venom composition in *Viperidae* can be classified as: L amino acid oxidase (LAAO), Kunitz peptides (KUN), disintegrins (DIS), cysteine rich secretory proteins

(CRiSP), C type lectins (CTL), and natriuretic peptides (NP) (Tasoulis & Isbister, 2022), bradykinin potentiating peptides (BPPs), crotamine, and antimicrobial peptides (Diniz-Sousa et al., 2023).

2.2. Arachnid Venoms

The class Arachnida includes over 60,000 species, making it a huge reservoir of venomous diversity (Cordeiro et al., 2015). Recently, peptides and acylpolyamines derived from arachnids have drawn considerable attention for their broad systemic effects, especially on the mammalian central nervous system (CNS). These bioactive compounds have strong therapeutic potential, including analgesic, antiepileptic, and neuroprotective properties. They mainly achieve these effects by selectively inhibiting or stimulating specific ion channels and neurotransmitter receptors (Monge-Fuentes et al., 2015).

2.2.1. Scorpion Venoms

Scorpion venom is a complex store of bioactive compounds. It contains a wide range of proteins, peptides, enzymes, nucleotides, lipids, inorganic salts, free amino acids, and small molecules, and it shows remarkable specificity in targeting cellular pathways (Ortiz et al., 2014). Among these components, venom peptides stand out for their ability to specifically interact with key biological targets such as ion channels and cellular receptors. Their high target specificity and low toxicity make them very promising candidates for developing new therapeutic treatments (Lafnoune et al., 2025). As a major focus of this therapeutic potential, scorpion venom components have strong anticancer effects through various molecular mechanisms, including triggering apoptosis, regulating the cell cycle, and targeting ion channels (Arcos et al., 2025). Beyond these anticancer mechanisms, the broader pharmacological properties of scorpion derived bioactive molecules also include antimicrobial, immunosuppressive, bradykinin potentiating, and analgesic effects, among others (Ahmadi et al., 2020).

2.2.2. Spider Venoms

As one of the most widespread and successful venomous predators, spiders use a highly complex venom to catch a wide range of prey (Saez et al., 2010). This venom is a rich mix of low molecular mass compounds, proteins, and peptides. Research shows that its disulfide rich components mainly target excitable membranes, changing how essential receptors and ion channels like Na+, K+, and Ca2+ work (Chen et al., 2018). Because of their strong activity on various neuronal receptors and channels such as TRP, ASICs, and voltage gated channels, these toxins are now widely recognized as important pharmacological tools and strong candidates for drug discovery (Pineda et al., 2014).

2.3. Cone Snail Venoms

Cone snail venoms have become a highly valuable source of selective ligands that target nervous system receptors, ion channels, and transporters (Safavi Hemami et al., 2018). Because of their compact structure, high stability, precise target specificity, and relatively simple synthesis, these molecules serve as excellent pharmacological tools. Specifically, various conotoxin families interact with neurological components of pain pathways, effectively blocking the key receptors and ion channels responsible for pain while keeping off target effects to a minimum (Vetter & Lewis, 2012). Historically, snake and lizard venoms have been the main source for cardiovascular peptide drug candidates. However, cone snail venoms have recently gained attention by producing new peptide leads for other therapeutic areas, particularly pain management. A well-known example of this clinical translation is the synthetic analogue of MVIIA, a calcium channel blocker derived from *Conus magus* venom. This compound became the first FDA approved conotoxin therapeutic and is currently given intrathecally under the brand name Prialt for managing chronic pain (Prashanth et al., 2014).

3. The Biochemical Arsenal of Insects: Composition and Mechanisms

Insect venoms are highly complex mixtures made up of biogenic amines, bioactive peptides, and high molecular weight proteins (Laxme et al., 2018). Table 1 gives a comprehensive overview of the major insect groups, their main toxic constituents, and their key physiological effects.

Table1. Major venomous insects, their scientific classifications, and the principal toxic components of their venoms (Adapted from Schmidt, 2019).

Insect Group (Common & Scientific Names)	**Toxic Components and Their Effects**
HYMENOPTERA	
Honey bees (*Apis mellifera*; Apidae)	Melittin: Inhibits protein kinases and ion transport; causes cell lysis. Phospholipase A2: Causes lung congestion and allergic reactions.
Wasps & Hornets (*Vespula*, *Vespa*, *Polistes* spp.; Vespidae)	Kinins: Cause hemolysis and pain. Phospholipase A1: Triggers allergic reactions. Mastoparans: Destroy mast cells.
Fire ants (*Solenopsis* spp.; Formicidae)	Solenopsin (piperidine alkaloids): Inhibits angiogenesis via kinase signaling; causes cytotoxicity, hemolysis, necrosis, and pain.
Bulldog ants (*Myrmecia* spp.; Formicidae)	Pilosulin: Enzyme causing severe allergic reactions, including anaphylaxis.

Insect Group (Common & Scientific Names)	**Toxic Components and Their Effects**
Bullet ant (*Paraponera clavata*; Formicidae)	Poneratoxin: Neurotoxic peptide acting on voltage-gated Na+ channels; causes paralysis and extreme pain.
Harvester ants (*Pogonomyrmex* spp.; Formicidae)	Barbatolysin and Phospholipases: Cause extreme pain and potential anaphylaxis.
LEPIDOPTERA	
Lonomia caterpillars (*Lonomia* spp.; Saturniidae)	Proteolytic enzymes: Break down fibrinogen in blood, causing hemorrhaging, heart, and kidney failure.
Processionary caterpillars (*Thaumetopoea* spp.; Thaumetopoeidae)	Thaumetopoein: Urticating toxin causing dermatitis, conjunctivitis, and respiratory distress.
Puss moth caterpillars (*Megalopyge* spp.; Megalopygidae)	Protein toxins: Cause intense radiating pain, edema, erythema, and rash.

While Table 1 shows the diversity of toxic components found in different insect groups, the amount of each component within a venom is also important for understanding its biological activity. Honey bee (*Apis mellifera*) venom is a good example of this complexity. It is made up of several bioactive compounds that are present in different proportions. Melittin is the most abundant component, followed by major proteins such as phospholipase A2, and smaller amounts of potent peptides such as apamin. This complex composition has encouraged researchers to study individual venom components separately, especially to identify molecules with specific therapeutic potential, rather than focusing only on the overall toxic effects of the venom (Figure 4) (Gajski et al., 2024).

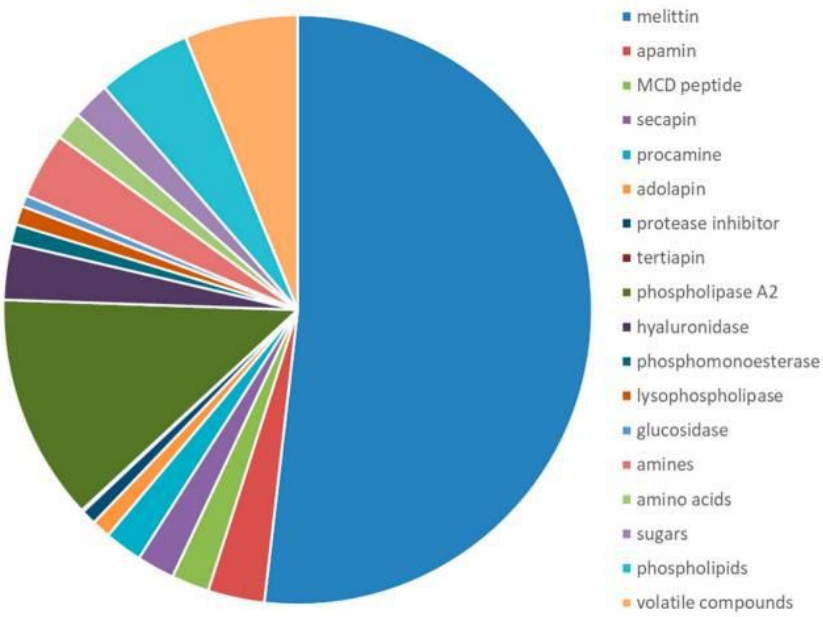


Figure 4. Composition of dry bee venom. Adapted from Gajski et al. (2024).

4. Therapeutic Applications of Insect Venoms

For the past thirty years, animal venoms have become an important source of new medicines. This has led to the sale of several peptide drugs made from venom that are now used to treat heart disease, high blood pressure, diabetes, multiple sclerosis, and pain (Ghodeif et al., 2025). The clearest clinical proof of this shift for insect venoms is the successful commercialization of whole venom products. Apitox® (made by Apimeds, Inc.) is a purified form of Apis mellifera venom given by injection under the skin. It has been approved by the FDA, which shows that venom-based treatments can successfully reach the clinic. It is currently used to relieve pain and inflammation linked to multiple sclerosis, rheumatoid arthritis, bursitis, and tendinitis (Alves et al., 2009).

4.1. Oncology: Targeted Cancer Therapeutics

One of the most widely studied areas for venom-based medicines is cancer, where insect peptides are used to destroy cancer cells. Bee venom has strong anticancer effects, mostly due to two parts of it called melittin and PLA2. These effects have been shown against many types of cancer, including leukemia, breast, prostate, lung, and liver cancer. The venom mainly fights cancer by causing cancer cells to self-destruct (apoptosis). This happens through the buildup of calcium (Ca^{2+}) and reactive oxygen species (ROS) inside the cells. Melittin also turns on PLA2, which breaks down the cancer cell membrane and makes the venom even more harmful to the cells (Soltan-Alinejad et al., 2022).

This target-specific cell-killing activity is not limited to Apis mellifera; social wasp venoms also show strong tumor-killing abilities by disrupting mitochondria. Mastoparan is a 14-amino-acid peptide that has both water-loving and water-fearing parts. It contains many hydrophobic and basic residues, which help it form pore-like helical structures in cell membranes. Because it acts on membranes, mastoparan can target mitochondria and trigger a strong mitochondrial permeability transition, which kills tumor cells. Many in vitro studies have confirmed the strong anti-tumor effects of mastoparan and its analogs (Moreno & Giralt, 2015). Beyond cancer, recent evidence shows it has other therapeutic uses. Mastoparan has strong antifungal activity and clearly speeds up wound healing by combining antioxidant, anti-inflammatory, and tissue-repair effects (Amin et al., 2026).

4.2. Antimicrobial and Antiviral Agents

As shown by the tissue-repair and antifungal properties of mastoparan, the way venom peptides break down cell membranes makes them very effective against resistant pathogens. Venom compounds from insects have been shown to fight a wide range of microbes very well. For example, melittin from honey bees has strong antibacterial and antifungal effects. It can stop harmful germs such as Borrelia burgdorferi, the bacterium that causes Lyme disease, and the yeast Candida albicans. It also works against Mycoplasma and Chlamydia infections. In the same way, solenopsin, which comes from fire ants, has many uses beyond just killing insects. It also has strong antibacterial, antifungal, and antiviral effects (Schmidt, 2019).

4.3. Neurodegenerative Diseases and Pain Management

Beyond breaking down membranes, the high target specificity of venom components on ion channels has opened new ways to treat complex neurological conditions. Apamin makes up about 2–3% of the dry weight of bee venom. It is a neurotoxin made of 18 amino acids and is well known as a very selective allosteric inhibitor of small-conductance Ca2+-activated K+ (SK) channels. These channels play a key role in many disease processes. By blocking them, apamin has strong potential for research and treatment in conditions such as atherosclerosis, Parkinson's disease, and liver fibrosis (Gu et al., 2020). Similar ion channel modulation is seen in ant venoms, which offer a wide range of neurotoxic peptides along with their defensive alkaloids. The venom of the fire ant (Solenopsis invicta) is a rich source of potential new drugs. This is because it contains a special mix of bioactive alkaloids and peptides. Its main components, such as solenopsin and the allergenic Sol i peptides, have strong antimicrobial, antifungal, and anticancer effects. In addition, certain neurotoxic parts, such as U5-ctenotoxin, may be useful for treating chronic pain and neurological disorders. They work by targeting and adjusting ion channels and specific receptor sites (Dioguardi et al., 2024). Also, venom enzymes like PLA2 have

shown strong potential in reducing neuroinflammation and nerve pain caused by chemotherapy. Bee venom PLA2 has been shown to reduce the harmful activation of microglia (immune cells in the brain) in a triple-transgenic mouse model of neuroinflammation. This suggests it may be a useful treatment for neurodegenerative diseases (Ye et al., 2016). Its clinical use also extends directly to pain management. Phospholipase A2 (PLA2) taken from the Egyptian honey bee (Apis mellifera lamarckii) has been shown to have blood-thinning effects. It mainly works by making prothrombin time longer. It also has strong pain-relieving effects on nerve pain caused by oxaliplatin, a common chemotherapy drug used for colorectal cancer that has spread (Moran et al., 2022).

4.4. Immune System Modulation and Inflammatory Diseases

While the neurotoxic and cell-killing effects of insect venoms are well documented, their ability to control the immune system is a very promising new area, deeply rooted in historical practices. Bee venom (BV) has been used in traditional medicine for a long time to treat long-term inflammatory conditions, especially rheumatoid arthritis. Its anti-rheumatic effects have been known for more than a century. Animal studies support this historical use. For example, injecting BV into the Zusanli acupoint clearly reduced both inflammation and pain in rats with Freund's adjuvant-induced arthritis (Hwang et al., 2015). Modern molecular studies continue to confirm these anti-inflammatory pathways in various tissues, including the skin. Recent studies show that bee venom (BV) may help treat skin diseases, especially atopic dermatitis, the most common long-term allergic skin disease. BV reduces symptoms by increasing CD55 expression through the activation of the ERK1/2 signaling pathways (Wehbe et al., 2019). This remarkable versatility balancing both immune modulation and defense against infections is a hallmark of venom-based therapies. Shi et al. (2022) showed that compounds from bee venom can work in both inflammatory and infectious diseases, which shows how versatile they are. In particular, melittin (MEL) may be a promising treatment for osteoarthritis because it protects IL-1β-stimulated C518 rat knee joint cells. MEL works by lowering iNOS expression, keeping cytosolic IκB stable, and as a result, blocking NF-κB from moving into the nucleus. In addition, whole bee venom (BV) has strong antimicrobial and antibiofilm effects against food-borne pathogens. BV stopped the growth of 16 Salmonella strains (MICs ranging from 256 to 1024 μg/ml) and broke down biofilm formation in most of these strains. This shows that BV could be a strong anti-infective agent. Ultimately, while current research strongly focuses on the anti-inflammatory uses of hymenopteran venoms like those of bees, the future of immune modulation may lie in parasitoid wasps (e.g., Venturia and Bracon species). Unlike defensive venoms, parasitoid venoms contain special proteins that expertly suppress host immune responses without causing tissue damage. This offers a unique blueprint for next-generation immunosuppressive therapeutics (Khalil et al., 2021).

5. Future Perspectives

Recent bibliometric data show a sharp, rapid rise in research on insect venom peptides. Nearly half of all translational studies have appeared in just the last five years. This fast growth since 2021 clearly points to the huge, still largely untapped pharmacological potential of these biochemical arsenals (Abbasi, 2025). This is where nanotechnology is truly changing venom-based drug delivery. Standard delivery methods often have problems with poor bioavailability and unwanted side effects, because powerful molecules can spread throughout the body without control. In contrast, engineered nanoparticles (NPs) offer a new solution by wrapping these active peptides inside them. For example, putting specific bee venom components inside targeted nanoparticles is a very promising way to cross biological barriers and deliver treatment directly to sites of neuroinflammation or tumor environments. By keeping the peptides inside nanoscale carriers until they reach their target, this approach not only improves tissue penetration and cellular uptake but also greatly reduces harmful systemic effects. As a result, NP-mediated delivery provides a safer and more precise way to use insect venoms against a range of complex illnes (Aher et al., 2024). Although nanotechnology offers a very promising preclinical framework for reducing toxicity, there is still a major gap when it comes to human translation. To fully achieve this biomedical vision, future research must focus on large clinical trials to firmly establish bee venom and other insect-derived compounds, as mainstream therapeutic agents in modern medicine (Bhardwaj et al., 2025.

6. Conclusion

Throughout history, animal venoms have mainly been viewed as lethal weapons. However, they are now increasingly recognized as valuable sources of bioactive molecules with potential applications in modern pharmacology. The successful development of venom-derived drugs from snakes, arachnids, and marine snails has already demonstrated that venom components can be translated into clinically useful therapies. In this context, insect venoms represent a particularly diverse and still underexplored source of molecules with therapeutic potential. Several insect venom components, including melittin, apamin, and mastoparan, have shown a wide range of biological activities. Their effects include inducing apoptosis in cancer cells, disrupting microbial membranes, and modulating ion channels involved in nervous system function. Parasitoid wasp venoms are also of particular interest because of their ability to regulate host immune responses. Understanding how these venoms suppress immunity while maintaining host viability may provide useful insights for the development of new immunomodulatory approaches.

Further progress in this field will depend on combining venomics with bioinformatics, molecular techniques, and modern drug delivery systems. Nanoparticle-based approaches, in particular, may help overcome some of the

limitations of venom-derived compounds, such as systemic toxicity and rapid degradation. Although many findings remain at the preclinical stage, they highlight the therapeutic potential of insect venoms and the need for further research. Ultimately, well-designed clinical studies will be necessary to determine their safety, efficacy, and possible applications in human medicine.

7. References

Abbasi, E. (2025). The role of Insects in Future Medicine: Diagnostic and therapeutic potential of Insect-Derived Biomolecules and Microbiota. *Entomologia Experimentalis Et Applicata*, *174*(1), 1–15. https://doi.org/10.1111/eea.70033

Aher, J., Jadhav, V., Bhagare, A., & Lokhande, D. (2024). Honey bee venom loaded nanomaterials: A promising avenue for therapeutic delivery. *Nano-Structures & Nano-Objects*, *39*, 101310. https://doi.org/10.1016/j.nanoso.2024.101310

Ahmadi, S., Knerr, J. M., Argemi, L., Bordon, K. C. F., Pucca, M. B., Cerni, F. A., Arantes, E. C., Çalışkan, F., & Laustsen, A. H. (2020). Scorpion Venom: Detriments and benefits. *Biomedicines*, *8*(5), 118. https://doi.org/10.3390/biomedicines8050118

Alves, E. M., Heneine, L. G. D., Pesquero, J. L., De Albuquerque Merlo, L., Funed, F. E. D.-., De Minas Gerais, U. F., De Amparo a Pesquisa Do Estado De Sao Paulo Fapesp, F., & De Amparo a Pesquisa Do Estado De Minas Gerais Fapemig, F. (2009, October 7). *WO2011041865A1 - Pharmaceutical composition containin an apitoxin fraction and use thereof - Google Patents*. https://patents.google.com/patent/WO2011041865A1/en

Amin, B. H., Elsharkawy, A. M., Galhom, R. A., Rady, M. H., Aboraya, D. M., Mekky, A. E., Helal, E. E., Abdelsamed, H. A., Yosri, M., & Amer, A. (2026). Mastoparan, a wasp venom-derived peptide, promotes healing in Candida albicans -infected wounds through antifungal and anti-inflammatory mechanisms. *Immunopharmacology and Immunotoxicology*, *48*(5), 830–843. https://doi.org/10.1080/08923973.2026.2705916

Anal, J. M. H., Mozhui, L., & Rokhum, S. L. (2025). Unveiling the therapeutic potential of insect-derived natural products for drug discovery. *Future Journal of Pharmaceutical Sciences*, *11*(1). https://doi.org/10.1186/s43094-024-00758-3

Arcos, S. S. S., Da Cunha Aguiar, M. R., De Oliveira, J., Da Silva, M. R., De Oliveira Cavalcante Pimentel, I., Anjos, N. G. D., Machado, G. H. R. S., Evangelista, K. B., Portaro, F. C. V., & Iwai, L. K. (2025). Scorpion Venom as a source of cancer drugs: A comprehensive proteomic analysis and therapeutic potential. *International Journal of Molecular Sciences*, *26*(20), 9907. https://doi.org/10.3390/ijms26209907

Bedraoui, A., Suntravat, M., Mejjad, S. E., Enezari, S., Oukkache, N., Sánchez, E. E., Galán, J. A., Fatimy, R. E., & Daouda, T. (2024). Therapeutic potential of snake venom: Toxin distribution and opportunities in deep learning for novel drug discovery. *Medicine in Drug Discovery*, *21*, 100175. https://doi.org/10.1016/j.medidd.2023.100175

Bhardwaj, V., Thakur, N., & Kumari, P. (2025). Harnessing bee venom for inflammatory diseases management: from traditional medicine to nanotechnology. *Naunyn-Schmiedeberg S Archives of Pharmacology*, *398*(8), 9797–9815. https://doi.org/10.1007/s00210-025-03991-6

Bose, D., Srinivasan, K., Patil, S. S., Nayak, A. G., & Hariharapura, R. C. (2026). The Venom Revolution in Biomedicine: Unlocking Nature's toxin toolkit for therapeutic innovation. *Toxicology Reports*, *16*, 102227. https://doi.org/10.1016/j.toxrep.2026.102227

Calderon, L. A., Sobrinho, J. C., Zaqueo, K. D., De Moura, A. A., Grabner, A. N., Mazzi, M. V., Marcussi, S., Nomizo, A., Fernandes, C. F. C., Zuliani, J. P., Carvalho, B. M. A., Da Silva, S. L., Stábeli, R. G., & Soares, A. M. (2014). Antitumoral activity of snake venom proteins: New trends in cancer therapy. *BioMed Research International*, *2014*, 1–19. https://doi.org/10.1155/2014/203639

Casewell, N. R., Wüster, W., Vonk, F. J., Harrison, R. A., & Fry, B. G. (2012). Complex cocktails: the evolutionary novelty of venoms. *Trends in Ecology & Evolution*, *28*(4), 219–229. https://doi.org/10.1016/j.tree.2012.10.020

Chen, N., Xu, S., Zhang, Y., & Wang, F. (2018). Animal protein toxins: origins and therapeutic applications. *Biophysics Reports*, *4*(5), 233–242. https://doi.org/10.1007/s41048-018-0067-x

Cordeiro, F. A., Amorim, F. G., Anjolette, F. a. P., & Arantes, E. C. (2015). Arachnids of medical importance in Brazil: main active compounds present in scorpion and spider venoms and tick saliva. *The Journal of Venomous Animals and Toxins Including Tropical Diseases*, *21*(1), 24. https://doi.org/10.1186/s40409-015-0028-5

De Castro Figueiredo Bordon, K., Cologna, C. T., Fornari-Baldo, E. C., Pinheiro-Júnior, E. L., Cerni, F. A., Amorim, F. G., Anjolette, F. a. P., Cordeiro, F. A., Wiezel, G. A., Cardoso, I. A., Ferreira, I. G., De Oliveira, I. S., Boldrini-França, J., Pucca, M. B., Baldo, M. A., & Arantes, E. C. (2020). From animal poisons and venoms to medicines: achievements, challenges and perspectives in drug discovery. *Frontiers in Pharmacology*, *11*, 1132. https://doi.org/10.3389/fphar.2020.0113

Diniz-Sousa, R., Silva, C. C. A., Pereira, S. D. S., Da Silva, S. L., Fernandes, P. A., Teixeira, L. M. C., Zuliani, J. P., & Soares, A. M. (2023). Therapeutic applications of snake venoms: An invaluable potential of new drug candidates. *International Journal of Biological Macromolecules*, *238*, 124357. https://doi.org/10.1016/j.ijbiomac.2023.124357

Dioguardi, M., Cantore, S., Sovereto, D., Sanesi, L., Martella, A., Almasri, L., Musella, G., Lo Muzio, L., & Ballini, A. (2024). Therapeutic Potential of Solenopsis invicta Venom: A Scoping Review of Its Bioactive Molecules,

Biological Aspects, and Health Applications. *Biomolecules*, *14*(12), 1499. https://doi.org/10.3390/biom14121499

El-Aziz, T. M. A., Soares, A., & Stockand, J. D. (2019). Snake Venoms in Drug Discovery: Valuable therapeutic tools for life saving. *Toxins*, *11*(10), 564. https://doi.org/10.3390/toxins11100564

Escoubas, P., & King, G. F. (2009). Venomics as a drug discovery platform. *Expert Review of Proteomics*, *6*(3), 221–224. https://doi.org/10.1586/epr.09.45

Gajski, G., Leonova, E., & Sjakste, N. (2024). Bee venom: Composition and anticancer properties. *Toxins*, *16*(3), 117. https://doi.org/10.3390/toxins16030117

Ghodeif, S. K., El-Fahla, N. A., Abdel-Rahman, M. A., & El-Shenawy, N. S. (2025). Arthropod venom peptides: Nanotechnology-enabled delivery and therapeutic potential in cancer treatment. *Cancer Pathogenesis and Therapy*, *4*(2), 81–97. https://doi.org/10.1016/j.cpt.2025.03.005

Gold, B. S., Dart, R. C., & Barish, R. A. (2002). *Bites of Venomous Snakes. New England Journal of Medicine, 347(5), 347–356.* doi:10.1056/nejmra013477

Gu, H., Han, S. M., & Park, K. (2020). Therapeutic effects of Apamin as a Bee venom component for Non-Neoplastic Disease. *Toxins*, *12*(3), 195. https://doi.org/10.3390/toxins12030195

Hwang, D., Kim, S., & Bae, H. (2015). Therapeutic effects of bee venom on immunological and neurological diseases. *Toxins*, *7*(7), 2413–2421. https://doi.org/10.3390/toxins7072413

Khalil, A., Elesawy, B. H., Ali, T. M., & Ahmed, O. M. (2021). Bee Venom: From venom to drug. *Molecules*, *26*(16), 4941. https://doi.org/10.3390/molecules26164941

Kim, E., Hwang, D. H., Prakash, R. L. M., Asirvatham, R. D., Lee, H., Heo, Y., Munawir, A., Seyedian, R., & Kang, C. (2025b). Animal venom in Modern Medicine: A Review of therapeutic applications. *Toxins*, *17*(8), 371. https://doi.org/10.3390/toxins17080371

Lafnoune, A., Darkaoui, B., Chbel, A., & Irahal, I. N. (2025). Emerging therapeutic applications of scorpion venom peptides in the Middle East and North Africa: A comprehensive review. *Toxicon*, *256*, 108270. https://doi.org/10.1016/j.toxicon.2025.108270

Laxme, R. S., Suranse, V., & Sunagar, K. (2018). Arthropod venoms: Biochemistry, ecology and evolution. *Toxicon*, *158*, 84–103. https://doi.org/10.1016/j.toxicon.2018.11.433

Messadi, E. (2023). Snake venom components as therapeutic drugs in ischemic heart disease. *Biomolecules*, *13*(10), 1539. https://doi.org/10.3390/biom13101539

Modahl, C. M., Brahma, R. K., Koh, C. Y., Shioi, N., & Kini, R. M. (2019). OMICS Technologies for Profiling Toxin Diversity and Evolution in snake venom: Impacts on the discovery of therapeutic and diagnostic agents. *Annual Review of Animal Biosciences*, *8*(1), 91–116. https://doi.org/10.1146/annurev-animal-021419-083626

Monge-Fuentes, V., Gomes, F. M. M., Campos, G. a. A., De Castro Silva, J., Biolchi, A. M., Anjos, L. C. D., Gonçalves, J. C., Lopes, K. S., & Mortari, M. R. (2015). Neuroactive compounds obtained from arthropod venoms as new therapeutic platforms for the treatment of neurological disorders. *The Journal of Venomous Animals and Toxins Including Tropical Diseases*, *21*(1), 31. https://doi.org/10.1186/s40409-015-0031-x

Moran, D., Dutta, U., Kunnumakkara, A. B., Daimari, E., & Deka, B. (2022). Insect Venoms and their Bioactive Components: A Novel Therapeutic Approach in Chronic Diseases and Cancer.

Moreno, M., & Giralt, E. (2015). Three Valuable Peptides from Bee and Wasp Venoms for Therapeutic and Biotechnological Use: Melittin, Apamin and Mastoparan. *Toxins*, *7*(4), 1126–1150. https://doi.org/10.3390/toxins7041126

Oliveira, A., Viegas, M. F., Da Silva, S. L., Soares, A. M., Ramos, M. J., & Fernandes, P. A. (2022). The chemistry of snake venom and its medicinal potential. *Nature Reviews Chemistry*, *6*(7), 451–469. https://doi.org/10.1038/s41570-022-00393-7

Ortiz, E., Gurrola, G. B., Schwartz, E. F., & Possani, L. D. (2014). Scorpion venom components as potential candidates for drug development. *Toxicon*, *93*, 125–135. https://doi.org/10.1016/j.toxicon.2014.11.233

Pineda, S. S., Undheim, E. A., Rupasinghe, D. B., Ikonomopoulou, M. P., & King, G. F. (2014). Spider Venomics: Implications for drug discovery. *Future Medicinal Chemistry*, *6*(15), 1699–1714. https://doi.org/10.4155/fmc.14.103

Prashanth, J. R., Brust, A., Jin, A., Alewood, P. F., Dutertre, S., & Lewis, R. J. (2014). Cone Snail Venomics: From Novel Biology to Novel Therapeutics. *Future Medicinal Chemistry*, *6*(15), 1659–1675. https://doi.org/10.4155/fmc.14.99

Rady, I., Siddiqui, I. A., Rady, M., & Mukhtar, H. (2017). Melittin, a major peptide component of bee venom, and its conjugates in cancer therapy. *Cancer Letters*, *402*, 16–31. https://doi.org/10.1016/j.canlet.2017.05.010

Román, J. J. M., Calderón-Arguedas, S., Solano, A. E., Rojas-Salas, M. F., González-Corrales, D., Brenes, D. M., & Redondo, G. M. (2022). Potential Applications of Drugs Obtained from Insect Venoms. *IAR Journal of Pharmacy*, *03*(01), 1–7. https://doi.org/10.47310/iarjp.2022.v03i01.002

Saez, N. J., Senff, S., Jensen, J. E., Er, S. Y., Herzig, V., Rash, L. D., & King, G. F. (2010). Spider-Venom peptides as therapeutics. *Toxins*, *2*(12), 2851–2871. https://doi.org/10.3390/toxins2122851

Safavi-Hemami, H., Brogan, S. E., & Olivera, B. M. (2018). Pain therapeutics from cone snail venoms: From Ziconotide to novel non-opioid pathways. *Journal of Proteomics*, *190*, 12–20. https://doi.org/10.1016/j.jprot.2018.05.009

Sanz, L., Ayvazyan, N., & Calvete, J. J. (2008). Snake venomics of the Armenian mountain vipers Macrovipera lebetina obtusa and Vipera raddei. *Journal of proteomics*, *71*(2), 198–209. https://doi.org/10.1016/j.jprot.2008.05.003

Schendel, V., Rash, L. D., Jenner, R. A., & Undheim, E. a. B. (2019). The diversity of Venom: The importance of behavior and venom system morphology in understanding its ecology and evolution. *Toxins*, *11*(11), 666. https://doi.org/10.3390/toxins11110666

Schmidt, J. O. (2019). Arthropod toxins and venoms. In *Medical and Veterinary Entomology* (pp. 23–31). https://doi.org/10.1016/b978-0-12-814043-7.00003-0

Shi, P., Xie, S., Yang, J., Zhang, Y., Han, S., Su, S., & Yao, H. (2022). Pharmacological effects and mechanisms of bee venom and its main components: Recent progress and perspective. *Frontiers in Pharmacology*, *13*, 1001553. https://doi.org/10.3389/fphar.2022.1001553

Soltan-Alinejad, P., Alipour, H., Meharabani, D., & Azizi, K. (2022). Therapeutic potential of bee and scorpion venom phospholipase A2 (PLA2): A narrative Review. *PubMed*, *47*(4), 300–313. https://doi.org/10.30476/ijms.2021.88511.1927

Stela, M., Cichon, N., Spławska, A., Szyposzynska, M., & Bijak, M. (2024). Therapeutic potential and mechanisms of Bee venom therapy: A Comprehensive review of Apitoxin applications and safety enhancement strategies. *Pharmaceuticals*, *17*(9), 1211. https://doi.org/10.3390/ph17091211

Tasoulis, T., & Isbister, G. K. (2022). A current perspective on snake venom composition andmconstituent protein families. *Archives of Toxicology*, *97*(1), 133–153. https://doi.org/10.1007/s00204-022-03420-0 .

Utkin, Y. N. (2017). Modern trends in animal venom research - omics and nanomaterials. *World Journal of Biological Chemistry*, *8*(1), 4. https://doi.org/10.4331/wjbc.v8.i1.4

Vetter, I., & Lewis, R. J. (2012). Therapeutic potential of cone snail venom peptides (Conopeptides). *Current Topics in Medicinal Chemistry*, *12*(14), 1546–1552. https://doi.org/10.2174/156802612802652457

Waheed, H., Moin, S. F., & Choudhary, M. I. (2017). Snake venom: From deadly toxins to life-saving therapeutics. *Current Medicinal Chemistry*, *24*(17). https://doi.org/10.2174/0929867324666170605091546

Wehbe, R., Frangieh, J., Rima, M., Obeid, D. E., Sabatier, J., & Fajloun, Z. (2019). Bee Venom: Overview of main compounds and bioactivities for therapeutic interests. *Molecules*, *24*(16), 2997. https://doi.org/10.3390/molecules24162997

Wiezel, G. A., dos Santos, P. K., Cordeiro, F. A., Bordon, K. C., Selistre-de-Araújo, H. S., Ueberheide, B., & Arantes, E. C. (2015). Identification of hyaluronidase and phospholipase B in Lachesis muta rhombeata venom. *Toxicon : official journal of the International Society on Toxinology*, *107*(Pt B), 359–368. https://doi.org/10.1016/j.toxicon.2015.08.029 .

Ye, M., Chung, H., Lee, C., Yoon, M. S., Yu, A. R., Kim, J. S., Hwang, D., Shim, I., & Bae, H. (2016). Neuroprotective effects of bee venom phospholipase A2 in the 3xTg AD mouse model of Alzheimer's disease. *Journal of Neuroinflammation*, *13*(1), 10. https://doi.org/10.1186/s12974-016-0476-z

CHAPTER 4

Plant Aging and Death Process – Senescence

Yüksel Keleş[1]

[1] Mersin University, Faculty of Education, Department of Biology Education MERSIN/TURKIYE

1. Introduction

The concept of senescence is derived from Latin and means the state of being old or the process of aging. Although it has a similar meaning to the concept of aging, senescence is more useful for expressing certain specific processes that occur in the final stages of the aging process. In higher plants, senescence refers to a slow-progressing, programmed process that results in the death of some organs or the entire plant. This process can also be seen as a strategy for plants to survive harsh conditions like winter and ensure the continuation of the species (Guo et al., 2021). Senescence is a metabolic transformation and recovery process controlled by a genetic program, triggered by environmental stimuli. The maturation and shedding of plant organs such as leaves, flowers, and fruits are called organ senescence. In annual or biennial plants that can reproduce only once during their life cycle, the process leading to the death of the entire plant is called organismal or monocarpic senescence. In this process, the entire plant dries up and dies after flowering and producing seeds and fruits.

The senescence program in photosynthetic organs of plants, such as leaves and cotyledons, can be initiated within days, weeks, months, or even years following maturation. This duration can depend on the genetic characteristics of the plant species and environmental conditions. While the process of senescence in plants typically begins with the transition to the reproductive phase under normal conditions, environmental factors can accelerate or slow down the senescence process. Environmental stress factors such as high and low light intensity, high and low temperature, drought, waterlogging, and salinity can cause early senescence. Inhibiting or promoting the senescence process significantly affects the quantity and quality of agricultural products. The control of the senescence process is a topic being studied to regulate harvest times and extend the shelf life of produce. Chemical substances known to inhibit (cytokinins, auxins, and gibberellins) or accelerate (abscisic acid (ABA), ethylene, salicylic acid (SA), jasmonic acid (JA), strigolactones, brassinolide, aminobenzamide, E64, 2,4-D) senescence can be used to increase agricultural productivity, regulate harvest times, or for experimental purposes (Öktem and Keleş, 2018; Guo et al., 2021) .

With the onset of leaf senescence, a large amount of reactive oxygen species (ROS), such as superoxide anion ($O_2^{\cdot-}$), hydrogen peroxide (H_2O_2), hydroxyl radical ($^{\cdot}OH$), singlet oxygen ($^1O_2$), and other harmful free radicals are produced (Prochazkova and Wilhelmova, 2007; Jing et al., 2008). Increased ROS leads to membrane lipid peroxidation, cellular damage, and programmed cell death. The amount of ascorbate and the rate of oxidation

among non-enzymatic antioxidant substances are a marker widely used for detecting oxidative stress and are important for regulating senescence (Pavet et al., 2005). In cereals, the timing and rate of leaf senescence depend on genotype and environmental conditions and are closely related to yield (Li et al., 2012). In cereal varieties, higher grain yield is obtained in those that remain green during the delayed leaf senescence or grain-filling period, whereas in those that enter early senescence, grain yield decreases because photosynthesis is inhibited significantly (Hongwei et al., 2014).

The genetic program of senescence requires the activation of some genes and the inhibition of others. There are numerous research reports indicating that new mRNAs and proteins are synthesized during senescence, and a metabolic transformation occurs. Although senescence is ultimately a destructive process, the synthesis of enzymes to function during this process is necessary. Using model plants such as *Arabidopsis*, barley, maize, and soybean, many genes associated with senescence (SAG) have been identified. Among the products of these genes are hydrolytic enzymes (proteases, lipases, RNases), protein kinases, and transcription factors. By manipulating SAG expression, it is possible to control the senescence process, meaning to delay or promote it. Buchanan-Wollaston et al. (2005) formed two main classes as regulatory and destructive genes by classifying SAG according to their functions and divided each class further into subfunctional groups within it.

In addition to defining the basic concepts related to the plant senescence process in this section, the signals that initiate the senescence process, metabolic changes, and genetic regulations are discussed. Leaf senescence is primarily addressed, and specific cases of flower and fruit senescence are not included. The level reached by senescence research and future expectations are also evaluated in the final section.

2. Symptoms of senescence

The typical symptom of leaf senescence is the transition from anabolic metabolism to catabolic metabolism. The number of catabolic genes expressed in aging leaves is twice the number of anabolic genes. The general symptom of monocarpic senescence, which results in the death of the entire plant, is the breakdown of membrane integrity, progressing in parallel with the degradation of proteins and chlorophyll. However, senescence processes resulting in the shedding of organs such as flowers, fruits, and leaves can exhibit different symptoms. Different symptoms can also be observed depending on the plant species and varieties, or on the stress factors that trigger senescence.

2.1. Membrane Degradation

The breakdown of the structural integrity of cell membranes is a general symptom that begins in the early stages of senescence. The onset of membrane degradation can be easily determined by measuring the increase in electrolyte and solute leakage. Membrane breakdown in organelles with active oxygenic metabolism, such as chloroplasts and mitochondria, begins earlier than the breakdown of the plasma membrane. This may be related to oxygen radicals acting as initiating signals for senescence. In addition, for the mobilization of degradation products within these organelles, an intact plasma membrane and other cytoplasmic membranes may be required for a longer period (Hopkins et al., 2007). Although the de-esterification of membrane lipids begins with an increase in lipolytic acyl hydrolase activity in the early stages of senescence, it is thought that the protein regions of the membrane remain functional until the later stages of senescence. Spherical lipid vesicles called plastoglobuli have been observed to form during the degradation of membrane lipids. The lipid degradation products protected in these vesicles are subsequently converted to sucrose and transported to developing seeds via the phloem.

2.2. Protein Degradation

In addition to leaf senescence, increased protease activity is an important stage of the senescence process. The activity of proteases is necessary for the autolysis process and subsequent nitrogen mobilization, primarily in chloroplasts. Chloroplasts contain 75% of the total leaf cell proteins and 70% of the nitrogen. In addition to LHCII apoproteins and other thylakoid proteins that bind chloroplast pigments, Rubisco proteins, which constitute 50% of chloroplast proteins, are also degraded for nitrogen mobilization. Dark treatments in barley have shown that the D1 protein in PSII is not easily degraded during senescence and is well-preserved. This may be related to the requirement for continued ATP synthesis during the dark-induced senescence process. Autophagy-related vesicles have been identified for the transport of degradation products from Rubisco and thylakoids in plastids (Nakamura et al., 2018). The protein degradation process is initiated within the organelle by proteases present in plastids, while it is sustained by the participation of active proteases in lytic vacuoles. There is evidence that the transcript levels and activity of serine endopeptidases and carboxypeptidases increase at the beginning and throughout senescence. The increased transcript levels of asparagine synthetase and aminotransferases, which are necessary for nitrogen transport in plants, in senescent leaves have been considered as evidence suggesting that nitrogen is converted into transportable forms and loaded into the phloem (Winichayakul et al., 2004) .

2.3. Chlorophyll Degradation

Chlorophyll degradation is the most typical and easily observed symptom of leaf senescence. When chlorophyll breakdown begins, carotenoid and anthocyanin pigments present in the leaves become visible, revealing the yellow, orange, and red tones of autumn leaves (Figure 1). The reaction sequences that cause chlorophyll degradation and the intermediate products formed have been elucidated using chlorophyll degradation-deficient mutant plants. The chlorophyll degradation process proceeds gradually. The enzyme chlorophyllase in chloroplasts cleaves the phytyl tail, Mg-dechelates separates the magnesium ion, and the resulting pheophytin is first converted to red, then fluorescent chlorophyll catabolites, thus causing the green color to disappear (Kuai et al., 2018). The activity of the enzymes responsible for the loss of green color prevents the accumulation of toxic catabolites and cell death. Further degradation processes of chlorophyll catabolites continue in the cytosol. The chlorophyll degradation process is thought to be a prerequisite for the degradation of LHCII proteins located in the thylakoid membranes.



Figure 1. Senescence observed in the leaves of ivy (*Epipremnum aureum*) with the development of chlorosis.

3. Senescence Signaling

The senescence process can be triggered by the influence of internal or external factors. Depending on the age of the plant, it may generate genetic program–initiating signals. Since changes in environmental conditions are closely linked to observed changes in hormone and ROS levels, signaling mechanisms are likely associated with these messengers.

3.1. Hormone Signals

In the senescence process, the delaying effect of cytokinins and the promoting effect of ethylene are well-known. Although other hormones have also been shown to be effective in senescence, their effects can vary depending on the plant species and tissues. The effect of auxins and gibberellins is mostly delaying, while ABA, JA, and SA are mostly promoting (Schippers et al., 2007) . There are differences in the mechanisms of action of these hormones or hormone-active substances. Some alter enzyme activities, while others affect gene expression.

3.1.1. Cytokinins

Application of cytokinin (zeatin, kinetin) to leaf cells delays leaf senescence by preventing chlorophyll degradation. The expression of the SAG12 gene stimulates cytokinin biosynthesis, and increased cytokinin delays senescence through extracellular invertase activity. Cytokinin applications reduce the expression of genes that produce peroxidases, some kinases, and ligases that promote the senescence process. The delay of senescence by cytokinin is linked to auxin levels, light duration, and sugar metabolism.

3.1.2. Ethylene

Increasing the internal levels of ethylene can trigger the senescence process. However, the effect of ethylene on senescence appears to depend on leaf age. Exogenously applied ethylene promoted senescence only in aged leaves, not in young leaves. Suppression of ACC oxidase, which is responsible for ethylene synthesis, leads to a delay in senescence. Ag^{+} ions can delay senescence by inhibiting ethylene biosynthesis. It has been determined that the expression of mitogen-activated protein kinase-6 (MAPK6), which controls ethylene signals, increases during the senescence process induced by environmental stresses in plants.

3.1.3. Other Growth Regulators

It has been shown that auxins (indole acetic acid - IAA, indole butyric acid - IBA) delay senescence by inhibiting the effect of ethylene. Studies suggest that the role of auxins in aging depends on their interaction with other hormones and the metabolic activities of tissues. Application of IAA to detached leaves significantly reduces the expression of SAG12, an important marker of the senescence process. Gibberellic acid (GA) delays leaf senescence by preventing chlorophyll and protein degradation in leaves and promoting transcription. It has been determined that the GA concentration in leaves is

tightly linked to the stages of development and that no GA is found in senescent leaves. ABA delays leaf, flower, and fruit abscission in some plants by inhibiting ethylene synthesis. ABA application to detached leaves triggers a rapid aging process, but this effect is quite limited in attached leaves. The activity of enzymes involved in ABA synthesis increases during the senescence process. The effect of ABA on senescence appears to be linked to the flow of sugar metabolism. High levels of glucose can suppress photosynthesis and initiate senescence (Rolland et al., 2002). Exogenous application of JA to leaf tissues significantly reduces the expression of genes encoding photosynthetic enzymes such as Rubisco. It has been reported that endogenous JA and SA levels can increase up to four times in aging leaves compared to normal leaves. Exogenous application of SA leads to increased SAG12 gene expression.

3.2. ROS Signals

At advanced stages of oxidative stress, the rate of ROS formation can exceed the capacity of the antioxidant defense system, leading to cell death. Oxidative damage occurs when the critical balance between oxidants and antioxidants is disrupted due to the depletion of antioxidants or excessive accumulation of ROS. Regardless of its source, increased intracellular ROS has two functions: the degradation of cellular components and the activation of specific signaling pathways. Oxidative damage in plant cells, especially during senescence, is characterized by a remarkable increase in ROS metabolism (Halliwell and Gutteridge, 2015) . Increased ROS levels also trigger the expression of many senescence-accelerating genes.

3.2.1. Superoxide anion

The production of superoxide in leaf tissues increases naturally or artificially induces senescence, but determining the mechanism of this induction is difficult. Because superoxide rapidly converts to hydrogen peroxide, and in many cases senescence induction can also result from the production of other ROSs. In barley, superoxide radical has been observed to increase during development and reach its highest level after the onset of senescence. While superoxide radical production declines toward the end of the senescence process, membrane fluidity simultaneously increases (Jajic et al., 2015).

3.2.2. Hydrogen peroxide

Hydrogen peroxide is formed in plant cells by the dismutation of the superoxide radical by SOD enzymes and by the activity of oxidase enzymes. Hydrogen peroxide levels are kept under control enzymatically and by antioxidants in a finely tuned network, and excessive accumulation is prevented (Foyer and Noctor, 2005). It is thought that the balance between SOD and different hydrogen peroxide scavenging enzymes within the cell is important in determining the steady-state hydrogen peroxide level (Keleş and Öncel, 2000; Mittler et al., 2004). Compared to other ROS, hydrogen peroxide is the most stable and least reactive ROS. Its ability to easily cross membranes and its stable structure make hydrogen peroxide a good signaling molecule. Hydrogen

peroxide plays variable roles in plant cells; at low concentrations, it is involved in the signaling regulation of various biotic and abiotic stresses, while at high concentrations, it contributes to the degradation of cell components, the progression of senescence, and cell death. It has been shown that hydrogen peroxide can be used as a signal to promote senescence in different plant tissues during the senescence process as part of a complex regulatory network (Bieker et al., 2012).

3.2.3. Singlet Oxygen

Consistent with the general increase in ROS production, singlet oxygen production also increases during senescence (Lee et al., 2012). Since the increase in singlet oxygen occurs simultaneously and in the same environment as other ROS, it is difficult to understand the specific role of singlet oxygen. The strong degradation of β-carotene and α-tocopherol in plants under drought stress has been associated with increased singlet oxygen production. While singlet oxygen is continuously produced at low levels in some naturally aging plants, in barley treated with hormone therapy at early stages, the mass production of singlet oxygen was observed to increase first and then decrease (Springer et al., 2015). A possible effect of singlet oxygen may be to increase lipid peroxidation (LPO), leading to cell death. A significant increase in lipid peroxidation is known to occur during senescence. Recently, it has been reported that singlet oxygen is responsible for more than 80% of non-enzymatic lipid peroxidation in *Arabidopsis* leaf tissues under optimal growth conditions (Triantaphyllides et al., 2008). It can lead to the formation of free radicals that promote lipid peroxidation senescence. The emergence of free radicals, in turn, increases the activity of lipid peroxidase enzymes and lipoxygenase, supporting the overproduction of singlet oxygen.

4. Factors Promoting Senescence

Various intrinsic and extrinsic factors can accelerate the senescence process or cause early senescence. In addition to pathogen attacks, extrinsic factors such as extreme climatic and soil conditions, darkness and the intensity of high light, or deficiencies in mineral nutrients can initiate or speed up the senescence process (Table 1). The most important intrinsic factors that trigger senescence are the age of the leaves or the stage of development of the plant's tissues (Keleş, 2009). In the leaves of annual plants, after full growth is reached, there is a continuous decrease in the rate of photosynthesis. In the leaves of *Arabidopsis*, under continuous light between days 4–6 of development, the photosynthetic capacity decreases by 50%. It is assumed that a drop in photosynthetic activity below a certain threshold value may be a senescence-inducing signal (Matile et al., 1996).

4.1. Darkness and High Light Intensity

There are many studies showing that insufficient light affects the initiation and progression of the senescence process. It has been understood that, in sunflower and corn, which are frequently sown, senescence initiation in the

shaded basal leaves is related to reduced light intensity, and especially to a deficiency in red light. Dark treatments are widely used in experimental senescence studies as a quick, easy, and effective method for triggering leaf aging (Öktem and Keleş, 2018). This facilitates the examination of the effects of aging regulators such as phytohormones, amino acids, fatty acids, sugars, secondary metabolites, free radicals, and gene expression (Doan et al., 2024). In Arabidopsis, dark treatments stimulate the expression of SAGs between 3–24 hours. The first signs of darkness-induced senescence are the cessation of chlorophyll and carotenoid pigment synthesis. This can be understood from the accumulation of different carotenoid compounds, as numerous light-regulated enzymes become inactive in the dark. While both the activities and gene expressions of CAT and SOD enzymes in wheat decreased during the darkness-induced senescence process, this decrease did not occur during the IAA-induced senescence process (Öktem and Keleş, 2018). In barley leaves during the darkness-triggered senescence process, the chlorophyll fluorescence decrease rate, also known as the vitality index ratio, rapidly declines (Paluch-Lubawa et al., 2021).

When seedlings kept in darkness for up to a week are re-exposed to light, chlorophyll, fluorescence, and PSII parameters recover, whereas in darkness treatments exceeding 7 days, the decrease in these parameters could not be reversed (Sobieszczuk-Nowicka et al., 2018). Leaf damage resembling senescence symptoms was observed under high light intensity. However, this damage could also be photo-oxidative due to increased ROS from excessive light. No significant evidence has been obtained from studies investigating the effect of light duration and photoperiod on senescence. It has been determined that increasing UV-B levels leads to ROS formation in *Arabidopsis*, causing chlorophyll and membrane degradation and inducing some senescence-related genes (SAG 12, 13, 14, 17) (John et al., 2001). Mature leaves of *Arabidopsis* are more affected by UV-B than young leaves. An increase in ethylene and JA levels has also been recorded in leaves exposed to UV-B.

4.2. Drought and Flooding

Senescence plays a critical role in the survival of plants under drought stress (Munne-Bosch and Alegre, 2004). The primary signals in the induction of senescence by drought stress can be considered as the cessation of growth and the initiation of solute accumulation. Under conditions where water is limited, the shedding of unproductive leaves both facilitates the transport of nutrients to productive leaves and reduces water loss through transpiration. Drought stress affects the internal levels of plant hormones, especially ABA. Under drought stress, the increase in ABA in cereal plants shows a positive correlation with increased carbon remobilization from senescing leaves to the seeds. The decrease in cytokinin levels, which is parallel to the decrease in photosynthetic rate and chlorophyll loss, is also observed under drought stress. There is also evidence suggesting that increased oxidative stress, resulting from the weakening of the antioxidant defense system under dry

conditions, triggers senescence. In plants under salt stress, signs of senescence, such as the shedding of older leaves, can also be observed under secondary drought stress (Keleş and Öncel, 2002). Data obtained by remote sensing methods showed that early autumn senescence was primarily induced by drought (Ma et al., 2024). GWAS analyses are used to identify loci, genes, and molecular markers associated with drought-induced senescence in crops such as barley, wheat, maize, and soybean. The findings contribute to understanding the genetic basis of adaptation to drought conditions and provide useful tools for the development of drought-resistant crop varieties (Doan et al., 2024).

Submerging plant roots and shoots in water leads to a lack of oxygen, carbon, and light, hindering plant growth and triggering early senescence. If the exposure period is prolonged, the plants may die completely even if conditions improve. The rapid decrease in cytokinin levels during flooding may be the main factor initiating early senescence. Although some evidence suggests a link between increased ethylene and chlorophyll degradation, the connection between ethylene and senescence caused by flooding is unclear. The senescence-stimulating effect of flood stress is more pronounced under high-temperature conditions (Keleş and Öncel, 2002).

4.3. High and Low Temperature

Since the temperature tolerance of plant species varies over a wide range, it can be suggested that temperature is the most important environmental factor determining the distribution of plants on Earth. High temperatures above tolerance limits, often combined with high light intensity and drought, effectively lead to early senescence (Keleş and Öncel 2002). Studies have shown that both drought and high temperatures have a limited effect on plant growth; however, the combination of drought and high temperatures has a much more serious impact on plant development (Mukherjee and Mishra 2021). High temperature can create a suitable environment for ROS formation, leading to lipid peroxidation of membranes and loss of enzyme activity. High temperatures can cause early senescence of mature leaves in cereals, shorten lifespan, and

lead to yield loss. An increase in soil temperature, similar to air temperature, also causes early senescence through root damage. Large-scale studies spread over time show that the increase in crop productivity due to global warming will reverse in the future, and rising temperatures will not continuously promote plant growth. The adverse conditions created by increasing drought along with warming cause leaves to age earlier (Ma et al., 2024).

Low temperature stress can have different effects on senescence depending on the decrease in enzyme activities and photosynthesis at chilling and freezing temperatures. It has been reported that the loss of activity of antioxidant defense enzymes at low temperatures can accelerate senescence due to increased ROS damage (Jajić et al., 2015). It has been observed that cold acclimation in plants significantly delays leaf senescence. This observation suggests a potential interaction between the acclimation process and the

metabolic regulation of the senescence process in a cold environment (Masclaux-Daubresse et al., 2007).

4.4. Nutrient Deficiency

Deficiency of mobile nutrients such as nitrogen and phosphorus primarily causes senescence in older structures, leading to the transport of nutrients to younger leaves or newly developing tissues. Nitrogen deficiency in cereals can lead to reduced photosynthesis, slowed growth, decreased biomass production, reduced grain yields, and early senescence. In GWAS studies of *Arabidopsis* plants grown under nitrogen deficiency conditions, several loci potentially associated with leaf yellowing were identified. These genomic regions were reported to contain genes related to nitrogen uptake, transport, and metabolism (Sakuraba et al., 2021). There are also studies showing the relationship between early senescence and the deficiency of other mobile macroelements, such as phosphorus and potassium (Doan et al., 2024). Studies on early senescence caused by nutrient deficiency have applications in modern agricultural practices. These advancements can enable targeted fertilization appropriate for plant growth stages, thus allowing for higher yields at a lower cost.

4.5. Biotic factors

Plant pathogens such as viruses, bacteria, and fungi, as well as invasive insects, can cause senescence and death of the organs they infect. This effect is mostly a result of lipid, protein, and chlorophyll degradation processes caused by specific toxins secreted by pathogens. Another mode of action is the induction of hypersensitive responses (HR) by pathogens, which stimulate plant defense mechanisms. HR responses are essentially a cell death process initiated by the plant to prevent the spread of infection, resulting in chlorosis and necrosis (Barna, 2022). Although hypersensitive responses and senescence serve different purposes, they may operate through the same molecular and genetic mechanisms. Plants can regulate leaf senescence to maintain overall physiological balance, thereby ensuring optimal conditions for the development of new organs and the continuation of the species. The interaction of pathogens and pests with plants depends on the physiological state of the plant and the age of the organs. Biotrophs prefer young tissues and organs, while necrotrophs prefer mature or old tissues and organs. The organ or mode of infestation by pests can affect the appearance of senescence symptoms. While two gall wasps that infest eucalyptus trees, *Leptocybe invasa*, which settle in the petiole and veins, did not cause chlorosis, *Ofelimus maskelli*, which settles in the leaf blade, caused chlorosis (Aytar and Keleş, 2025).

There is evidence showing that some different SAGs are activated during plant-pathogen interactions. Knockout *Arabidopsis* mutants were compared with overexpressing lines to determine the roles of WRKY transcription factors induced by pathogens in plant defense against microbial pathogens. Continuous expression of WRKY18 was reported to make plants

resistant to the bacterial pathogen *Pseudomonas syringae*, while its expression along with WRKY40 and WRKY60 caused susceptibility (Xu et al., 2006) . It is thought that ethylene and hydrogen peroxide levels increase during the pathogen-induced senescence process, and SA and JA play a role in the signaling mechanism. In *Arabidopsis*, pathogen-related genes (PR1) and receptor-like protein (RLP23) genes enhance systemic acquired resistance in combating fungi. A phenotype exhibiting leaf chlorosis has been interpreted as a response to penetration resistance against microbial infections, and it has been emphasized that it ensures the redistribution of nutrients in climates with short growing seasons. This adaptation mechanism can accelerate leaf senescence during the reproductive phase, directing more nutrients toward seed development (Johansson, 2014). Senescence triggered by biotic stress in plants depends on the balance between defense mechanisms and growth and provides insights into the adaptation strategies between pathogens and plants.

5. Factors Delaying Senescence

5.1. Removal of Reproductive Organs

In wheat, flag leaf senescence is delayed by the removal of reproductive organs after pollination. In cereals, the removal of reproductive organs during monocarpic senescence has been shown to reduce oxidative stress, inhibit lipid peroxidation, decrease oxidative damage, and preserve proteins for a longer period. The presence of reproductive organs promotes nitrogen mobilization, leading to increased ROS levels and accelerated protein degradation through enhanced proteolytic activity (Srivalli and Khanna-Chopra, 2004) .

5.2. Abundance of Nutrient Elements

Among nutrient elements, nitrogen is the most influential on senescence. Plants grown in environments with sufficient nitrogen exhibit slower leaf senescence. Low nitrogen accelerates senescence, while excessive nitrogen fertilization increases vegetative growth and delays senescence. Deficiency in all elements, including N, P, K, S, Ca, and Mg promotes senescence, whereas an excess of only nitrogen and phosphorus results in delayed senescence. In soybeans, increasing phosphate in the nutrient solution delayed senescence. Spraying wheat leaves with nitrogen and phosphorus compounds delayed aging, while other elements did not show the same effect.

Table 1. Internal and external factors that accelerate or delay the leaf senescence process.

Factors	**Senscence inhibitors**	**Senescence inducers**
Hormones and Growth Regulators	Auxins Cytokinins Gibberellic acid	Abscisic acid Ethylene Jasmonic acid Salicylic acid Strigolactones Brassinolide
Oxidants / Antioxidants	Ascorbic acid Glutathione Tocopherol Carotenoids	Superoxide anions Hidrogen peroxide Singlet oxygene
Enzmes	Superoxide dismutase Proxidases Catalase Histone methyltransferase Histon deacetylase	Proteases Chlorophyllase lipolytic acyl hydrolase Histone demethylase Histone acetyltransferase
Mineral Nutrients	Ag+ Nitrogen Phosphore	Mineral nutrient deficiencies
Environmental Conditions	Red light Long day Removal of the terminal bud Removal of generative organs	Far-red light Ultraviolet light Darkness Short day Salt stress Osmotic stress Pathogens and pests

6. SenescenceAssociated Genes

It is proposed that the primary cause of cellular aging is DNA damage. There is evidence showing a connection between changes in epigenetic information and senescence (Zhang et al., 2023). Even if there is no change in the DNA code, the alteration of gene expression via chromatin modification is referred to as epigenetic. Under stress conditions, the triggering of senescence may be linked to epigenetic regulation. Through ATP-dependent chromatin remodeling complexes, the nucleosome structure can be loosened or tightened, thereby selectively turning specific genes **"**on**"** or **"**off**"** for transcription and thus expression.

The activation of the genetic program of senescence due to various reasons leads to the degradation of nucleic acids, proteins, carbohydrates, and lipids, and ultimately to the death of organs or the entire plant. The senescence process is carried out through quite complex hormone and ROS signals. Messengers carrying the senescence signal regulate gene expression at the transcription and translation levels and manage cytoplasmic intermediate metabolism by altering enzyme activities. Through PCR-based hybridization, microarray technology, and expressed sequence tag (EST)

analyses, numerous genes whose expression increases and decreases during the senescence process have been identified and named senescence-associated genes (SAGs) (Tripathi and Tuteja, 2007; Xu et al., 2007). Large-scale transcriptome studies have determined that in *Arabidopsis* leaves undergoing senescence, numerous genes responsible for anabolic metabolism are downregulated, while genes associated with catabolic metabolism are generally upregulated. It has been reported that the number of SAGs upregulated during senescence in *Arabidopsis* leaves exceeds 2000, and approximately 500 transcription factors are involved in the expression of these genes (Buchanan-Wollaston et al., 2005). During the developmental aging process, changes in the expression of approximately 30% of the *Arabidopsis* genome have been reported. Genome-wide association studies (GWAS) are widely used to determine the genetic basis of complex traits by associating genetic markers with phenotypic variations. This approach allows for the mapping of loci associated with desired traits and the identification of candidate genes for functional research. GWAS studies have successfully identified genes involved in leaf senescence in *Arabidopsis* and some agricultural species (Doan et al., 2024).

Although it is difficult to classify SAGs due to their large number and the fact that their functions are not fully defined, a classification has been made in terms of some general functions. Accordingly: 1) genes related to macromolecule degradation (including subgroups related to protein, lipid, nucleic acid, and chlorophyll degradation), 2) genes related to nutrient scavenging and transport, 3) genes related to defense against pathogens and detoxification, and 4) regulatory genes (including subgroups of transcription factors, kinases-phosphatases, hormones, and other signaling molecules).

Two superfamilies of transcription factors determined to be associated with senescence in the genomes of model plants such as *Arabidopsis*, rice, wheat, and maize were identified. Numerous genes in the NAC superfamily play a central role in plant development and senescence processes (Li et al., 2024). Some genes from the WRKY superfamily regulate the senescence process by affecting the expression of hormone-related SAGs. WRKY6, 53, and 75 genes have been shown to be related to leaf senescence and to be regulators in both developmental and stress-induced senescence. NAC transcription factor NAM-B1 plays a critical role in regulating wheat leaf senescence and the remobilization of nutrients such as iron and zinc. In *Oryza sativa*, WRKY5 regulates the senescence process by modulating the expression or activity of the NAP and NAC (NAC-2) transcription factors, and even by modulating genes that enable ABA biosynthesis and chlorophyll breakdown (Li et al., 2024). Antioxidant or ROS scavenger genes are involved in controlling ROS levels at different stages of plant growth and development, including responses formed against stress and organ senescence. Along with an increase in the levels of ROS in aging leaves and petals, genes responsible for protection against ROS are regulated differently. Transcriptome studies have shown that in the leaves of

Arabidopsis mutants, the expression of Cu-ZnSODs, FeSOD, KAT1, ferritin1, PODs, glutathione peroxidase (GPX2/GPX7), stromal APX, GR, and alternative oxidase (AOX) genes increased in response to oxidative stress, while the expression of FeSOD1, KAT3, thylakoid APX, and DHAR genes decreased (Mylona and Polidoros, 2010). Mutations that lead to the overaccumulation of ROS and reduce the activity of ROS-scavenging enzymes have been associated with the early onset of senescence in plants.

7. Control of Senescence

Controlling the senescence process is economically important as it affects parameters such as plant product quality and shelf life. Delaying senescence in both cotyledons and leaves can have economic value by reducing yield losses associated with early senescence. In cultivated crops, delaying cotyledon senescence in seedling production and delaying leaf senescence in vegetable and fruit production can provide increases in yield and quality. Early senescence caused by abiotic stresses can lead to yield losses of up to 50% in major crops and is probably the most important cause of crop losses worldwide (Zentgraf, 2018).

Regulation of leaf senescence is crucial for yield in cereal crops and has long been a subject of great interest. Studying the mechanism of leaf senescence can provide important information for the genetic improvement of high-yielding cereal varieties. The senescence process can be utilized by producers for various purposes. For example, in crops harvested for their stems and leaves, product increase can be achieved by delaying senescence, or yield increase can be achieved by transferring the contents of crops with induced early senescence to storage organs. In cereal crops, after leaf senescence begins, nutrients are transferred from the leaves to the spikes (Gregersen et al., 2013). Early senescence is a factor that reduces cereal quantity and quality, and in recent years, due to global climate change, the phenomenon of early senescence in crops has been increasing (Xiaochuan et al., 2011).

Understanding the relationship between environmental factors that cause senescence and the antioxidant defense system can contribute to studies on senescence control. Although the loss of antioxidant defense capacity during senescence progression has been reported in different plants, the relationship between lifespan and oxidative stress tolerance is still unclear. Analyses of late-flowering, long-lived mutants of *Arabidopsis* have revealed that lifespan and oxidative stress tolerance are closely linked. According to genetic evidence, oxidative stress tolerance in plants is controlled by leaf lifespan (Woo et al., 2004). The amount of antioxidant compounds per chlorophyll was found to be significantly higher in trees and shrubs with longer leaf lifespan than in herbaceous plants (Keleş and Everest, 2008).

Plant senescence is regulated by both internal signals, such as age and hormone levels, and external factors that lead to biotic and abiotic stresses. Since photosynthesis is vital for plants, they primarily use mineral nutrients and other resources to develop chloroplasts. Therefore, chloroplasts play a leading and central

role in the regulation of senescence. Molecular genetic and metabolic analyses have shown that the breakdown of chlorophyll and chloroplasts is tightly regulated throughout the senescence process (Lei et al., 2023). Another key feature in the regulation of cellular senescence is the loss of protein homeostasis. Plant cells have developed complex protein degradation systems, such as the ubiquitin-proteasome system (UPS), autophagy, and other vacuole-dependent degradation pathways, to maintain protein homeostasis in response to changing environmental and developmental cues. The proteasome positively regulates aging; mutations in proteasome subunits typically lead to a delayed onset of aging. Autophagy is one of the fundamental cellular degradation pathways and plays a role in the removal of damaged or unnecessary proteins and organelles, as well as the reuse of nutrients. Autophagy is controlled by a highly conserved set of autophagy-related genes (ATGs). Recently, high-throughput transcriptomic studies have revealed the transcriptional reprogramming that occurs throughout the genome during plant senescence (Lei et al., 2023). Several TF families, such as NACs and WRKYs, play a role in the transcriptional regulation of leaf senescence. Depending on the specific TF, these genes can act as positive or negative regulators of aging.

In discussions focusing on the control of plant senescence, it is emphasized that due to the continuous division properties of meristem cells through telomerase, epigenetic regulations play a more significant role in the timing of senescence than telomere shortening (Fojtová, et al., 2025). Research on the control of senescence encompasses the regulation of DNA methylation, histone methylation and acetylation, chromatin remodeling, non-coding RNAs, and RNA methylation. Molecular manipulations using these methods have the potential to increase the quality and quantity of agricultural products (Shen et al., 2023). While increased DNA and histon methylation delays leaf senescence, increased histone acetylation progresses alongside leaf senescence. Chromatin remodeling, on the other hand, affects stress-induced senescence (Table 2).

Table 2. Four-stage control of the senescence process. When leaf senescence is triggered by the plant's age or changes in environmental conditions, a complex mechanism begins to operate. This mechanism includes epigenetic modifications, changes in gene expression, post-transcriptional and post-translational regulation.

Stage of control	Tools of control	Explain
Epigenetik modifications DNA modifications Histone modifications Chromatine remodelling	DNA methyltransferase/methylase Histone methyltransferase/demethylase Histone acetyltransferase/deacetylase	Methylation or acetylation of DNA and histones (especially H3) affects gene expression. Methylation delays senescence, while acetylation promotes it.
Gen expession changing	Transcription factors (WRKYs, NACs, MYBs) SAGs	During senescence, an increase or decrease in the expression of numerous genes (SAGs) can be observed. Transcription factors regulate the expression of these genes.
RNA processing	miRNAs / smRNAs RNA splaysosome RNA editosome	The processing of mRNA, the transcription product of genes, determines the quantity and characteristics of the proteins it will produce. Non-coding micro (mi) or small (sm) RNAs can inhibit mRNA or silence genes.
Protein modifications Ubiquitination Phosphorylation Autophagy Proteosome	Ubiquitin ligase/hydrolase Protein kinase Autophagy SAPs	Synthesized proteins and enzymes must be modified to acquire their functional forms. The localization and activity of proteins depend on these modifications. Autophagy inhibits senescence, while ubiquitin-proteasome senescence is promoted. Senescence-associated proteins (SAPs) are products of these modifications.

8. The Future of Senescence Research

Findings from senescence studies can contribute to understanding the relationship between senescence and antioxidants. The potential use of antioxidant compounds in controlling senescence is an area open to research. Although the role of hormones in controlling the senescence process, which is extremely important for the production, distribution, and marketing stages of

agricultural products, is better known, the functions of ROS and antioxidants have not yet been fully understood. In addition to preserving the nutritional value of plant products from producers to consumers, preventing product loss due to spoilage and decay is linked to the control of the senescence process. Identifying senescence characteristics specific to plants and organs requires large-scale research to understand the molecular regulation mechanisms of plant aging and to create desired aging characteristics in future agricultural products. Senescence research has the potential to make valuable contributions to the knowledge base in the fields of agricultural production and plant biotechnology, in addition to understanding plant metabolism.

Leaf senescence occurs with dynamic changes in metabolites. GWAS studies focusing on the links between phenotype and genotype are being combined with metabolomic approaches. mGWAS brings a new dimension to traditional GWAS by relating genomic variation to metabolite profiles and can be used to determine the genetic basis of metabolic changes observed during aging. It is necessary to investigate how plants balance developmental signals with environmental signals to enter this tightly controlled unique degradation process. A potential challenge for these studies is to analyze the general or species-specific control mechanisms by evaluating phenomic data together with genomic and metabolomic data.

Literature

Aytar, F., & Keleş, Y. (2025). Gall wasps change the biochemical composition of *Eucalyptus* leaves. *Anatolian Journal of Botany, 9*(2), 141–149. https://doi.org/10.30616/ajb.1701359

Barna, B. (2022). Manipulation of senescence of plants to improve biotic stress resistance. *Life (Basel), 12*(10), 1496. https://doi.org/10.3390/life12101496

Bieker, S., Riester, L., Stahl, M., Franzaring, J., & Zentgraf, U. (2012). Senescence-specific alteration of hydrogen peroxide levels in *Arabidopsis thaliana* and oilseed rape spring variety *Brassica napus* L. cv. Mozart. *Journal of Integrative Plant Biology, 54*, 540–554. https://doi.org/10.1111/j.1744-7909.2012.01147.x

Buchanan-Wollaston, V., Page, T., Harrison, E., Breeze, E., Lim, P. O., Nam, H. G., Lin, J.-F., Wu, S.-H., Swidzinski, J., Ishizaki, K., & Leaver, C. J. (2005). Comparative transcriptome analysis reveals significant differences in gene expression and signalling pathways between developmental and dark/starvation-induced senescence in *Arabidopsis*. *The Plant Journal, 42*, 567–585. https://doi.org/10.1111/j.1365-313X.2005.02399.x

Doan, P. P. T., Vuong, H. H., & Kim, J. (2024). Genetic foundation of leaf senescence: Insights from natural and cultivated plant diversity. *Plants, 13*, 3405. https://doi.org/10.3390/plants13233405

Fojtová, M., Procházková Schrumpfová, P., & Fajkus, J. (2025). The leaves fall, yet the tree endures. *Cellular and Molecular Life Sciences, 82*, 368. https://doi.org/10.1007/s00018-025-05874-8

Foyer, C. H., & Noctor, G. (2005). Redox homeostasis and antioxidant signaling: A metabolic interface between stress perception and physiological responses. *Plant Cell, 17*, 1866–1875. https://doi.org/10.1105/tpc.105.033589

Gregersen, P. L., Culetic, A., Boschian, L., & Krupinska, K. (2013). Plant senescence and crop productivity. *Plant Molecular Biology, 82*, 603–622. https://doi.org/10.1007/s11103-013-0013-8

Guo, Y., Ren, G., Zhang, K., & Li, Z. (2021). Leaf senescence: Progression, regulation, and application. *Molecular Horticulture, 1*, 5. https://doi.org/10.1186/s43897-021-00006-9

Halliwell, B., & Gutteridge, J. M. C. (2015). Oxidative stress and redox regulation: Adaptation, damage, repair, senescence, and death. In *Free Radicals in Biology and Medicine* (5th ed.). Oxford Academic. https://doi.org/10.1093/acprof:oso/9780198717478.003.0005

Hongwei, L., Gui, W., Shudong, L., Qiang, A., Zheng, Q., Bin, L., & Zhensheng, L. (2014). Comparative changes in the antioxidant system in the flag leaf of early and normally senescing near-isogenic lines of wheat (*Triticum aestivum*

L.). *Plant Cell Reports, 14*, 16–24. https://doi.org/10.1007/s00299-014-1600-0

Hopkins, M., McNamara, L., Taylor, C., Wang, T.-W., & Thompson, J. (2007). Membrane dynamics and regulation of subcellular changes during senescence. In S. Gan (Ed.), *Annual Plant Reviews Volume 26: Senescence Processes in Plants*. https://doi.org/10.1002/9780470988855.ch3

Jajic, I., Sarna, T., & Strzalka, K. (2015). Senescence, stress, and reactive oxygen species. *Plants, 4*, 393–411. https://doi.org/10.3390/plants4030393

Jing, H. C., Hebeler, R., Oeljeklaus, S., Sitek, B., Stuhler, K., & Meyer, H. E. (2008). Early leaf senescence is associated with an altered cellular redox balance in *Arabidopsis* cpr5/old1 mutants. *Plant Biology, 10*, 85–98. https://doi.org/10.1111/j.1438-8677.2008.00087.x

Johansson, O. N., Fantozzi, E., Fahlberg, P., Nilsson, A. K., Buhot, N., Tör, M., & Andersson, M. X. (2014). Role of the penetration-resistance genes PEN1, PEN2 and PEN3 in the hypersensitive response and race-specific resistance in *Arabidopsis thaliana*. *Plant Journal, 79*, 466–476. https://doi.org/10.1111/tpj.12571

John, C. F., Morris, K., Jordan, B. R., Thomas, B., & Mackerness, N. S. A.-H. (2001). Ultraviolet-B exposure leads to up-regulation of senescence-associated genes in *Arabidopsis thaliana*. *Journal of Experimental Botany, 52*(359), 1367–1373. https://doi.org/10.1093/jxb/52.359.1367

Keleş, Y., & Öncel, I. (2000). Changes of superoxide dismutase activity in wheat seedlings exposed to natural environmental stresses. *Communications Faculty of Sciences University of Ankara Series C Biology, 18*, 1–8. https://doi.org/10.1501/Commuc_0000000089

Keleş, Y., & Öncel, I. (2002). Response of antioxidative defence system to temperature and water stress combinations in wheat seedlings. *Plant Science, 163*(4), 783–790. https://doi.org/10.1016/S0168-9452(02)00213-3

Keleş, Y. (2009). Changes in antioxidant defense capacity in crop plants depend on leaf developmental periods. *Journal of Applied Biological Sciences, 3*(3), 39–46.

Keleş, Y., & Everest, A. (2008). Relation to altitude adaptation and antioxidant defense system in five shrubs and tree species from the middle Taurus Mountains. *International Journal of Natural and Engineering Sciences, 2*, 45–49.

Kuai, B., Chen, J., & Hortensteiner, S. (2018). The biochemistry and molecular biology of chlorophyll breakdown. *Journal of Experimental Botany, 69*, 751–767. https://doi.org/10.1093/jxb/erx322

Lee, S., Seo, P. J., Lee, H. J., & Park, C. M. (2012). A NAC transcription factor ntl4 promotes reactive oxygen species production during drought-induced leaf senescence in *Arabidopsis*. *Plant Journal, 70*, 831–844. https://doi.org/10.1111/j.1365-313X.2012.04932.x

Lei, P., Yu, F., & Liu, X. (2023). Recent advances in cellular degradation and nuclear control of leaf senescence. *Journal of Experimental Botany, 74*(18), 5472–5486. https://doi.org/10.1093/jxb/erad273

Li, H. W., Lin, F. Y., Wang, G., Jing, R. L., Zheng, Q., Li, B., & Li, Z. S. (2012). Quantitative trait loci mapping of dark-induced senescence in winter wheat (*Triticum aestivum* L.). *Journal of Integrative Plant Biology, 54*, 33–44. https://doi.org/10.1111/j.1744-7909.2011.01088.x

Li, S., Li, S., Tan, S., Liu, Z., & Li, Z. (2024). Transcription factors-regulated leaf senescence in major crops: Insights, applications, and challenges. *Current Plant Biology, 40*, 100428. https://doi.org/10.1016/j.cpb.2024.100428

Ma, C., Wang, X., & Wu, C. (2024). Early leaf senescence under drought conditions in the Northern hemisphere. *Agricultural and Forest Meteorology, 358*, 110231. https://doi.org/10.1016/j.agrformet.2024.110231

Masclaux-Daubresse, C., Purdy, S., Lemaitre, T., Pourtau, N., Taconnat, L., Renou, J. P., & Wingler, A. (2007). Genetic variation suggests interaction between cold acclimation and metabolic regulation of leaf senescence. *Plant Physiology, 143*, 434–446. https://doi.org/10.1104/pp.106.091355

Matile, P., Hoertensteiner, S., Thomas, H., & Kraeutler, B. (1996). Chlorophyll breakdown in senescent leaves. *Plant Physiology, 112*, 1403–1409. https://doi.org/10.1104/pp.112.4.1403

Mukherjee, S., & Mishra, A. K. (2021). Increase in compound drought and heatwaves in a warming world. *Geophysical Research Letters, 48*, e2020GL090617. https://doi.org/10.1029/2020GL090617

Munné-Bosch, S., & Alegre, L. (2004). Die and let live: Leaf senescence contributes to plant survival under drought stress. *Functional Plant Biology, 31*(3), 203–216. https://doi.org/10.1071/fp03236

Mylona, P. V., & Polidoros, A. N. (2010). ROS regulation of antioxidant genes. In *Reactive Oxygen Species and Antioxidants in Higher Plants* (pp. 101–127). CRC Press. https://doi.org/10.1201/9781439854082

Nakamura, S., Hidema, J., Sakamoto, W., Ishida, H., & Izumi, M. (2018). Selective elimination of membrane-damaged chloroplasts via microautophagy. *Plant Physiology, 177*, 1007–1026. https://doi.org/10.1104/pp.18.00444

Öktem, M., & Keleş, Y. (2018). The role of silver ions in the regulation of the senescence process in *Triticum aestivum*. *Turkish Journal of Biology, 42*, 517–526. https://doi.org/10.3906/biy-1802-95

Paluch-Lubawa, E., Stolarska, E., & Sobieszczuk-Nowicka, E. (2021). Dark-induced barley leaf senescence – A crop system for studying senescence and autophagy mechanisms. *Frontiers in Plant Science, 12*, 635619. https://doi.org/10.3389/fpls.2021.635619 (doi.org in Bing)

Pavet, V., Olmos, E., Kiddle, G., Mowla, S., Kumar, S., & Antoniw, J. (2005). Ascorbic acid deficiency activates cell death and disease resistance in *Arabidopsis thaliana*. *Plant Physiology, 139*, 1291–1303. https://doi.org/10.1104/pp.105.067686

Prochazkova, D., & Wilhelmova, N. (2007). Leaf senescence and activities of the antioxidant enzymes. *Biologia Plantarum, 51*, 401–406. https://doi.org/10.1007/s10535-007-0088-7

Rolland, F., Moore, B., & Sheen, J. (2002). Sugar sensing and signalling in plants. *Plant Cell, 14*, 185–205. https://doi.org/10.1105/tpc.010455

Sakuraba, Y., Mabuchi, C., Iba, K., & Yanagisawa, S. (2021). Enhanced NRT1.1/NPF6.3 expression in shoots improves growth under nitrogen deficiency stress in *Arabidopsis*. *Communications Biology, 4*, 256. https://doi.org/10.1038/s42003-021-01775-1

Shen, L., Ma, J., Li, P., Wu, Y., & Yu, H. (2023). Recent advances in the plant epitranscriptome. *Genome Biology, 24*, 43. https://doi.org/10.1186/s13059-023-02872-6 (doi.org in Bing)

Sobieszczuk-Nowicka, E., Wrzesinski, T., Bagniewska-Zadworna, A., Kubala, S., Rucinska-Sobkowiak, R., Polcyn, W., Misztal, L., & Mattoo, A. K. (2018). Physio-genetic dissection of dark-induced leaf senescence and timing its reversal in barley. *Plant Physiology, 178*, 654–671. https://doi.org/10.1104/pp.18.00516

Springer, A., Acker, G., Bartsch, S., Bauerschmitt, H., Reinbothe, S., & Reinbothe, C. (2015). Differences in gene expression between natural and artificially induced leaf senescence in barley. *Journal of Plant Physiology, 176*, 180–191. https://doi.org/10.1016/j.jplph.2015.01.004

Srivalli, B., & Khanna-Chopra, R. (2004). The developing reproductive 'sink' induces oxidative stress to mediate nitrogen mobilization during monocarpic senescence in wheat. *Biochemical and Biophysical Research Communications, 325*(1), 198–202. https://doi.org/10.1016/j.bbrc.2004.09.221

Triantaphylides, C., Krischke, M., Hoeberichts, F. A., Ksas, B., Gresser, G., Havaux, M., Van Breusegem, F., & Mueller, M. J. (2008). Singlet oxygen is the major reactive oxygen species involved in photooxidative damage to plants. *Plant Physiology, 148*(2), 960–968. https://doi.org/10.1104/pp.108.125690

Tripathi, S. K., & Tuteja, N. (2007). Integrated signaling in flower senescence: An overview. *Plant Signaling & Behavior, 2*, 437–445. https://doi.org/10.4161/psb.2.6.4991

Van Breusegem, F., & Dat, J. F. (2006). Reactive oxygen species in plant cell death. *Plant Physiology, 141*(2), 384–390. https://doi.org/10.1104/pp.106.078295

Winichayakul, S., Moyle, R. L., Ryan, D. J., Farnden, K. J. F., Davies, K. M., & Coupe, S. A. (2004). Distinct cis-elements in the *Asparagus officinalis* asparagine synthetase promoter respond to carbohydrate and senescence signals. *Functional Plant Biology, 31*(6), 573–582. https://doi.org/10.1071/FP03198

Woo, H. R., Kim, J. H., Nam, H. G., & Lim, P. O. (2004). The delayed leaf senescence mutants of *Arabidopsis*, ore1, ore3, and ore9 are tolerant to oxidative stress. *Plant and Cell Physiology, 45*(7), 923–932. https://doi.org/10.1093/pcp/pch110

Xu, X., Chen, C., Fan, B., & Chen, Z. (2006). Physical and functional interactions between pathogen-induced *Arabidopsis* WRKY18, WRKY40, and WRKY60 transcription factors. *Plant Cell, 18*, 1310–1326. https://doi.org/10.1105/tpc.105.037523

Xu, X., Gookin, T., Jiang, C. Z., & Reid, M. S. (2007). Genes associated with opening and senescence of *Mirabilis jalapa* flowers. *Journal of Experimental Botany, 58*, 2193–2201. https://doi.org/10.1093/jxb/erm058

Zentgraf, U. (2018). Oxidative stress and leaf senescence. In J. A. Roberts (Ed.), *Annual Plant Reviews Online*. Wiley. https://doi.org/10.1002/9781119312994.apr0265

Zhang, Y., Huang, D., & Miao, Y. (2023). Epigenetic control of plant senescence and cell death and its application in crop improvement. *Frontiers in Plant Science, 14*, 1258487. https://doi.org/10.3389/fpls.2023.1258487

CHAPTER 5

Investigation of Tert-Butanol/Water Mixture Using Two Types of TD-NMR Devices

Cengiz Okay[1]

[1] Assoc. Prof. Dr., Marmara University Faculty of Science, Department of Physics, Istanbul-Turkey, ORCID: 0000-0001-9609-2912

1. INTRODUCTION

Alcohols are compounds in organic chemistry that contain a hydroxyl (-OH) group and have a wide range of uses in both daily life and industry. These compounds, with the general formula R–OH, are noteworthy for their physical and chemical behavior due to their ability to form hydrogen bonds. Alcohols are classified as primary, secondary, and tertiary according to the degree to which they are bonded to a carbon atom. This classification directly affects the reactivity of alcohols and their interactions with solvent environments. Tert-butanol (TBA) is a compound belonging to the tertiary alcohol class, in which a hydroxyl group is attached to a carbon atom surrounded by three methyl groups. This bulky structure limits tert-butanol's hydrogen bonding capacity and causes it to form specific microstructures when mixed with water. In its mixtures with water, tert-butanol alters its hydrogen bonding network by arranging its molecules into localized clusters, and this directly affects the physical properties of the mixture. In this context, the study of tert-butanol/water mixtures is important both from a fundamental chemistry perspective and for industrial applications. In particular, relaxation time (T_2) measurements using time-domain nuclear magnetic resonance imaging (TD-NMR) techniques offer a powerful tool for understanding the microstructural arrangement and hydrogen bond interactions of the mixture.

Different liquid compounds and their combinations (such as alcohol-water mixtures) can be detected and distinguished using a range of procedures, which is essential for industrial and safety scenarios. These include nuclear magnetic resonance (NMR) (Jora et al., 2017; Rameev et al., 2012), X-ray scattering (Takamuku et al., 2002), infrared (IR) (Parker et al., 2014), and molecular dynamics simulations (MDS) (Pothoczki et al., 2018). There are numerous NMR subtypes within these approaches, including Time Domain NMR (TD-NMR), Earth's Magnetic Field NMR (EF-NMR), Solid State NMR (ss-NMR), Zero Field NMR, and High Field NMR. High field (HF) NMR spectroscopy is a highly sensitive technique for analyzing chemical structures, but it requires a cryogenic environment due to the usage of a superconducting magnet system. In this instance, NMR spectroscopy is too expensive and challenging to use in real-world settings. Since TD-NMR employs permanent magnet technology, a cryogenic apparatus is not necessary. Due to its low cost, ease of use, and portability, it might be better for applications involving security and quality control. The time-domain NMR (TD-NMR) technique differs from traditional NMR spectroscopy in that it measures relaxation times rather than spectrum information (Balcı 2020). TD-NMR yields two primary parameters: spin-spin (transverse, T_2) and spin-lattice (longitudinal, T_1) relaxation times. Different materials exhibit distinct relaxation behaviors, making the T_1 and T_2 relaxation times critical parameters for effective liquid screening and analysis (Malcolm H. Levitt et al., 2021). However, when multiple alcohols are present in the discrimination process,

relying solely on T_1 and T_2 values does not provide a sufficiently rapid or accurate detection method.

In this study, the spin-spin (T_2) and spin-lattice (T_1) relaxation times in tert-butanol/water mixtures were determined using both the Spinsolve device, which offers ease of desktop use, and the Minispec device, which stands out for its industrial reliability. The Magritek Spinsolve TD-NMR device operates at high resolution (42 MHz, 1 Tesla) using 5 mm NMR tubes, whereas the Bruker Minispec device functions at lower resolution (20 MHz, 0.5 Tesla) with 10 mm NMR tubes

2. MATERIAL and METHODS

Tert-butanol (99%, Sigma-Aldrich®) and deionized water (Milli-Q, 18.2 MΩ) were combined at varying molar fractions, and the mixtures were kept at room temperature. The samples were left motionless in the NMR apparatus for ten minutes before each measurement, and relaxation times T_2 and T_1 were subsequently determined in a series of alcohol–water mixtures with varying alcohol concentrations using two commercial instruments (Figures 1. a and b).



Figure 1. a) Bruker Minispec mq20 TD-NMR (20MHz-0.5Tesla) **(b)** Magritek Spinsolve NMR (42MHz-1Tesla)

3. RESULTS AND DISCUSSION

3.1.TD-NMR Properties of propanol-water mixtures

Two TD-NMR instruments were employed to determine T_1 and T_2 relaxation times using inversion recovery (IR) and Carr-Purcell–Meiboom–Gill (CPMG) pulse sequences, respectively, with the number of scans set to 2 for IR (T_1) and 4 for CPMG (T_2). The IR sequence, widely used for measuring spin-lattice relaxation (T_1), and the CPMG sequence, commonly applied for determining spin-spin relaxation (T_2), represent the standard approaches in TD-NMR analysis.

The relaxation curves for spin-lattice (T_1) and spin-spin (T_2) for each sample are presented in Figures 2 and 3.

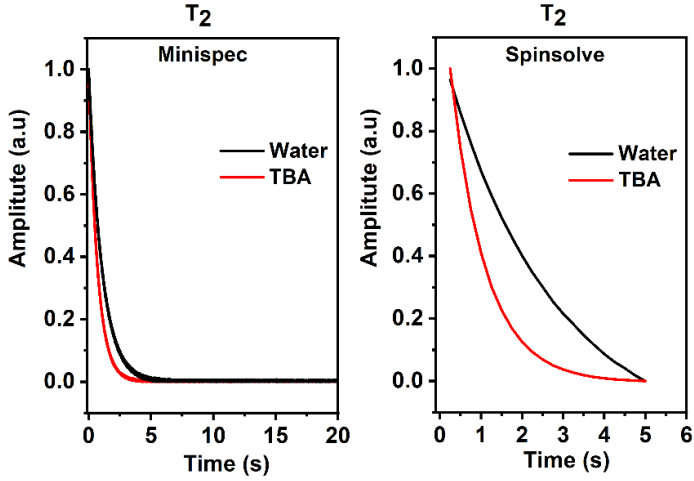


Figure 2. Spin-spin spectra for the Minispec and Spinsolve devices

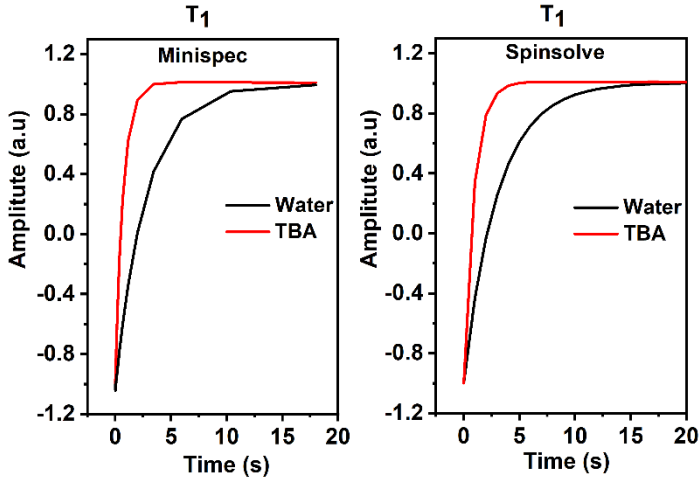


Figure 3. Spin-lattice spectra for the Minispec and Spinsolve devices

The T_1 and T_2 values were determined by applying exponential fitting to each sample's relaxation time curve. The graphs of T_2-relaxation rates T_2 and T_1, and relaxation rates T_1 for the molar fractions of TBA-water mixtures are displayed in Figures 4 and 5.

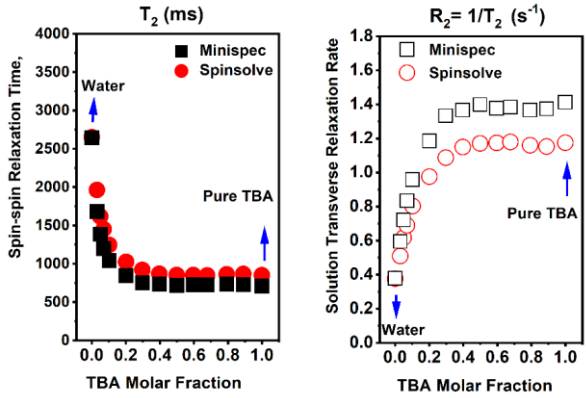


Figure 4. Spin-spin and relaxation rate times for the mixture.

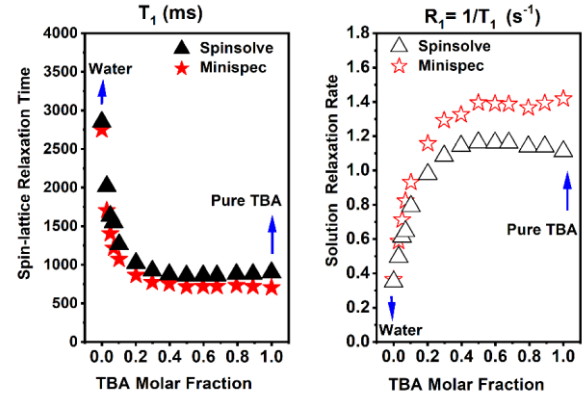


Figure 5. Spin-lattice and relaxation rate times for the mixture.

The graphs indicate that T_1 and T_2 values show similar trends across both instruments for identical chemical solutions, although the Bruker Minispec consistently yields lower relaxation times than the Magritek Spinsolve. The use of two different instruments enhanced the reliability of the results and allowed testing for device dependence. The comparison of findings obtained from the Spinsolve and Minispec devices demonstrates the consistency of the measurement techniques, while minor differences between the instruments can be attributed to magnetic field homogeneity. According to Maraşlı et al. (2023), the Magritek Spinsolve device exhibits significantly superior magnetic field homogeneity compared to the Bruker Minispec TD-NMR, which explains why higher T_1 and T_2 values are obtained when field homogeneity is improved. As expected for liquids, the results show that T_1 values are consistently slightly higher than T_2 values across all substances. This difference arises from the fundamental mechanisms of relaxation, where spin-lattice energy transfer governs T_1 and spin-spin interactions determine T_2. Since the spin-lattice distance

is greater than the distance between individual spins, T_1 is anticipated to be longer than T_2. Accordingly, the measurements obtained in this study support the hypothesis proposed by Ma et al. (2018). The findings obtained are consistent with the trends reported in the literature for alcohol–water mixtures (Jora et al., 2017). In similar systems reported in the literature (e.g., alcohol–water mixtures), T_2 has been shown to vary with solvent composition, with relaxation times decreasing as water content diminishes in solvents possessing high hydrogen-bonding capacity (Jora et al., 2017). Our findings are consistent with this trend and highlight that the sterically hindered structure of tert-butanol restricts its interactions with water, thereby exerting a significant influence on relaxation dynamics.

Moreover, the agreement between the results from the two different instruments demonstrates the reliability of T_2 measurements and their independence from device type. This approach not only serves as a powerful tool for understanding the microstructural organization of mixtures but also has potential applications in industrial contexts such as food quality control and solvent system characterization.

In this study, the proton spin–spin relaxation time (T_2) of tert-butanol/water mixtures were measured, and it was observed that T_2 values decreased as the water content diminished. This finding is consistent with changes in the mixture's microstructure. When water decreases, water molecules can no longer form an extensive hydrogen-bonding network; instead, they engage in more localized and stronger interactions with tert-butanol. This restricts the mobility of protons, enhances dipolar interactions, and consequently shortens T_2. In water-rich environments, molecules move more freely, and the hydrogen-bonding network becomes more dynamic, allowing protons to maintain coherence for longer periods and thereby extending T_2. In tert-butanol-rich environments, however, the bulky structure of tert-butanol encapsulates water molecules into localized clusters, increasing proton density within these regions and accelerating relaxation, which results in shorter T_2 values.

4. CONCLUSION

In this study, spin-lattice (T_1) and spin-spin (T_2) relaxation times of TBA/water mixtures were measured using two commercial TD-NMR instruments. The results obtained from both devices were consistent, with concentration-dependent relaxation times exhibiting the same trend for alcohol–water systems. Moreover, the Magritek Spinsolve produced longer T_1 and T_2 values compared to the Bruker Minispec, confirming congruence between the two instruments while highlighting device-specific differences.

Acknowledgment

I would like to thank Prof. Dr. Bulat Rami and Dr. Ayşe Maraşlı from Gebze Technical University for providing laboratory facilities and access to equipment.

REFERENCES

Balcı, M. (2020). Nükleer Manyetik Rezonans Spektroskopisi Eğitim Yaynevi. In Eğitim yayınevi (4.Baskı). -Türkiye.

Jora, M. Z., Cardoso, M. V. C., & Sabadini, E. (2017). Correlation between viscosity, diffusion coefficient and spin-spin relaxation rate in 1H NMR of water-alcohols solutions. *Journal of Molecular Liquids*, *238*, 341–346. https://doi.org/10.1016/j.molliq.2017.05.006

Malcolm H. Levitt, Svirmickas, A., Wood, M., Cunha, S. C., Oliveira, M. B. P. P., Moresi, G., Magin, R., Řezanka, T., Řezanková, H., Ancora, D., Milavec, J., Gradišek, A., Cifelli, M., Sepe, A., Apih, T., Zalar, B., Domenici, V., Mason, J., Nmr, M., … Liu, M. M. (2021). Spin Dynamics Basics of Nuclear Magnetic Resonance. *Physical Review*, *8*(1), 1–9. https://doi.org/10.1002/cmr.a.20130

Maraşlı, A., Okay, C., Karataş, Ö., Mozzhukhin, G., & Rameev, B. (2023). Comparison of homemade TD-NMR device and commercial devices for detection of oil adulteration. *European Physical Journal Plus*, *138*(5). https://doi.org/10.1140/epjp/s13360-023-03980-9

Ma, Y., Liu, Y., Su, H., Wang, L., & Zhang, J. (2018). Relationship between hydrogen bond and viscosity for a series of pyridinium ionic liquids: Molecular dynamics and quantum chemistry. *Journal of Molecular Liquids*, *255*, 176–184. https://doi.org/10.1016/j.molliq.2018.01.121

Parker, T., Limer, E., Watson, A. D., Defernez, M., Williamson, D., & Kemsley, E. K. (2014). 60MHz 1H NMR spectroscopy for the analysis of edible oils. In *TrAC - Trends in Analytical Chemistry*. Elsevier Ltd. https://doi.org/10.1016/j.trac.2014.02.006

Pothoczki, S., Pusztai, L., & Bakó, I. (2018). Temperature dependent dynamics in water-ethanol liquid mixtures. *Journal of Molecular Liquids*, *271*, 571–579. https://doi.org/10.1016/j.molliq.2018.09.027

Rameev, B., Mozzhukhin, G., & Aktaş, B. (2012). Magnetic Resonance Detection of Explosives and Illicit Materials. *Applied Magnetic Resonance*, *43*(4), 463–467. https://doi.org/10.1007/s00723-012-0423-9

Takamuku, T., Saisho, K., Aoki, S., & Yamaguchi, T. (2002). Large-angle X-ray scattering investigation of the structure of 2-propanol-water mixtures. *Zeitschrift Fur Naturforschung - Section A Journal of Physical Sciences*, *57*(12), 982–994. https://doi.org/10.1515/zna-2002-1213

CHAPTER 6

Optimal Boundary Control of Vibration Problems: Modeling, Regularization, and The Adjoint Method

Hakkı Güngör[1]

[1] Ufuk University, ORCİD: 0000-0002-9546-665X

Introduction

Boundary control of a vibrating string seeks time-dependent endpoint forces that produce a desired motion. The displacement evolves according to a wave equation, so an input applied at an endpoint influences the interior through propagation and reflection. Although there are only two possible actuation locations in the model considered here, each input is a function of time and the optimization problem is infinite-dimensional.

The formulation requires separate specifications of actuation and observation. Endpoint forces may be chosen to track prescribed endpoint displacements, an interior displacement field, or both. This distinction is part of the classical formulation of optimal control for systems governed by partial differential equations (Lions, 1971). Modern treatments develop the associated functional analysis, adjoint equations, and numerical approximation in a common framework (Hinze et al., 2009; Manzoni et al., 2021).

Several related studies motivate the present formulation. Subaşı et al. (2012) considered a hyperbolic boundary control problem with a final-state objective, derived its Fréchet derivative through an adjoint problem, and used a variational inequality to characterize constrained optimal controls. Gugat et al. (2016) investigated optimal Neumann control of a one-dimensional wave equation with one fixed endpoint, including boundary tracking and the effect of the time horizon. These configurations differ from the two independently actuated endpoints and time-integrated displacement observations used below.

This chapter develops an expository treatment motivated by the vibration control problem studied in the author's doctoral thesis (Güngör, 2017). It retains the variable-coefficient wave model and presents a unified formulation for endpoint and distributed displacement tracking, single-actuator restrictions, and pointwise control bounds. The control variables throughout are boundary fluxes; the observed quantities are displacements. Velocity observations would require a separate trace analysis.

The main argument connects the energy solution of the state equation to a strongly convex reduced objective. A positive quadratic control penalty yields a unique minimizer and stability with respect to the target. An adjoint wave equation gives an explicit gradient, from which unconstrained and constrained optimality conditions follow. The final sections describe a projected-gradient method and construct an exact analytical benchmark. The optimization results are standard consequences of linear-quadratic control theory, stated with proofs for the present setting; the benchmark is intended for verification of numerical implementations.

Mathematical Model and Boundary Actuation

Let $l > 0$ be the length of the string, $T > 0$ the observation horizon, and $\Omega = (0, l) \times (0, T)$. The displacement $u = u(x, t)$ satisfies

$$\rho(x)u_{tt} - (k(x)u_x)_x = F(x,t),\ (x,t) \in \Omega. \tag{1}$$

Here ρ is the mass density, k is an effective elastic coefficient, and F is a prescribed distributed force. We assume

$$\rho, k \in C^1([0,l]), 0 < \rho_0 \le \rho(x) \le \rho_1, 0 < k_0 \le k(x) \le k_1. \tag{2}$$

The initial conditions and data spaces are

$$\begin{gathered} u(x,0) = \varphi_1(x), u_t(x,0) = \varphi_2(x), \\ \varphi_1 \in H^1(0,l), \varphi_2 \in L^2(0,l), F \in L^2(\Omega). \end{gathered} \tag{3}$$

We introduce the controls through the Neumann conditions

$$k(0)u_x(0,t) = f(t),\ k(l)u_x(l,t) = g(t). \tag{4}$$

With the spatial coordinate directed from left to right, the outward fluxes are $-f$ and g, respectively. This convention fixes the boundary signs in the weak formulation and the adjoint gradient.

The control space is $\mathcal{U} = L^2(0,T) \times L^2(0,T)$, with $h = (f, g)$ and

$$\langle h, \tilde{h} \rangle_{\mathcal{U}} = \int_0^T \left(f\tilde{f} + g\tilde{g} \right)\, dt,\ \| h \|_{\mathcal{U}}^2 = \int_0^T (f^2 + g^2)\, dt. \tag{5}$$

The admissible set $\mathcal{U}_{\mathrm{ad}} \subset \mathcal{U}$ is nonempty, closed, and convex. Unrestricted actuation corresponds to $\mathcal{U}_{\mathrm{ad}} = \mathcal{U}$. Pointwise amplitude restrictions take the form

$$f_a(t) \le f(t) \le f_b(t),\ g_a(t) \le g(t) \le g_b(t) \text{ a.e. in } (0,T), \tag{6}$$

where the bounds belong to $L^\infty(0,T)$ and are ordered almost everywhere. A single left actuator can be represented by $\mathcal{U}_{\mathrm{ad}} = \{(f, 0) : f \in \mathcal{F}_{\mathrm{ad}}\}$, for a nonempty closed convex set $\mathcal{F}_{\mathrm{ad}} \subset L^2(0,T)$. In this case the inactive right endpoint has zero Neumann data. A fixed right displacement would instead require a different boundary condition in the state equation.

Weak solutions permit square-integrable inputs without imposing classical corner compatibility conditions. The use of integral identities and energy estimates for hyperbolic initial-boundary value problems follows the framework described by Ladyzhenskaya (1985). In the present model, a displacement with $u(\cdot, 0) = \varphi_1$ satisfies

$$\int_0^T \int_0^l (-\rho u_t v_t + k u_x v_x)\ dx\ dt = \int_0^T \int_0^l F\ v\ dx\ dt + \int_0^T [g(t)v(l,t) - f(t)v(0,t)]\ dt + \int_0^l \rho\,(x)\varphi_2(x)v(x,0)\ dx \tag{7}$$

for every $v \in H^1(\Omega)$ with $v(\cdot, T) = 0$. Endpoint evaluation is continuous on $H^1(0, l)$. For example,

$$|v(0)|^2 + |v(l)|^2 \leq \frac{4}{l} \parallel v \parallel^2_{L^2(0,l)} + 4l \parallel v_x \parallel^2_{L^2(0,l)}. \tag{8}$$

For smooth v, this follows by expressing an endpoint value in terms of $v(x)$ and the integral of v_x, applying Cauchy–Schwarz, and averaging over x. Density extends the inequality to $H^1(0, l)$. Applying it at almost every time establishes the boundedness of the endpoint displacement traces used below.

For sufficiently smooth solutions, the mechanical energy and its balance law are

$$E(t) = \frac{1}{2}\int_0^l \left(\rho u_t^2 + k u_x^2\right)\ dx, \qquad E'(t) = \int_0^l F\, u_t\ dx + g(t)u_t(l,t) - f(t)u_t(0,t). \tag{9}$$

The boundary terms represent mechanical power. This identity is used here as a physical interpretation for smooth data. Its extension to weak solutions requires boundary velocity estimates; inequality (8), which concerns displacement, does not by itself provide them.

Tracking Objectives and Regularization

Let $y_1, y_2 \in L^2(0, T)$ be desired endpoint displacements and $u_d \in L^2(\Omega)$ a desired interior displacement. Consider

$$J_\alpha(h) = \frac{\beta_1}{2}\int_0^T [u(0,t;h) - y_1(t)]^2\ d t + \frac{\beta_2}{2}\int_0^T [u(l,t;h) - y_2(t)]^2\ dt + \frac{\mu}{2}\int_0^T \int_0^l [u(x,t;h) - u_d(x,t)]^2\ dx\ dt + \frac{\alpha}{2}\int_0^T [f(t)^2 + g(t)^2]\ dt, \tag{10}$$

where $\beta_1, \beta_2, \mu \geq 0, \beta_1 + \beta_2 + \mu > 0$, and $\alpha > 0$. The problem is to minimize J_α over $\mathcal{U}_{\text{ad}}$.

The observation configurations are distinguished as follows:

- Endpoint tracking: $\mu = 0$ and $\beta_1 + \beta_2 > 0$.
- Distributed tracking: $\beta_1 = \beta_2 = 0$ and $\mu > 0$.

- Combined tracking: $\mu > 0$ and $\beta_1 + \beta_2 > 0$.

The controls remain boundary forces in each case. The final term in (10) penalizes their squared magnitude and is therefore a control-effort penalty. It is not mechanical work, which also depends on endpoint velocity. The weights must account for the physical units or nondimensionalization of the quantities being compared.

The quadratic penalty has the structure of Tikhonov regularization for an operator equation (Engl et al., 1996). In optimal control, it also represents the chosen cost of applying an input. These interpretations do not require the same parameter-selection rule: a prescribed actuator cost and a regularization parameter chosen from noisy data serve different purposes. Here α is fixed and positive; convergence as $\alpha \to 0$ is not asserted.

Define $\mathcal{X} = L^2\big(0,T;H^1(0,l)\big)$ and $\mathcal{Y} = L^2(0,T) \times L^2(0,T) \times L^2(\Omega)$. The observation operator and target vector are

$$\begin{aligned} \mathcal{O}u &= \big(\sqrt{\beta_1}u(0,\cdot), \sqrt{\beta_2}u(l,\cdot), \sqrt{\mu}u\big), \\ y_d &= \big(\sqrt{\beta_1}y_1, \sqrt{\beta_2}y_2, \sqrt{\mu}u_d\big). \end{aligned} \tag{11}$$

Inequality (8) implies that $\mathcal{O}: \mathcal{X} \to \mathcal{Y}$ is bounded. Hence the objective can be written as

$$J_\alpha(h) = \tfrac{1}{2} \| \mathcal{O}u(h) - y_d \|_{\mathcal{Y}}^2 + \tfrac{\alpha}{2} \| h \|_U^2. \tag{12}$$

Well-Posedness and Existence of Optimal Controls

Under (2)–(4), the one-dimensional Neumann wave problem has a unique energy solution with

$$u \in C\Big([0,T];H^1(0,l)\Big),\ u_t \in C\Big([0,T];L^2(0,l)\Big), \tag{13}$$

and the estimate

$$\begin{aligned} &\| u \|_{C([0,T];H^1)} + \| u_t \|_{C([0,T];L^2)} \\ &\le C\big(\| \varphi_1 \|_{H^1} + \| \varphi_2 \|_{L^2} + \| F \|_{L^2(\Omega)} + \| h \|_U\big). \end{aligned} \tag{14}$$

The spatial spaces without explicit intervals in (14) are defined on $(0,l)$. The constant may depend on the coefficients, l, and T, but not on h.

The boundary-input regularity in (14) needs more than the displacement trace estimate. A precise route is to set $z = (\rho u_t, u_x)^{\mathsf{T}}$ and write

$$z_t = P_1(\mathcal{H}z)_x + \binom{F}{0},\ P_1 = \begin{pmatrix} 0 & 1 \\ 1 & 0 \end{pmatrix},\ \mathcal{H} = \begin{pmatrix} \rho^{-1} & 0 \\ 0 & k \end{pmatrix}. \tag{15}$$

The homogeneous Neumann realization is conservative in its weighted energy space. Positivity and C^1 regularity provide a C^1 characteristic diagonalization, with characteristic speeds $\pm\sqrt{k/\rho}$. The one-dimensional boundary well-posedness result of Zwart et al. (2010, Theorem 2.4) therefore applies to the momentum and strain variables. The distributed source is included by the variation-of-constants formula. Recovering u from its initial value and u_t also controls its spatially constant component, which the strain alone cannot determine. The abstract distinction between an unbounded boundary input operator and its admissible action over time is treated by Tucsnak and Weiss (2009).

Let $u^{(0)} = u(0)$ denote the state for zero boundary control, with the original source and initial data retained. Linearity and (14) give

$$u(h) = u^{(0)} + Sh,\ S{:}\,\mathcal{U} \to \mathcal{X} \text{ bounded and linear.} \tag{16}$$

With $G = \mathcal{O}S$ and $d = y_d - \mathcal{O}u^{(0)}$, the reduced objective is

$$J_\alpha(h) = \frac{1}{2} \parallel Gh - d \parallel_{\mathcal{Y}}^2 + \frac{\alpha}{2} \parallel h \parallel_{\mathcal{U}}^2. \tag{17}$$

The following propositions specialize the standard Hilbert-space arguments for quadratic optimal control to this reduced problem (Lions, 1971; Hinze et al., 2009).

Proposition 1. Existence and uniqueness. *If $G{:}\,\mathcal{U} \to \mathcal{Y}$ is bounded and linear, $\alpha > 0$, and $\mathcal{U}_{ad}$ is nonempty, closed, and convex, then J_α has a unique minimizer on $\mathcal{U}_{ad}$.*

Proof. *Since $J_\alpha(h) \geq (\alpha/2) \parallel h \parallel_{\mathcal{U}}^2$, a minimizing sequence is bounded. A subsequence converges weakly to some $h^* \in \mathcal{U}$. The admissible set is weakly closed because it is closed and convex. Bounded linearity of G preserves weak convergence, and squared norms are weakly lower semicontinuous. Thus h^* is admissible and attains the infimum. For $0 < \theta < 1$, direct expansion gives*

$$\begin{aligned} J_\alpha(\theta h_1 + (1-\theta)h_2) &= \theta J_\alpha(h_1) + (1-\theta) J_\alpha(h_2) \\ &\quad - \frac{\theta(1-\theta)}{2}\left(\parallel G(h_1 - h_2) \parallel_{\mathcal{Y}}^2 + \alpha \parallel h_1 - h_2 \parallel_{\mathcal{U}}^2 \right). \end{aligned} \tag{18}$$

If $h_1 \neq h_2$, the last term is strictly negative. Strict convexity proves uniqueness.

For any perturbation $\delta h \in \mathcal{U}$, the exact expansion is

$$\begin{aligned} J_\alpha(h + \delta h) - J_\alpha(h) &= \langle G^*(Gh - d) + \alpha h, \delta h \rangle_{\mathcal{U}} \\ &\quad + \frac{1}{2} \parallel G\delta h \parallel_{\mathcal{Y}}^2 + \frac{\alpha}{2} \parallel \delta h \parallel_{\mathcal{U}}^2. \end{aligned} \tag{19}$$

The remainder is $O(\| \delta h \|_{\mathcal{U}}^2)$*, which establishes Fréchet differentiability. Identifying the derivative with its Riesz representative in* $\mathcal{U}$ *yields*

$$\nabla J_\alpha(h) = G^*(Gh - d) + \alpha h,\ L = \| G \|^2 + \alpha. \tag{20}$$

The gradient is Lipschitz with constant L. It is also strongly monotone, since

$$\begin{aligned}\langle \nabla J_\alpha(h_1) - \nabla J_\alpha(h_2), h_1 - h_2 \rangle_{\mathcal{U}} &= \| G(h_1 - h_2) \|_Y^2 \\ &+ \alpha \| h_1 - h_2 \|_{\mathcal{U}}^2 \geq \alpha \| h_1 - h_2 \|_{\mathcal{U}}^2.\end{aligned} \tag{21}$$

Proposition 2. Stability with respect to the target. *Let* h_1^*, h_2^* *minimize (17) for targets* d_1, d_2*, with* G*,* α*, and* $\mathcal{U}_{ad}$ *fixed. Then*

$$\| h_1^* - h_2^* \|_{\mathcal{U}} \leq \frac{\|G\|}{\alpha} \| d_1 - d_2 \|_Y. \tag{22}$$

Proof. Convex minimization gives $\langle G^*(Gh_i^* - d_i) + \alpha h_i^*, h - h_i^* \rangle_{\mathcal{U}} \geq 0$ for every admissible h. Use $h = h_2^*$ in the first inequality and $h = h_1^*$ in the second. With $\Delta h = h_1^* - h_2^*$, addition yields

$$\| G\Delta h \|_Y^2 + \alpha \| \Delta h \|_{\mathcal{U}}^2 \leq \langle d_1 - d_2, G\Delta h \rangle_Y.$$

Cauchy–Schwarz and boundedness of G *prove (22), including the trivial case* $\Delta h = 0$*. This estimate concerns target perturbations; changes in the coefficients or observation operator also change* G *and need separate estimates.*

The effect of the control penalty can be characterized without an explicit solution. Write $R(h) = \frac{1}{2} \| Gh - d \|_Y^2$ *and* $Q(h) = \frac{1}{2} \| h \|_{\mathcal{U}}^2$*. For* $0 < \alpha_1 < \alpha_2$*, optimality of* h_{α_1} *and* h_{α_2} *gives*

$$\begin{aligned}R(h_{\alpha_1}) + \alpha_1 Q(h_{\alpha_1}) &\leq R(h_{\alpha_2}) + \alpha_1 Q(h_{\alpha_2}), \\ R(h_{\alpha_2}) + \alpha_2 Q(h_{\alpha_2}) &\leq R(h_{\alpha_1}) + \alpha_2 Q(h_{\alpha_1}).\end{aligned}$$

Adding these inequalities, then substituting back into the first, proves

$$\| h_{\alpha_2} \|_{\mathcal{U}} \leq \| h_{\alpha_1} \|_{\mathcal{U}},\ \| Gh_{\alpha_1} - d \|_Y \leq \| Gh_{\alpha_2} - d \|_Y. \tag{23}$$

These comparisons hold for exact minimizers with the same data and admissible set. They are useful consistency checks when varying α *in computations.*

The Adjoint Method and Optimality Conditions

The abstract gradient (20) can be evaluated through an adjoint PDE. This is the standard approach in PDE-constrained optimization (Hinze et al., 2009); a related hyperbolic boundary-control derivation appears in Subaşı et al. (2012). Here the observation terms determine the adjoint boundary conditions and source explicitly.

For $\delta h = (\delta f, \delta g)$, the increment $w = S\delta h$ solves the homogeneous wave equation with zero initial data and boundary fluxes $\delta f, \delta g$. Set $e_1 = u(0,\cdot) - y_1$, $e_2 = u(l,\cdot) - y_2$, and $e = u - u_d$. Differentiation gives

$$J_\alpha'(h)[\delta h] = \beta_1 \int_0^T e_1\, w(0,t)\, dt + \beta_2 \int_0^T e_2\, w(l,t)\, dt + \mu \int_\Omega e\, w\, dx\, dt + \alpha \int_0^T (f\delta f + g\delta g)\, dt. \tag{24}$$

Choose the Lagrangian sign convention $J_\alpha + \int_\Omega \eta\, [\rho u_{tt} - (k u_x)_x - F]$. The corresponding adjoint problem is

$$\begin{gathered} \rho\eta_{tt} - (k\eta_x)_x = -\mu e \text{in } \Omega, \\ k(0)\eta_x(0,t) = \beta_1 e_1(t), k(l)\eta_x(l,t) = -\beta_2 e_2(t), \\ \eta(x,T) = 0, \eta_t(x,T) = 0. \end{gathered} \tag{25}$$

The terminal conditions are zero because (10) has no terminal observation term. Time reversal converts (25) into a forward problem of the same regularity class as the state equation. In particular, its endpoint displacement traces belong to $L^2(0,T)$.

For smooth functions, Green's identity gives

$$\int_\Omega [\eta(\rho w_{tt} - (k w_x)_x) - w(\rho\eta_{tt} - (k\eta_x)_x)]\, dx\, dt = \int_0^T [k(w\eta_x - \eta w_x)]_0^l\, dt.$$

where the temporal boundary terms vanish by the initial conditions of w and terminal conditions of η. Substituting their equations and boundary data yields

$$\beta_1 \int_0^T e_1\, w(0,t)\, dt + \beta_2 \int_0^T e_2\, w(l,t)\, dt + \mu \int_\Omega e\, w\, dx\, dt = \int_0^T [\eta(0,t)\delta f - \eta(l,t)\delta g]\, dt. \tag{26}$$

Approximation by smooth data extends (26) to energy solutions using (14) and the displacement trace estimate. Thus

$$\nabla J_\alpha(h) = \big(\alpha f + \eta(0,\cdot),\ \alpha g - \eta(l,\cdot)\big). \tag{27}$$

For unrestricted controls, the unique minimizer satisfies

$$f^*(t) = -\frac{\eta^*(0,t)}{\alpha},\ g^*(t) = \frac{\eta^*(l,t)}{\alpha}. \tag{28}$$

For a general admissible set, the necessary and sufficient condition is

$$\langle \nabla J_\alpha(h^*), h - h^* \rangle_U \geq 0 \text{ for all } h \in \mathcal{U}_{\text{ad}}. \tag{29}$$

The equivalence with a projection fixed point follows from the characterization of metric projections onto closed convex sets in Hilbert spaces (Bauschke & Combettes, 2017):

$$h^* = P_{\mathcal{U}_{\text{ad}}}\big(h^* - \tau \nabla J_\alpha(h^*)\big),\ \tau > 0. \tag{30}$$

For the box constraints (6), this becomes

$$\begin{aligned} f^*(t) &= P_{[f_a(t), f_b(t)]}\left(-\frac{\eta^*(0,t)}{\alpha}\right), \\ g^*(t) &= P_{[g_a(t), g_b(t)]}\left(\frac{\eta^*(l,t)}{\alpha}\right), \end{aligned} \tag{31}$$

where $P_{[a,b]}(s) = \min\{b, \max\{a, s\}\}$. The state, adjoint, and projected control must be solved together. In general, clipping a previously computed unconstrained control once does not solve the constrained problem, because the resulting state changes the adjoint.

Computational Strategies

The projected-gradient iteration is

$$h^{m+1} = P_{\mathcal{U}_{\text{ad}}}\big(h^m - \tau_m \nabla J_\alpha(h^m)\big),\ h^0 \in \mathcal{U}_{\text{ad}}. \tag{32}$$

At each iteration, solve the state equation forward, evaluate the observation errors, solve (25) backward, and form (27). Select a step length, apply the projection, and test the optimality residual. A fixed-step update needs one forward and one adjoint solve to evaluate its gradient; a line search can require additional forward solves for trial objective values. The connection between reduced objectives, adjoint gradients, and their numerical approximation is discussed by Manzoni et al. (2021).

For this quadratic problem, convergence follows directly. The self-adjoint operator $A = G^*G + \alpha I$ has spectrum in $[\alpha, L]$, where L is defined in (20). Nonexpansiveness of the projection gives

$$\begin{aligned} \| h^{m+1} - h^* \|_{\mathcal{U}} &\leq q \| h^m - h^* \|_{\mathcal{U}}, \\ q &= \max\{|1 - \tau\alpha|, |1 - \tau L|\}. \end{aligned} \tag{33}$$

Thus $0 < \tau < 2/L$ ensures $q < 1$. Choosing $\tau = 1/L$ gives $q \leq 1 - \alpha/L$. A small α relative to $\| G \|^2$ can therefore make the basic gradient method slow. The nonexpansive-operator framework underlying this estimate is developed by Bauschke and Combettes (2017).

When L is unavailable, a backtracking rule can enforce sufficient decrease. Such line-search principles are treated by Nocedal and Wright (2006). For $h^+ = P_{\mathcal{U}_{\text{ad}}}\big(h - \tau \nabla J_\alpha(h)\big)$, require

$$J_\alpha(h^+) \le J_\alpha(h) - \frac{\sigma}{\tau} \| h^+ - h \|_{\mathcal{U}}^2, \ 0 < \sigma < 1. \tag{34}$$

The projection inequality and Lipschitz gradient bound imply acceptance whenever $\tau \le 2(1-\sigma)/L$. Repeatedly multiplying the trial step by a fixed factor in $(0,1)$ therefore terminates.

A suitable stopping measure is the projected-gradient residual

$$r_\tau(h) = \frac{1}{\tau}\left[h - P_{\mathcal{U}_{\text{ad}}}\left(h - \tau \nabla J_\alpha(h)\right)\right], \ \frac{\|r_\tau(h^m)\|_{\mathcal{U}}}{\max\{1, \|h^m\|_{\mathcal{U}}\}} \le \varepsilon_{\text{opt}}. \tag{35}$$

For a fixed positive test step, $r_\tau(h) = 0$ is equivalent to (29). Objective changes and iteration counts are useful additional diagnostics, but do not replace this optimality check.

The discrete gradient should be consistent with both the discretized objective and the chosen control inner product. For amplitude-constrained controls, pointwise clipping is appropriate only when it represents the projection associated with that inner product (Hinze et al., 2009).

A directional derivative check should be performed before optimization:

$$R(\varepsilon) = \left| J_\Delta(h + \varepsilon \delta h) - J_\Delta(h) - \varepsilon \langle \nabla J_\Delta(h), \delta h \rangle_{\mathcal{U}_\Delta} \right|. \tag{36}$$

For a consistent gradient, $R(\varepsilon)$ decays quadratically until solver or floating-point errors dominate. The control inner product and quadrature must be identical in this check and in the algorithm. An adjoint of the discrete state equations provides a direct way to preserve the derivative of the discrete objective.

Wave discretizations also require refinement checks. Ervedoza and Zuazua (2013) analyze numerical approximation of exact wave controls, where high-frequency behavior can obstruct uniform discrete controllability. Those results do not automatically imply convergence for the present regularized tracking problem. They do motivate checking state accuracy, objective values, and optimality residuals together as the spatial and temporal grids are refined. No finite-element or finite-difference convergence theorem is claimed here.

An Analytical Boundary Control Example

We construct an exact example to verify both gradient signs and the complete optimality system. Set $l = 1$, $T = 1/2$, $\rho = k = 1$, $F = 0$, and take zero initial displacement and velocity. The boundary conditions remain $u_x(0,t) = f(t)$ and $u_x(1,t) = g(t)$. Choose $\alpha = 1$, $\beta_1 = \beta_2 = 1$, $\mu = 0$, and unrestricted controls.

Because $T < 1$, an input at either endpoint cannot reach the opposite endpoint during the observation interval. For arbitrary controls in $L^2(0,T)$, the state is

$$u(x,t) = -\int_0^{(t-x)_+} f(s)\, ds + \int_0^{\left(t-(1-x)\right)_+} g(s)\, ds,$$

$$r_+ = \max\{r, 0\}. \tag{37}$$

In particular, $u(0,t) = -(Vf)(t)$ and $u(1,t) = (Vg)(t)$, where $(Vq)(t) = \int_0^t q\,(s)\,ds$. Cauchy–Schwarz gives

$$\| Vq \|^2_{L^2(0,T)} \leq \int_0^T t \int_0^t |q(s)|^2 \; ds\, dt \leq \frac{T^2}{2} \| q \|^2_{L^2(0,T)}. \tag{38}$$

Thus the observation map is bounded directly, with $G = \mathrm{diag}(-V, V)$ in the two nonzero observation components.

Define $\phi(s) = \sin^4(\pi s/T)$ for $0 \leq s \leq T$, and set $\phi(s) = 0$ outside this interval. Let $W(s) = \int_0^s \phi\,(r)\,dr$. On $[0,T]$,

$$W(s) = \frac{3s}{8} - \frac{T}{4\pi}\sin\left(\frac{2\pi s}{T}\right) + \frac{T}{32\pi}\sin\left(\frac{4\pi s}{T}\right). \tag{39}$$

For real amplitudes a, b, prescribe

$$\begin{aligned} f^*(t) = -a\phi(t), g^*(t) = b\phi(t), \\ u^*(x,t) = aW(t-x) + bW\big(t-(1-x)\big). \end{aligned} \tag{40}$$

Since W vanishes for negative arguments, (40) satisfies the initial conditions. Differentiation verifies the wave equation and boundary conditions, while the endpoint displacements are $u^*(0,t) = aW(t)$ and $u^*(1,t) = bW(t)$.

Choose the desired trajectories as

$$y_1(t) = a[W(t) - \phi'(t)],\; y_2(t) = b[W(t) - \phi'(t)]. \tag{41}$$

These are manufactured targets chosen so that the optimizer is known. Consider

$$\eta^*(x,t) = a\phi(T-t-x) + b\phi\big(T-t-(1-x)\big). \tag{42}$$

Each summand is a traveling wave, and the support and endpoint derivatives of ϕ give $\eta^*(\cdot,T) = \eta^*_t(\cdot,T) = 0$. The identities $\phi(T-t) = \phi(t)$ and $\phi'(T-t) = -\phi'(t)$ imply

$$\begin{aligned} \eta^*_x(0,t) = a\phi'(t) = u^*(0,t) - y_1(t), \\ \eta^*_x(1,t) = -b\phi'(t) = -[u^*(1,t) - y_2(t)]. \end{aligned} \tag{43}$$

Hence (43) solves the adjoint problem. Its endpoint values are $a\phi(t)$ and $b\phi(t)$, so

$$f^* + \eta^*(0,\cdot) = 0,\; g^* - \eta^*(1,\cdot) = 0. \tag{44}$$

Equation (27) gives $\nabla J_1(h^*) = 0$. Proposition 1 therefore proves that the constructed pair is the unique global minimizer.

The benchmark provides exact objective values as well. Elementary integration yields

$$\int_0^T \phi\,(t)^2\,dt = \frac{35T}{128},\ \int_0^T \phi\,'(t)^2\,dt = \frac{5\pi^2}{8T}. \tag{45}$$

Consequently,

$$\begin{gathered} \| h^* \|_{\mathcal{U}}^2 = (a^2+b^2)\frac{35T}{128}, \\ \| u^*(0,\cdot) - y_1 \|_{L^2}^2 + \| u^*(1,\cdot) - y_2 \|_{L^2}^2 = (a^2+b^2)\frac{5\pi^2}{8T}, \\ J_1(h^*) = (a^2+b^2)\left(\frac{5\pi^2}{16T} + \frac{35T}{256}\right). \end{gathered} \tag{46}$$

For $a = 1$, $b = 1/2$, and $T = 1/2$, the squared control norm is 0.1708984375, the sum of squared endpoint tracking errors is approximately 15.4212568767, and $J_1(h^*) \approx 7.7960776571$. The continuous optimality residual is exactly zero. These values are analytical reference quantities, not results of a discretized optimization experiment.

Taking $b = 0$ gives a left-actuator benchmark, while $a = b$ gives equal-amplitude actuation. If box constraints contain (41), the same pair remains optimal. Bounds excluding it require a new solution of the coupled constrained system. The short horizon makes (38) especially simple; longer horizons introduce reflections and cannot use the same representation without modification.

Discussion and Conclusions

The displacement-tracking formulation leads to a well-defined, strongly convex optimization problem once the one-dimensional boundary-input estimate is established. Its optimality system makes the effect of the observations explicit: endpoint errors enter the adjoint Neumann data, while interior errors enter its source. Control constraints are incorporated through a variational inequality and projection, and the analytical benchmark supplies a complete state–adjoint–control solution with exact objective values.

The analysis assumes linear dynamics, positive C^1 coefficients, displacement observations, and a positive quadratic control penalty. It does not establish exact controllability, convergence as the penalty vanishes, or numerical convergence under mesh refinement. Velocity tracking and penalties on temporal control derivatives require different observation or control spaces. A natural computational continuation is to use the benchmark to verify the discrete gradient, then study variable coefficients, active amplitude constraints, and horizons long enough to include reflected waves.

References

Bauschke, H. H., & Combettes, P. L. (2017). *Convex analysis and monotone operator theory in Hilbert spaces* (2nd ed.). Cham, Switzerland: Springer. doi:10.1007/978-3-319-48311-5

Engl, H. W., Hanke, M., & Neubauer, A. (1996). *Regularization of inverse problems*. Dordrecht, Netherlands: Kluwer Academic Publishers.

Ervedoza, S., & Zuazua, E. (2013). *Numerical approximation of exact controls for waves*. New York, NY: Springer. doi:10.1007/978-1-4614-5808-1

Gugat, M., Trélat, E., & Zuazua, E. (2016). Optimal Neumann control for the 1D wave equation: Finite horizon, infinite horizon, boundary tracking terms and the turnpike property. *Systems & Control Letters, 90*, 61–70. doi:10.1016/j.sysconle.2016.02.001

Güngör, H. (2017). *Bir titreşim probleminde uç noktalardaki hız için optimal kontrol problemi* (Unpublished doctoral dissertation). Atatürk University, Erzurum, Turkey.

Hinze, M., Pinnau, R., Ulbrich, M., & Ulbrich, S. (2009). *Optimization with PDE constraints*. Dordrecht, Netherlands: Springer. doi:10.1007/978-1-4020-8839-1

Ladyzhenskaya, O. A. (1985). *The boundary value problems of mathematical physics*. New York, NY: Springer. doi:10.1007/978-1-4757-4317-3

Lions, J.-L. (1971). *Optimal control of systems governed by partial differential equations*. Berlin, Germany: Springer.

Manzoni, A., Quarteroni, A., & Salsa, S. (2021). *Optimal control of partial differential equations: Analysis, approximation, and applications*. Cham, Switzerland: Springer. doi:10.1007/978-3-030-77226-0

Nocedal, J., & Wright, S. J. (2006). *Numerical optimization* (2nd ed.). New York, NY: Springer. doi:10.1007/978-0-387-40065-5

Subaşı, M., Saraç, Y., & Kaçar, A. (2012). A variational technique for optimal boundary control in a hyperbolic problem. *Applied Mathematics and Computation, 218*(12), 6629–6636. doi:10.1016/j.amc.2011.12.053

Tucsnak, M., & Weiss, G. (2009). *Observation and control for operator semigroups*. Basel, Switzerland: Birkhäuser. doi:10.1007/978-3-7643-8994-9

Zwart, H., Le Gorrec, Y., Maschke, B., & Villegas, J. (2010). Well-posedness and regularity of hyperbolic boundary control systems on a one-dimensional spatial domain. *ESAIM: Control, Optimisation and Calculus of Variations, 16*(4), 1077–1093. doi:10.1051/cocv/2009036

CHAPTER 7

Drug Resistance in Breast Cancer: Subtype-Specific Mechanisms and Strategies to Overcome Treatment Failure

İdil Çetin[1]
Mehmet Topçul[2]

[1] Assoc. Prof. Dr., Department of Biology, Faculty of Science, Istanbul University, Istanbul, Turkey, ORCID: 0000-0002-3961-6422
[2] Prof. Dr., Department of Biology, Faculty of Science, Istanbul University, Istanbul, Turkey, ORCID: 0000-0002-9685-9404

1. Introduction

Breast cancer does not represent a molecularly or clinically homogeneous disease. Rather, it comprises a collection of biologically distinct entities that happen to arise from the same organ. The Luminal A, Luminal B, HER2-enriched, and triple-negative (TNBC) subtypes, defined according to estrogen receptor (ER), progesterone receptor (PR), and HER2 expression status, were first delineated through gene expression profiling as the "intrinsic subtypes" of breast cancer, a classification that reorganized the disease around its underlying molecular drivers rather than histological appearance alone (Perou et al., 2000; Sørlie et al., 2001). These subtypes are each associated with distinct treatment approaches and, consequently, distinct patterns of resistance (Prat et al., 2015). In hormone receptor–positive tumors, resistance to endocrine therapy predominates; in HER2-positive tumors, resistance to anti-HER2 agents; and in TNBC, resistance to cytotoxic chemotherapy and, increasingly, to immunotherapy.

This subtype framework, while clinically indispensable, represents a simplification of a more continuous and heterogeneous biological reality. Within a single clinically defined subtype, intratumoral heterogeneity at the genomic, transcriptomic, and cellular level is now well documented, and even individual tumors can harbor subpopulations that would be classified differently if sampled in isolation (Turashvili & Brogi, 2017). This heterogeneity has direct implications for resistance: a treatment that eliminates the dominant clonal population within a tumor may leave a minority subpopulation, biologically distinct from the bulk tumor at diagnosis, to expand under the resulting selective pressure. The subtype-specific mechanisms discussed in this chapter should therefore be understood as the predominant or best-characterized resistance routes for each clinical subtype rather than as mutually exclusive, deterministic pathways confined strictly within subtype boundaries.

The clinical significance of this problem is substantial. Despite considerable therapeutic progress over the past two decades — including the introduction of CDK4/6 inhibitors in hormone receptor–positive disease, HER2-targeted antibody-drug conjugates, and immune checkpoint inhibitors in TNBC — the majority of deaths from breast cancer occur in the metastatic setting, where acquired resistance to sequential lines of therapy is the rule rather than the exception (Harbeck et al., 2019). Resistance is consequently not a peripheral complication of treatment but the central obstacle standing between current therapeutic capability and durable disease control, which is why understanding its molecular basis has become a research priority commensurate with the effort historically directed at identifying therapeutic targets themselves.

These subtype-specific resistance mechanisms illustrate how the general principles established in cancer biology more broadly — target alterations,

activation of compensatory survival pathways, evasion of apoptosis, and cellular plasticity — operate within the molecular context specific to breast tissue, and specifically within the context of the ER, HER2, and DNA-repair-pathway biology that defines each subtype's dependencies. Viewed this way, breast cancer resistance offers a useful case study in how the same limited repertoire of cancer-general escape strategies becomes channeled through different molecular routes depending on which pathway a given subtype's treatment approach depends upon.

This chapter addresses the molecular basis of resistance development in the major subtypes of breast cancer, its relationship to the shared cellular mechanisms that recur across subtypes, the experimental model approaches most commonly used to study these mechanisms in vitro, and current and emerging strategies aimed at anticipating or overcoming resistance in clinical practice.

2. Resistance in Hormone Receptor–Positive (Luminal) Breast Cancer

2.1. Tamoxifen Resistance

Tamoxifen, a selective estrogen receptor modulator (SERM), binds ER and blocks estrogen-driven proliferative signaling. Resistance is often associated not with complete loss of ER signaling but with the pathway becoming ligand-independent or being sustained through crosstalk with alternative growth factor signaling. Acquired mutations in the ESR1 gene, particularly within the ligand-binding domain (notably the Y537S and D538G hotspots), can cause the receptor to remain in an active conformation even in the absence of estrogen, and these mutations are detectable in circulating tumor DNA as an early indicator of emerging resistance (Jeselsohn et al., 2015; Robinson et al., 2013; Toy et al., 2013).

Beyond genomic alterations in ER itself, resistance can also arise through non-genomic mechanisms. Altered expression of steroid receptor coactivators, particularly SRC-3/AIB1, shifts the balance of coregulator recruitment such that tamoxifen behaves as a partial agonist rather than an antagonist at the ER (Osborne et al., 2003). Increased signaling through HER2, EGFR, and downstream MAPK/PI3K pathways further reduces ER's dependence on ligand and can phosphorylate ER and its coactivators at sites that promote ligand-independent transcriptional activity (Osborne & Schiff, 2011). Pharmacogenomic factors also contribute at the population level: polymorphisms in CYP2D6, the enzyme responsible for converting tamoxifen to its active metabolite endoxifen, are associated with reduced metabolic activation and consequently diminished clinical response in some patient populations (Goetz et al., 2018). Finally, autophagy has been proposed as a survival mechanism that allows tamoxifen-exposed cells to withstand therapeutic stress, with autophagy inhibition shown experimentally to resensitize resistant cells (Cook et al., 2014).

2.2. Aromatase Inhibitor Resistance

Aromatase inhibitors (AIs) act by blocking estrogen synthesis in peripheral tissues. Resistance to this class has been associated with ligand-independent activating mutations of ESR1, which are found to be particularly enriched in metastatic disease following prolonged AI therapy — a selection pattern less commonly seen after tamoxifen alone, since AIs remove the extracellular ligand entirely and thereby exert stronger selective pressure toward ligand-independent ER activation (Fribbens et al., 2016; Jeselsohn et al., 2015; Schiavon et al., 2015; Toy et al., 2013). This finding aligns with the clonal evolution framework, in which resistance arises from subclones selected under treatment pressure, and serial ctDNA sampling has demonstrated that ESR1 mutant clonal fractions can rise measurably over the course of AI treatment (Fribbens et al., 2016).

Local, intratumoral estrogen synthesis via residual aromatase activity or alternative steroidogenic pathways within the tumor microenvironment has also been proposed as a mechanism sustaining ER signaling despite systemic estrogen suppression (Chumsri, 2015). In addition, bidirectional crosstalk between ER and HER2/growth factor receptor pathways, similar to that described for tamoxifen resistance, contributes to AI resistance and provides rationale for the co-targeting strategies discussed in Section 7.

2.3. CDK4/6 Inhibitor Resistance

CDK4/6 inhibitors arrest the cell cycle at the G1 phase by blocking phosphorylation of the retinoblastoma protein (RB). Resistance mechanisms include loss of RB function, cyclin E1 (CCNE1) amplification, and CDK6 overexpression; these alterations render cell cycle progression independent of CDK4/6 (Herrera-Abreu et al., 2016; Turner et al., 2019). Analyses of the PALOMA-3 trial cohort further identified RB1 loss-of-function alterations as an acquired resistance mechanism arising specifically under CDK4/6 inhibitor pressure, distinguishing it from pre-existing resistance drivers present at treatment initiation (Condorelli et al., 2018).

Non-canonical activation of the cell cycle also contributes to resistance: cyclin D1–CDK2 complexes and FAT1 loss have been implicated in restoring RB phosphorylation through CDK4/6-independent routes (Herrera-Abreu et al., 2016; Li et al., 2018). Additionally, compensatory activation of the PI3K/AKT/mTOR pathway has emerged as a shared resistance mechanism against both endocrine therapy and CDK4/6 inhibitors, and cells under prolonged CDK4/6 inhibition have been shown to evade the intended senescence-like arrest, instead resuming proliferation through these compensatory routes (Herrera-Abreu et al., 2016).

2.4. Compensatory Activation of the PI3K/AKT/mTOR Pathway

PIK3CA mutations — most commonly at the E545K and H1047R hotspots — are among the genetic alterations frequently observed in Luminal breast cancer and contribute to both primary and acquired endocrine resistance. Loss of PTEN and activating mutations in AKT1 produce a convergent effect on the same pathway (Miller et al., 2011). Activation of this pathway supports ER's ligand-independent transcriptional activity and sustains cell survival, thereby reducing the efficacy of endocrine therapy. A feedback loop further complicates this mechanism: mTOR inhibition alone can paradoxically reactivate upstream AKT signaling, providing a rationale for combining mTOR or PI3K inhibitors directly with endocrine agents rather than using either alone (O'Reilly et al., 2006).

This mechanistic rationale has been validated clinically: the BOLERO-2 trial demonstrated that combining the mTOR inhibitor everolimus with an aromatase inhibitor improved progression-free survival in AI-resistant, hormone receptor–positive metastatic breast cancer (Baselga et al., 2012), and subsequent trials of alpha-specific PI3K inhibitors in combination with endocrine therapy have extended this approach specifically to PIK3CA-mutant disease.

3. Resistance in HER2-Positive Breast Cancer

3.1. Trastuzumab Resistance

Trastuzumab is a monoclonal antibody that binds domain IV of the extracellular region of the HER2 receptor, blocking ligand-independent HER2 homodimerization and triggering antibody-dependent cellular cytotoxicity (ADCC) in addition to direct signaling inhibition. Among the best-characterized resistance mechanisms is proteolytic cleavage of the HER2 extracellular domain by matrix metalloproteinases, which removes the trastuzumab binding site and generates the constitutively active, truncated p95HER2 fragment; tumors expressing p95HER2 have been clinically associated with reduced response to trastuzumab-based therapy (Arribas et al., 2011; Scaltriti et al., 2007).

Downstream of the receptor itself, activating PIK3CA mutations and loss of PTEN sustain activity of the PI3K/AKT pathway independently of HER2 signaling, reducing response to trastuzumab; PTEN loss specifically has also been shown to impair the ADCC component of trastuzumab's mechanism by altering natural killer cell engagement (Berns et al., 2007; Nagata et al., 2004). Increased crosstalk with the insulin-like growth factor receptor (IGF-1R) has also been described as a contributing resistance component, with IGF-1R forming a heterodimeric complex with HER2 that sustains PI3K/AKT signaling and physically interferes with trastuzumab binding (Nahta et al., 2005). Reduced antibody accessibility due to steric hindrance from the cell-surface mucin MUC4 has similarly been proposed as a mechanism limiting effective HER2 engagement (Nagy et al., 2005). At the immune level, Fc-gamma receptor (FcγR)

polymorphisms affecting ADCC efficiency, and an immunosuppressive tumor microenvironment more broadly, have been implicated in variable trastuzumab response independent of tumor-intrinsic signaling changes (Musolino et al., 2008).

3.2. Resistance to Trastuzumab Emtansine (T-DM1) and Tyrosine Kinase Inhibitors

Resistance to T-DM1, an antibody-drug conjugate that delivers the microtubule-disrupting agent DM1 following HER2-mediated internalization, has been associated with reduced HER2 expression or heterogeneity of expression across the tumor, impaired lysosomal processing and degradation capacity required to release active DM1 intracellularly, and overexpression of drug efflux transporters such as ABCB1, which extrude the released payload before it can act (Barok et al., 2014; Loganzo et al., 2016). Impaired trafficking of the HER2-antibody complex to lysosomes, rather than degradation capacity alone, has also been reported as a distinct contributing factor (Sung et al., 2018).

Resistance to small-molecule tyrosine kinase inhibitors such as lapatinib and neratinib, which act intracellularly on the HER2 kinase domain rather than the extracellular domain, can develop through increased HER2/HER3 heterodimerization with compensatory upregulation of the HER3 ligand heregulin, restoring downstream PI3K/AKT signaling despite kinase inhibition (Sergina et al., 2007). Activation of alternative receptor tyrosine kinases, including MET and FGFR, provides parallel bypass signaling routes that similarly circumvent HER2 blockade (Garrett & Arteaga, 2011). Because lapatinib and neratinib act at the kinase domain rather than the extracellular domain, resistance mechanisms specific to this class are largely non-overlapping with those affecting trastuzumab and T-DM1, which is part of the rationale for sequencing or combining agents from different structural classes in clinical practice.

4. Resistance in Triple-Negative Breast Cancer (TNBC)

4.1. Chemotherapy Dependence and Resistance Development Due to Lack of Targets

Because ER, PR, and HER2 expression are absent, treatment options in TNBC are largely limited to cytotoxic chemotherapy, most commonly anthracyclines, taxanes, and platinum agents. This dependence creates conditions under which tumor cells undergo rapid selection under treatment pressure, and the resistance pathways described in the general mechanisms (ABC transporter overexpression, enhanced DNA damage repair, evasion of apoptosis) become particularly prominent in this subtype (Bianchini et al., 2016). TNBC itself is not molecularly uniform: transcriptomic profiling has identified distinct subgroups — including basal-like, mesenchymal, and luminal androgen receptor (LAR) subtypes — that

differ in their baseline chemosensitivity and in the specific resistance pathways that predominate, which has implications for treatment selection beyond a one-size-fits-all chemotherapy approach (Lehmann et al., 2011).

Platinum agents (e.g., carboplatin) occupy a particular position in this subtype given the enrichment of homologous recombination deficiency (HRD) in TNBC; resistance to platinum-based regimens is mechanistically linked to the same reversion mutations and repair-capacity restoration discussed below for PARP inhibitors, reflecting substantial mechanistic overlap between these two drug classes despite their different modes of action (Isakoff et al., 2015).

4.2. PARP Inhibitor Resistance

In BRCA1/2-mutated TNBC, PARP inhibitors act through the principle of synthetic lethality, exploiting the tumor's dependence on PARP-mediated single-strand break repair in the absence of functional homologous recombination. Resistance has been most extensively associated with reversion mutations that restore the BRCA reading frame, partially recovering homologous recombination repair capacity and thereby re-establishing tolerance to PARP inhibition (Edwards et al., 2008). Loss of 53BP1, a component of the non-homologous end joining pathway whose absence paradoxically restores DNA end resection and homologous recombination in BRCA1-deficient cells, has also been described as an additional resistance component, alongside loss of the Shieldin complex, which functions similarly downstream of 53BP1 (Bunting et al., 2010; Dev et al., 2018).

Beyond DNA repair restoration, overexpression of drug efflux transporters (notably ABCB1) reduces intracellular PARP inhibitor accumulation, and stabilization of stalled replication forks — limiting the degradation of nascent DNA that would otherwise sensitize HR-deficient cells to further damage — has been proposed as a repair-independent resistance mechanism (Rondinelli et al., 2017).

4.3. Resistance to Immune Checkpoint Inhibitors (PD-L1)

Although TNBC is considered relatively more immunogenic than other subtypes, owing to higher tumor mutational burden and greater baseline lymphocytic infiltration, response to immune checkpoint inhibitors is heterogeneous. Resistance has been linked to insufficient T-cell infiltration in the tumor microenvironment (the so-called "cold" tumor phenotype), defects in antigen presentation such as loss of beta-2 microglobulin or downregulation of MHC class I, and activation of alternative immunosuppressive signals including TGF-β and indoleamine 2,3-dioxygenase (IDO) (Emens, 2018; Gatalica et al., 2014). Expansion of immunosuppressive cell populations within the tumor microenvironment, particularly regulatory T cells (Tregs) and myeloid-derived suppressor cells (MDSCs), further contributes to an environment resistant to

checkpoint blockade (Stovgaard et al., 2018). Loss-of-function mutations in the JAK1/JAK2 signaling pathway, which is required for interferon-gamma–induced upregulation of PD-L1 and antigen presentation machinery, have also been reported as a tumor-intrinsic mechanism of primary resistance to checkpoint inhibition (Zaretsky et al., 2016).

4.4. The Prominent Role of Cancer Stem Cells and EMT in TNBC

TNBC is a group in which cell populations exhibiting cancer stem cell (CSC) properties, commonly identified by the CD44+/CD24-/low surface marker profile or by high aldehyde dehydrogenase (ALDH) activity, are more pronounced compared to other subtypes (Al-Hajj et al., 2003). Activation of the epithelial-mesenchymal transition (EMT) program has been associated both with acquisition of the CSC phenotype and with increased chemotherapy resistance and metastatic potential (Mani et al., 2008). Key EMT-driving transcription factors — including SNAIL, SLUG, TWIST, and ZEB1 — not only suppress epithelial adhesion but also directly upregulate ABC transporter expression and anti-apoptotic signaling, linking the EMT/CSC phenotype mechanistically to the efflux- and apoptosis-based resistance pathways discussed elsewhere in this chapter (Kurrey et al., 2009). Chemotherapy exposure itself has additionally been shown to enrich for CSC populations within residual tumor burden, suggesting a bidirectional relationship in which treatment pressure actively selects for and expands the stem-like, drug-tolerant subpopulation rather than merely failing to eliminate it (Creighton et al., 2009).

5. Shared Cellular Mechanisms (with Breast Cancer–Specific Findings)

5.1. Overexpression of ABC Transporters (ABCB1/P-gp)

Overexpression of ABCB1 (P-glycoprotein) has been identified as an important component of multidrug resistance in breast cancer, particularly against anthracycline and taxane-class chemotherapeutics, both of which are established substrates of the transporter. ABCB1 upregulation is frequently driven at the transcriptional level, with NF-κB and the nuclear receptor PXR implicated as regulators that increase ABCB1 promoter activity in response to chemotherapeutic exposure, alongside epigenetic mechanisms such as promoter demethylation that can stably lock in the resistant phenotype across passages (Chen et al., 2016). Increased ABCB1 expression in TNBC and in patients who have received prolonged chemotherapy has been associated with post-treatment recurrence (Wind & Holen, 2011).

Resistant sublines developed with paclitaxel or doxorubicin in TNBC cell lines such as MDA-MB-231 are common experimental models demonstrating increased expression of this transporter; in such models, ABCB1 inhibitors (e.g., verapamil, tariquidar) or efflux-independent taxane analogs are frequently used to functionally confirm that the transporter itself, rather than a co-occurring

mechanism, accounts for the observed resistance (Nanayakkara et al., 2018). Clinically, first- and second-generation ABCB1 inhibitors largely failed in trials due to pharmacokinetic interference with co-administered chemotherapy and dose-limiting toxicity, which has shifted more recent efforts toward transporter-independent taxane formulations rather than direct pump inhibition (Robey et al., 2018).

5.2. Evasion of Apoptosis: BCL-2/BCL-xL Overexpression

Overexpression of anti-apoptotic BCL-2 family members (BCL-2, BCL-xL, MCL-1) is a shared mechanism that blocks chemotherapy-induced cell death across both hormone receptor–positive and TNBC subtypes by sequestering pro-apoptotic BH3-only proteins (e.g., BIM, BID) and preventing BAX/BAK-mediated mitochondrial outer membrane permeabilization (Vaillant et al., 2013). Notably, BCL-2 expression itself is at least partly ER-driven, which explains its particular enrichment in Luminal tumors and provides a mechanistic link between hormone receptor signaling and apoptotic threshold (Vaillant et al., 2013).

Investigation of BH3-mimetic agents (e.g., venetoclax) in BCL-2–overexpressing tumors, particularly within the Luminal subtype, underscores the therapeutic relevance of this mechanism; because these agents directly occupy the BH3-binding groove of BCL-2 to release sequestered pro-apoptotic proteins, they can restore chemosensitivity independently of upstream DNA damage signaling. In TNBC and other high-MCL-1 contexts, however, BCL-2–selective agents such as venetoclax are frequently ineffective on their own, since MCL-1 can substitute for BCL-2's sequestering function — a finding that has driven interest in MCL-1–selective inhibitors and in dual BCL-2/BCL-xL/MCL-1–targeting combination strategies for this subtype (Merino et al., 2018).

5.3. Tumor Microenvironment: Cancer-Associated Fibroblasts and Hypoxia

Cancer-associated fibroblasts (CAFs) can enhance resistance to chemotherapy and endocrine therapy by supporting tumor cell survival signaling through cytokine and growth factor secretion, most notably IL-6, CXCL12/SDF-1, and hepatocyte growth factor (HGF), which activate STAT3, PI3K/AKT, and MET signaling in adjacent tumor cells (Tchou & Conejo-Garcia, 2012). CAFs additionally remodel the extracellular matrix, and the resulting increase in matrix stiffness has itself been shown to activate mechanotransduction pathways (e.g., integrin/FAK signaling) that independently promote a drug-tolerant cell state (Insua-Rodríguez & Oskarsson, 2016).

Hypoxia, through HIF-1α–mediated transcriptional reprogramming, contributes to resistance development — particularly in solid, rapidly growing TNBC tumors — by promoting both drug efflux transporter expression and the EMT/cancer stem cell phenotype. HIF-1α also directly suppresses components of

the intrinsic apoptotic pathway and has been shown to upregulate ABCB1 and ABCG2 transcriptionally, providing a direct mechanistic bridge between the hypoxic microenvironment and the efflux-mediated resistance described in Section 5.1 (Samanta et al., 2014). Because hypoxic regions are typically poorly vascularized, they are also associated with reduced drug delivery independent of any cell-intrinsic resistance mechanism — a pharmacokinetic barrier that compounds, rather than substitutes for, the molecular mechanisms discussed above.

6. Experimental Model Approaches

6.1. Approaches to Developing Resistant Sublines in Cell Lines such as MCF-7 and MDA-MB-231

Resistant sublines are typically developed through chronic or stepwise exposure of the parental cell line to increasing drug concentrations; this approach mimics the process of clonal selection under treatment pressure in vitro (McDermott et al., 2014). Two general exposure strategies are used in practice: continuous exposure, in which cells are maintained at a fixed, sub-lethal drug concentration until proliferation recovers before the concentration is incrementally raised, and pulsed (intermittent) exposure, in which cells are exposed to higher, near-IC50 or supra-IC50 concentrations for a defined interval followed by a drug-free recovery period before the next pulse; the pulsed approach has been reported to more closely approximate the intermittent pharmacokinetic exposure seen in clinical dosing schedules, whereas continuous exposure more directly models sustained selective pressure (McDermott et al., 2014).

In MCF-7 cells, representing the Luminal A subtype, tamoxifen- or paclitaxel-resistant sublines are commonly generated using this method, while in MDA-MB-231 cells, a TNBC model, doxorubicin- or paclitaxel-resistant sublines are frequently preferred; HER2-positive models such as SKBR3 or BT-474 are similarly used to generate trastuzumab- or lapatinib-resistant sublines when HER2-specific resistance mechanisms are under investigation (Liu et al., 2023). The resulting resistant lines allow comparative evaluation, against the parental line, of resistance mechanisms such as ABC transporter expression, apoptotic protein profile, and EMT markers.

Beyond drug-induced sublines, resistant models can also be derived through genetic engineering (e.g., CRISPR-mediated knockout of RB1 or PTEN to model specific resistance drivers directly) or isolated from single-cell clones surviving drug exposure without prior population-level chronic selection, an approach that can better preserve pre-existing clonal heterogeneity for studying which subpopulations were selected rather than which adaptations were acquired de novo (Ramirez et al., 2016). This distinction matters mechanistically: chronic selection protocols favor the emergence of acquired resistance mechanisms (e.g.,

new mutations, epigenetic reprogramming) that develop under sustained pressure, whereas isolating surviving clones from a brief high-dose exposure more directly captures pre-existing, intrinsically resistant subpopulations, and the two approaches are not necessarily interchangeable for a given research question.

Several methodological points warrant particular attention in resistant subline development. The resistance index (IC50 resistant/IC50 parental) should be reported clearly, together with the specific IC50 calculation method and software used, since values are not always directly comparable across studies using different curve-fitting approaches. Whether resistance was maintained across a defined number of passages in drug-free medium — i.e., the stability of the resistant phenotype — should be explicitly stated, as some resistant phenotypes are transient and reflect adaptive plasticity rather than stable genetic or epigenetic change, while others persist for many passages after drug withdrawal (Sharma et al., 2010). The parental line should be maintained as a parallel control across matched passage ranges to minimize the confounding effect of genetic drift, since prolonged culture of any line, resistant or not, can independently alter baseline drug sensitivity. Short tandem repeat (STR) profiling of both parental and resistant lines is additionally recommended to confirm cell line identity and rule out cross-contamination, a documented and non-trivial concern in long-term selection experiments spanning many months (Capes-Davis et al., 2010).

6.2. In Vitro Combination Therapy Designs

In combination studies aimed at overcoming resistance, testing resistant and parental lines in parallel is important for demonstrating that the combination genuinely overcomes resistance, as distinct from a merely additive effect that would also be observed in drug-naïve cells. Dose-response matrices — in which each agent is tested across a full concentration range both alone and in fixed-ratio or full-matrix combination with the other — and synchronized experimental designs (matched treatment duration, plating density, and endpoint assay across all conditions being compared) are recommended for reliable synergy assessment.

Explicitly stating the method used for such analyses is important for methodological transparency, since different reference models rest on different underlying assumptions and are not always concordant for the same dataset. Bliss independence assumes the two agents act through statistically independent mechanisms and calculates an expected combined effect from that assumption, whereas Loewe additivity assumes the two agents behave as dilutions of the same underlying agent and is generally considered more appropriate when the two drugs are believed to share a common mechanistic target or pathway (Foucquier & Guedj, 2015). Synergy scoring frameworks built on these models, such as SynergyFinder, are increasingly used to visualize synergy landscapes across the full dose-response matrix rather than at a single dose pair, which helps distinguish

synergy that is consistent across the tested dose range from synergy that is an artifact of a narrow concentration window (Ianevski et al., 2020).

Regardless of the specific reference model selected, it should be reported alongside the raw dose-response data (not only a single summary synergy score), and the model choice should be justified based on the presumed mechanistic relationship between the two agents under study, since results derived from one framework should not be presented as though they were computed by another.

7. Strategies to Overcome Resistance and Future Directions

7.1. Rational Combination Therapies

Simultaneously targeting compensatory signaling pathways is a prominent approach for overcoming resistance to single agents, since monotherapy resistance frequently arises from a single dominant escape route that a second, mechanistically distinct agent can close off. Combining endocrine therapy with CDK4/6 inhibitors has become standard first-line practice in hormone receptor–positive metastatic disease, with the MONALEESA and MONARCH trial programs demonstrating substantial progression-free survival benefit over endocrine therapy alone; combining endocrine therapy with PI3K inhibitors in PIK3CA-mutant disease follows the same compensatory-pathway rationale discussed in Section 2.4 (André et al., 2019).

Dual anti-HER2 blockade in HER2-positive disease (e.g., trastuzumab plus pertuzumab) works by targeting non-overlapping epitopes on the HER2 extracellular domain — pertuzumab blocks HER2/HER3 heterodimerization rather than competing with trastuzumab's domain IV binding site — which explains why the combination outperforms either antibody alone and why it retains activity against several trastuzumab-resistance mechanisms described in Section 3.1 (Swain et al., 2015). In TNBC, combining PARP inhibitors with agents targeting the DNA damage response, such as ATR or WEE1 inhibitors, aims to prevent the replication-stress tolerance that underlies both reversion-mutation and replication-fork-stabilization resistance mechanisms discussed in Section 4.2 (Yap et al., 2019).

A general principle underlying rational combination design is that agents should ideally target nodes that lie downstream of, or parallel to, the anticipated resistance mechanism rather than simply combining two agents with independent single-agent activity; combinations chosen without this mechanistic rationale have in several cases failed to show benefit over sequential monotherapy despite additive activity in preclinical models, underscoring that synergy demonstrated in vitro (Section 6.2) does not automatically translate to clinical benefit (Bardia et al., 2021).

7.2. Next-Generation Agents and Antibody-Drug Conjugates

Next-generation antibody-drug conjugates such as trastuzumab deruxtecan have shown efficacy even in patients resistant to prior HER2-targeted therapies, demonstrating that optimizing linker chemistry and payload can partially overcome resistance (Modi et al., 2020). Mechanistically, this reflects two design improvements over first-generation conjugates such as T-DM1: a cleavable linker that allows released payload to diffuse into and kill neighboring HER2-low or HER2-negative tumor cells (the so-called "bystander effect"), and a substantially higher drug-to-antibody ratio that increases cytotoxic payload delivery per binding event, partially compensating for reduced or heterogeneous HER2 expression — one of the principal T-DM1 resistance mechanisms discussed in Section 3.2 (Ogitani et al., 2016).

Similarly, Trop-2–targeted conjugates in TNBC, such as sacituzumab govitecan, offer an alternative approach to the treatment limitations arising from the lack of targetable receptors, exploiting the broad overexpression of Trop-2 across TNBC regardless of molecular subtype (Bardia et al., 2019). More broadly, this shift toward conjugate-based and bystander-effect-dependent agents reflects an emerging strategy in which cell-surface target expression need not be uniform across the tumor for the agent to achieve therapeutic effect, addressing the intratumoral heterogeneity that undermines many single-target approaches described elsewhere in this chapter.

7.3. Biomarker-Guided Personalized Therapy

Monitoring resistance-associated mutations such as ESR1 or PIK3CA in circulating tumor DNA via liquid biopsy may allow treatment changes to be guided before clinical progression is evident on imaging, since ctDNA mutant allele fraction has been shown in several cohorts to rise weeks to months ahead of radiographic progression (Turner et al., 2020). Beyond single-mutation tracking, serial ctDNA sampling additionally allows monitoring of clonal dynamics over the course of treatment — for example, tracking whether an ESR1-mutant subclone is expanding or contracting relative to wild-type disease — providing a window into the ongoing evolutionary process described in the clonal evolution framework introduced in Section 2 rather than a single static readout (Fribbens et al., 2016 — Bölüm 2 kaynakçası).

This approach is consistent with the principle that resistance is a dynamic rather than a static process, and it supports real-time adaptation of treatment strategy; practical implementation nonetheless faces limitations, including variable assay sensitivity for low-shedding tumors, the cost and infrastructure required for serial testing, and, most importantly, a current lack of prospective randomized evidence that ctDNA-guided early treatment switching actually improves survival outcomes compared with switching at radiographic or clinical progression (Cescon et al., 2020).

7.4. Future Directions

Single-cell RNA sequencing technologies may contribute to identifying intratumoral heterogeneity and resistant subclones prior to treatment, and, when applied longitudinally across paired pre- and post-treatment biopsies, can additionally resolve whether resistant populations emerging on therapy reflect pre-existing subclones undergoing selection or newly acquired adaptive states arising within initially drug-sensitive cells — a distinction with direct relevance to the pulsed-versus-continuous subline selection methods discussed in Section 6.1 (Kim et al., 2018).

Organoid and patient-derived xenograft (PDX) models, by better reflecting the tumor microenvironment and heterogeneity compared to conventional 2D cell lines, hold potential for increasing the clinical validity of resistance studies; PDX models in particular preserve stromal and architectural features absent from cell culture, while patient-derived organoids offer a more scalable platform better suited to medium-throughput drug screening, and the two approaches are increasingly used complementarily rather than as substitutes for one another (Bruna et al., 2016). Looking further ahead, integration of multi-omic data (genomic, transcriptomic, and proteomic) with machine learning approaches has been proposed to predict resistance risk and optimal combination strategy at the level of the individual tumor, though such approaches remain largely at the retrospective, hypothesis-generating stage and will require prospective clinical validation before informing treatment decisions.

8. Conclusion

Drug resistance in breast cancer is not the result of a single molecular event but rather the outcome of compensatory activation of subtype-specific signaling pathways, target alterations, cellular plasticity, and interaction with the tumor microenvironment. In the Luminal subtype, ESR1 mutations and activation of the PI3K/AKT/mTOR pathway; in HER2-positive disease, receptor cleavage and compensatory signaling pathways; and in TNBC, chemotherapy dependence arising from the absence of targetable receptors together with the cancer stem cell phenotype have been identified as the predominant mechanisms. These differences underscore the importance of addressing resistance research within a subtype-specific framework rather than assuming a single unifying resistance pathway applies uniformly across breast cancer as a whole.

At the same time, several mechanisms recur across subtypes rather than remaining confined to one: ABC transporter overexpression, evasion of apoptosis through BCL-2 family proteins, and tumor microenvironment contributions from hypoxia and cancer-associated fibroblasts each appear, in modified form, in Luminal, HER2-positive, and TNBC disease alike (Sections 5.1–5.3). This recurrence suggests that resistance is best understood not as a fixed set of subtype-specific mutations alone, but as the convergence of subtype-defining signaling

dependencies with a smaller set of shared cellular survival programs — a distinction with direct implications for how combination strategies are designed (Section 7.1).

A further point warranting emphasis is that resistance mechanisms within a given tumor are rarely singular or static. Longitudinal ctDNA and single-cell sequencing studies discussed in Sections 6 and 7 have demonstrated that resistant subclones can pre-exist treatment, expand under selective pressure, and in some cases be succeeded by distinct resistant populations later in the treatment course, consistent with the clonal evolution framework introduced at the outset of this chapter (Kim et al., 2018 — Bölüm 7 kaynakçası). This temporal dimension has practical consequences: a resistance mechanism identified at one point in a patient's treatment history does not necessarily predict the mechanism that will emerge subsequently, which argues against static, one-time biomarker assessment in favor of the dynamic, serial monitoring approaches discussed in Section 7.3.

In vitro studies using resistant cell sublines allow these mechanisms to be examined at the molecular level and rational combination strategies to be tested, and remain an essential and accessible first step in resistance research given their relative speed, cost, and experimental tractability compared to in vivo or patient-derived systems. Nonetheless, it should be recognized that conventional two-dimensional cell line models reflect the tumor microenvironment and heterogeneity only to a limited extent, lacking the stromal, immune, and architectural context increasingly understood to shape resistance outcomes in vivo. The potential of organoid, PDX, and single-cell analysis approaches to overcome this limitation warrants further evaluation, and the field appears to be converging on a tiered experimental strategy — mechanistic hypothesis generation in 2D cell lines, validation in organoid or 3D culture, and confirmation in PDX or in vivo models — rather than treating any single model system as sufficient on its own (Bruna et al., 2016).

The integration of biomarker-guided, dynamic treatment approaches into clinical practice reflects a paradigm shift toward treating resistance as an evolving process rather than a static state. Realizing this shift in routine clinical practice will nonetheless require prospective evidence that acting on early molecular signals of resistance — rather than waiting for radiographic or clinical progression — translates into measurable survival benefit, a question that remains open for most of the biomarkers discussed in this chapter (Cescon et al., 2020). In this sense, the central challenge for the field going forward lies less in identifying further resistance mechanisms, which have now been characterized in considerable molecular detail across all major breast cancer subtypes, and more in translating that mechanistic understanding into treatment strategies that anticipate and intercept resistance before it manifests clinically.

References

Al-Hajj, M., Wicha, M. S., Benito-Hernandez, A., Morrison, S. J., & Clarke, M. F. (2003). Prospective identification of tumorigenic breast cancer cells. Proc Natl Acad Sci U S A., 100(7), 3983–3988. doi: 10.1073/pnas.0530291100.

André, F., Ciruelos, E., Rubovszky, G., Campone, M., Loibl, S., Rugo, H. S., ... Juric, D. (2019). Alpelisib for PIK3CA-mutated, hormone receptor–positive advanced breast cancer. New England Journal of Medicine, 380(20), 1929–1940. doi:10.1056/NEJMoa1813904

Arribas, J., Baselga, J., Pedersen, K., & Parra-Palau, J. L. (2011). p95HER2 and breast cancer. Cancer Research, 71(5), 1515–1519.

Bardia, A., Hurvitz, S. A., Tolaney, S. M., Loirat, D., Punie, K., Oliveira, M., ... Rugo, H. S. (2021). Sacituzumab govitecan in metastatic triple-negative breast cancer. New England Journal of Medicine, 384(16), 1529–1541. doi:10.1056/NEJMoa2028485

Bardia, A., Mayer, I. A., Vahdat, L. T., Tolaney, S. M., Isakoff, S. J., Diamond, J. R., ... Kalinsky, K. (2019). Sacituzumab govitecan-hziy in refractory metastatic triple-negative breast cancer. New England Journal of Medicine, 380(8), 741–751. doi:10.1056/NEJMoa1814213

Barok, M., Joensuu, H., & Isola, J. (2014). Trastuzumab emtansine: Mechanisms of action and drug resistance. Breast Cancer Research, 16(2), 209. doi:10.1186/bcr3621

Baselga, J., Campone, M., Piccart, M., Burris, H. A., Rugo, H. S., Sahmoud, T., ... Hortobagyi, G. N. (2012). Everolimus in postmenopausal hormone-receptor-positive advanced breast cancer. New England Journal of Medicine, 366(6), 520–529. doi:10.1056/NEJMoa1109653

Berns, K., Horlings, H. M., Hennessy, B. T., Madiredjo, M., Hijmans, E. M., Beelen, K., ... Bernards, R. (2007). A functional genetic approach identifies the PI3K pathway as a major determinant of trastuzumab resistance in breast cancer. Cancer Cell, 12(4), 395–402. doi:10.1016/j.ccr.2007.08.030

Bianchini, G., Balko, J. M., Mayer, I. A., Sanders, M. E., & Gianni, L. (2016). Triple-negative breast cancer: Challenges and opportunities of a heterogeneous disease. Nature Reviews Clinical Oncology, 13(11), 674–690. doi: 10.1038/nrclinonc.2016.66.

Bruna, A., Rueda, O. M., Greenwood, W., Batra, A. S., Callari, M., Batra, R. N., ... Caldas, C. (2016). A biobank of breast cancer explants with preserved intra-tumor heterogeneity to screen anticancer compounds. Cell, 167(1), 260–274. doi:10.1016/j.cell.2016.08.041

Bunting, S. F., Callén, E., Wong, N., Chen, H.-T., Polato, F., Gunn, A., ... Nussenzweig, A. (2010). 53BP1 inhibits homologous recombination in

Brca1-deficient cells by blocking resection of DNA breaks. Cell, 141(2), 243–254. doi:10.1016/j.cell.2010.03.012

Capes-Davis, A., Theodosopoulos, G., Atkin, I., Drexler, H. G., Kohara, A., MacLeod, R. A. F., ... Freshney, R. I. (2010). Check your cultures! A list of cross-contaminated or misidentified cell lines. International Journal of Cancer, 127(1), 1–8. doi: 10.1002/ijc.25242

Cescon, D. W., Bratman, S. V., Chan, S. M., & Siu, L. L. (2020). Circulating tumor DNA and liquid biopsy in oncology. Nature Cancer, 1(3), 276–290. doi:10.1038/s43018-020-0043-5

Chen, Z., Shi, T., Zhang, L., Zhu, P., Deng, M., Huang, C., ... Li, J. (2016). Mammalian drug efflux transporters of the ATP binding cassette (ABC) family in multidrug resistance: A review of the past decade. Cancer Letters, 370(1), 153–164. doi:10.1016/j.canlet.2015.10.010

Chumsri, S. (2015). Clinical utilities of aromatase inhibitors in breast cancer. International Journal of Women's Health, 7, 493–499. doi:10.2147/IJWH.S69907

Condorelli, R., Spring, L., O'Shaughnessy, J., Lacroix, L., Bailleux, C., Scott, V., ... Bardia, A. (2018). Polyclonal RB1 mutations and acquired resistance to CDK 4/6 inhibitors in patients with metastatic breast cancer. Annals of Oncology, 29(3), 640–645. doi:10.1093/annonc/mdx784

Cook, K. L., Wärri, A., Soto-Pantoja, D. R., Clarke, P. A. G., Cruz, M. I., Zwart, A., & Clarke, R. (2014). Hydroxychloroquine inhibits autophagy to potentiate antiestrogen responsiveness in ER+ breast cancer. Clinical Cancer Research, 20(12), 3222–3232. doi:10.1158/1078-0432.CCR-13-3227

Creighton, C. J., Li, X., Landis, M., Dixon, J. M., Neumeister, V. M., Sjolund, A., ... Chang, J. C. (2009). Residual breast cancers after conventional therapy display mesenchymal as well as tumor-initiating features. Proceedings of the National Academy of Sciences, 106(33), 13820–13825. doi:10.1073/pnas.0905718106

Dev, H., Chiang, T.-W. W., Lescale, C., de Krijger, I., Martin, A. G., Pilger, D., ... Jackson, S. P. (2018). Shieldin complex promotes DNA end-joining and counters homologous recombination in BRCA1-null cells. Nature Cell Biology, 20(8), 954–965. doi:10.1038/s41556-018-0140-1

Edwards, S. L., Brough, R., Lord, C. J., Natrajan, R., Vatcheva, R., Levine, D. A., ... Ashworth, A. (2008). Resistance to therapy caused by intragenic deletion in BRCA2. Nature, 451(7182), 1111–1115. doi:10.1038/nature06548

Emens, L. A. (2018). Breast cancer immunotherapy: Facts and hopes. Clinical Cancer Research, 24(3), 511–520. doi:10.1158/1078-0432.CCR-16-3001

Foucquier, J., & Guedj, M. (2015). Analysis of drug combinations: Current methodological landscape. Pharmacology Research & Perspectives, 3(3), e00149. doi:10.1002/prp2.149

Fribbens, C., O'Leary, B., Kilburn, L., Hrebien, S., Garcia-Murillas, I., Beaney, M., ... Turner, N. C. (2016). Plasma ESR1 mutations and the treatment of estrogen receptor-positive advanced breast cancer. Journal of Clinical Oncology, 34(25), 2961–2968. doi:10.1200/JCO.2016.67.3061

Garrett, J. T., & Arteaga, C. L. (2011). Resistance to HER2-directed antibodies and tyrosine kinase inhibitors: Mechanisms and clinical implications. Cell Cycle, 10(9), 793–800. doi:10.4161/cbt.11.9.15045

Gatalica, Z., Snyder, C., Maney, T., Ghazalpour, A., Holterman, D. A., Xiao, N., ... Hamid, O. (2014). Programmed cell death 1 (PD-1) and its ligand (PD-L1) in common cancers and their correlation with molecular cancer type. Cancer Epidemiology, Biomarkers & Prevention, 23(12), 2965–2970. doi:10.1158/1055-9965.EPI-14-0654

Goetz, M. P., Sangkuhl, K., Guchelaar, H.-J., Schwab, M., Province, M., Whirl-Carrillo, M., ... Klein, T. E. (2018). Clinical Pharmacogenetics Implementation Consortium (CPIC) guideline for CYP2D6 and tamoxifen therapy. Clinical Pharmacology & Therapeutics, 103(5), 770–777. doi:10.1002/cpt.1007

Harbeck, N., Penault-Llorca, F., Cortes, J., Gnant, M., Houssami, N., Poortmans, P., ... Cardoso, F. (2019). Breast cancer. Nature Reviews Disease Primers, 5, 66. doi:10.1038/s41572-019-0111-2

Herrera-Abreu, M. T., Palafox, M., Asghar, U., Rivas, M. A., Cutts, R. J., Garcia-Murillas, I., ... Serra, V. (2016). Early adaptation and acquired resistance to CDK4/6 inhibition in estrogen receptor–positive breast cancer. Cancer Research, 76(8), 2301–2313. doi:10.1158/0008-5472.CAN-15-0728

Ianevski, A., Giri, A. K., & Aittokallio, T. (2020). SynergyFinder 2.0: Visual analytics of multi-drug combination synergies. Nucleic Acids Research, 48(W1), W488–W493. doi:10.1093/nar/gkaa216

Insua-Rodríguez, J., & Oskarsson, T. (2016). The extracellular matrix in breast cancer. Advanced Drug Delivery Reviews, 97, 41–55. doi:10.1016/j.addr.2015.12.017

Isakoff, S. J., Mayer, E. L., He, L., Traina, T. A., Carey, L. A., Krag, K. J., ... Ellisen, L. W. (2015). TBCRC009: A multicenter phase II clinical trial of platinum monotherapy with biomarker assessment in metastatic triple-negative breast cancer. Journal of Clinical Oncology, 33(17), 1902–1909. doi:10.1200/JCO.2014.57.6660

Jeselsohn, R., Buchwalter, G., De Angelis, C., Brown, M., & Schiff, R. (2015). ESR1 mutations—a mechanism for acquired endocrine resistance in breast cancer.

Nature Reviews Clinical Oncology, 12(10), 573–583. doi:10.1038/nrclinonc.2015.117

Kim, C., Gao, R., Sei, E., Brandt, R., Hartman, J., Hatschek, T., ... Navin, N. E. (2018). Chemoresistance evolution in triple-negative breast cancer delineated by single-cell sequencing. Cell, 173(4), 879–893. doi:10.1016/j.cell.2018.03.041

Kurrey, N. K., Jalgaonkar, S. P., Joglekar, A. V., Ghanate, A. D., Chaskar, P. D., Doiphode, R. Y., & Bapat, S. A. (2009). Snail and Slug mediate radioresistance and chemoresistance by antagonizing p53-mediated apoptosis and acquiring a stem-like phenotype in ovarian cancer cells. Stem Cells, 27(9), 2059–2068. doi:10.1002/stem.154

Lehmann, B. D., Bauer, J. A., Chen, X., Sanders, M. E., Chakravarthy, A. B., Shyr, Y., & Pietenpol, J. A. (2011). Identification of human triple-negative breast cancer subtypes and preclinical models for selection of targeted therapies. Journal of Clinical Investigation, 121(7), 2750–2767. doi:10.1172/JCI45014

Li, Z., Razavi, P., Li, Q., Toy, W., Liu, B., Ping, C., ... Chandarlapaty, S. (2018). Loss of the FAT1 tumor suppressor promotes resistance to CDK4/6 inhibitors via the Hippo pathway. Cancer Cell, 34(6), 893–905. doi: 10.1016/j.ccell.2018.11.006.

Liu, H., Ruan, S., Larsen, M. E., Tan, C., Liu, B., & Lyu, H. (2023). Trastuzumab-resistant breast cancer cells-derived tumor xenograft models exhibit distinct sensitivity to lapatinib treatment in vivo. Biological Procedures Online, 25, 19. doi:10.1186/s12575-023-00212-3

Loganzo, F., Sung, M., & Gerber, H.-P. (2016). Mechanisms of resistance to antibody-drug conjugates. Molecular Cancer Therapeutics, 15(12), 2825–2834. doi: 10.1158/1535-7163.MCT-16-0408.

Mani, S. A., Guo, W., Liao, M.-J., Eaton, E. N., Ayyanan, A., Zhou, A. Y., ... Weinberg, R. A. (2008). The epithelial-mesenchymal transition generates cells with properties of stem cells. Cell, 133(4), 704–715. doi:10.1016/j.cell.2008.03.027

McDermott, M., Eustace, A. J., Busschots, S., Breen, L., Crown, J., Clynes, M., O'Donovan, N., & Stordal, B. (2014). In vitro development of chemotherapy and targeted therapy drug-resistant cancer cell lines: A practical guide with case studies. Frontiers in Oncology, 4, 40. doi:10.3389/fonc.2014.00040

Merino, D., Kelly, G. L., Lessene, G., Wei, A. H., Roberts, A. W., & Strasser, A. (2018). BH3-mimetic drugs: Blazing the trail for new cancer medicines. Cancer Cell, 34(6), 879–891. doi:10.1016/j.ccell.2018.11.004

Miller, T. W., Balko, J. M., & Arteaga, C. L. (2011). Phosphatidylinositol 3-kinase and antiestrogen resistance in breast cancer. Journal of Clinical Oncology, 29(33), 4452–4461. doi:10.1200/JCO.2010.34.4879

Modi, S., Saura, C., Yamashita, T., Park, Y. H., Kim, S.-B., Tamura, K., Andre, F., Iwata, H., Ito, Y., Tsurutani, J., Sohn, J., Denduluri, N., Perrin, C., Aogi, K., Tokunaga, E., Im, S.-A., Lee, K. S., Hurvitz, S. A., Cortes, J., ... Krop, I. E. (2020). Trastuzumab deruxtecan in previously treated HER2-positive breast cancer. New England Journal of Medicine, 382(7), 610–621. doi:10.1056/NEJMoa1914510

Musolino, A., Naldi, N., Bortesi, B., Pezzuolo, D., Capelletti, M., Missale, G., ... Ardizzoni, A. (2008). Immunoglobulin G fragment C receptor polymorphisms and clinical efficacy of trastuzumab-based therapy in patients with HER-2/neu-positive metastatic breast cancer. Journal of Clinical Oncology, 26(11), 1789–1796. doi:10.1200/JCO.2007.14.8957

Nagata, Y., Lan, K.-H., Zhou, X., Tan, M., Esteva, F. J., Sahin, A. A., ... Yu, D. (2004). PTEN activation contributes to tumor inhibition by trastuzumab, and loss of PTEN predicts trastuzumab resistance in patients. Cancer Cell, 6(2), 117–127. doi:10.1016/j.ccr.2004.06.022

Nagy, P., Friedländer, E., Tanner, M., Kapanen, A. I., Carraway, K. L., Isola, J., & Jovin, T. M. (2005). Decreased accessibility and lack of activation of ErbB2 in JIMT-1, a herceptin-resistant, MUC4-expressing breast cancer cell line. Cancer Research, 65(2), 473–482.

Nahta, R., Yuan, L. X. H., Zhang, B., Kobayashi, R., & Esteva, F. J. (2005). Insulin-like growth factor-I receptor/human epidermal growth factor receptor 2 heterodimerization contributes to trastuzumab resistance of breast cancer cells. Cancer Research, 65(23), 11118–11128. doi:10.1158/0008-5472.CAN-04-3841

Nanayakkara, A. K., Follit, C. A., Chen, G., Williams, N. S., Vogel, P. D., & Wise, J. G. (2018). Targeted inhibitors of P-glycoprotein increase chemotherapeutic-induced mortality of multidrug resistant tumor cells. Scientific Reports, 8, 967. doi: 10.1038/s41598-018-19325-x.

Ogitani, Y., Aida, T., Hagihara, K., Yamaguchi, J., Ishii, C., Harada, N., ... Agatsuma, T. (2016). DS-8201a, a novel HER2-targeting ADC with a novel DNA topoisomerase I inhibitor, demonstrates a promising antitumor efficacy with differentiation from T-DM1. Clinical Cancer Research, 22(20), 5097–5108. doi:10.1158/1078-0432.CCR-15-2822

O'Reilly, K. E., Rojo, F., She, Q.-B., Solit, D., Mills, G. B., Smith, D., ... Rosen, N. (2006). mTOR inhibition induces upstream receptor tyrosine kinase signaling and activates Akt. Cancer Research, 66(3), 1500–1508. doi: 10.1158/0008-5472.CAN-05-2925.

Osborne, C. K., & Schiff, R. (2011). Mechanisms of endocrine resistance in breast cancer. Annual Review of Medicine, 62, 233–247. doi:10.1146/annurev-med-070909-182917

Osborne, C. K., Bardou, V., Hopp, T. A., Chamness, G. C., Hilsenbeck, S. G., Fuqua, S. A. W., ... Schiff, R. (2003). Role of the estrogen receptor coactivator AIB1 (SRC-3) and HER-2/neu in tamoxifen resistance in breast cancer. Journal of the National Cancer Institute, 95(5), 353–361. doi:10.1093/jnci/95.5.353

Perou, C. M., Sørlie, T., Eisen, M. B., van de Rijn, M., Jeffrey, S. S., Rees, C. A., ... Botstein, D. (2000). Molecular portraits of human breast tumours. Nature, 406(6797), 747–752. doi:10.1038/35021093

Prat, A., Pineda, E., Adamo, B., Galván, P., Fernández, A., Gaba, L., ... Muñoz, M. (2015). Clinical implications of the intrinsic molecular subtypes of breast cancer. The Breast, 24, S26–S35. doi:10.1016/j.breast.2015.07.008

Ramirez, M., Rajaram, S., Steininger, R. J., Osipchuk, D., Roth, M. A., Morinishi, L. S., ... Altschuler, S. J. (2016). Diverse drug-resistance mechanisms can emerge from drug-tolerant cancer persister cells. Nature Communications, 7, 10690. doi:10.1038/ncomms10690

Robey, R. W., Pluchino, K. M., Hall, M. D., Fojo, A. T., Bates, S. E., & Gottesman, M. M. (2018). Revisiting the role of ABC transporters in multidrug-resistant cancer. Nature Reviews Cancer, 18(7), 452–464. doi:10.1038/s41568-018-0005-8

Robinson, D. R., Wu, Y.-M., Vats, P., Su, F., Lonigro, R. J., Cao, X., ... Chinnaiyan, A. M. (2013). Activating ESR1 mutations in hormone-resistant metastatic breast cancer. Nature Genetics, 45(12), 1446–1451. doi:10.1038/ng.2823

Rondinelli, B., Gogola, E., Yücel, H., Duarte, A. A., van de Ven, M., van der Sluijs, R., ... D'Andrea, A. D. (2017). EZH2 promotes degradation of stalled replication forks by recruiting MUS81 through histone H3 trimethylation. Nature Cell Biology, 19(11), 1371–1378. doi:10.1038/ncb3626

Samanta, D., Gilkes, D. M., Chaturvedi, P., Xiang, L., & Semenza, G. L. (2014). Hypoxia-inducible factors are required for chemotherapy resistance of breast cancer stem cells. Proceedings of the National Academy of Sciences, 111(50), E5429–E5438. doi:10.1073/pnas.1421438111

Scaltriti, M., Rojo, F., Ocaña, A., Anido, J., Guzman, M., Cortes, J., ... Baselga, J. (2007). Expression of p95HER2, a truncated form of the HER2 receptor, and response to anti-HER2 therapies in breast cancer. Journal of the National Cancer Institute, 99(8), 628–638. doi:10.1093/jnci/djk134

Schiavon, G., Hrebien, S., Garcia-Murillas, I., Cutts, R. J., Pearson, A., Tarazona, N., ... Turner, N. C. (2015). Analysis of ESR1 mutation in circulating tumor DNA demonstrates evolution during therapy for metastatic breast cancer. Science Translational Medicine, 7(313), 313ra182. doi:10.1126/scitranslmed.aac7551

Sergina, N. V., Rausch, M., Wang, D., Blair, J., Hann, B., Shokat, K. M., & Moasser, M. M. (2007). Escape from HER-family tyrosine kinase inhibitor therapy by

the kinase-inactive HER3. Nature, 445(7126), 437–441. doi:10.1038/nature05474

Sharma, S. V., Lee, D. Y., Li, B., Quinlan, M. P., Takahashi, F., Maheswaran, S., ... Settleman, J. (2010). A chromatin-mediated reversible drug-tolerant state in cancer cell subpopulations. Cell, 141(1), 69–80. doi:10.1016/j.cell.2010.02.027

Sørlie, T., Perou, C. M., Tibshirani, R., Aas, T., Geisler, S., Johnsen, H., ... Børresen-Dale, A.-L. (2001). Gene expression patterns of breast carcinomas distinguish tumor subclasses with clinical implications. Proceedings of the National Academy of Sciences, 98(19), 10869–10874. doi:10.1073/pnas.191367098

Stovgaard, E. S., Nielsen, D., Hogdall, E., & Balslev, E. (2018). Triple negative breast cancer – prognostic role of immune-related factors: A systematic review. Acta Oncologica, 57(1), 74-82. doi: 10.1080/0284186X.2017.1400180.

Sung, M., Tan, X., Lu, B., Golas, J., Hosselet, C., Wang, F., ... Loganzo, F. (2018). Caveolae-mediated endocytosis as a novel mechanism of resistance to trastuzumab emtansine (T-DM1). Molecular Cancer Therapeutics, 17(1), 243-253. doi:10.1158/1535-7163.MCT-17-0403

Swain, S. M., Baselga, J., Kim, S.-B., Ro, J., Semiglazov, V., Campone, M., ... Cortés, J. (2015). Pertuzumab, trastuzumab, and docetaxel in HER2-positive metastatic breast cancer. New England Journal of Medicine, 372(8), 724–734. doi:10.1056/NEJMoa1413513

Tchou, J., & Conejo-Garcia, J. (2012). Targeting the tumor stroma as a novel treatment strategy for breast cancer: Shifting from the neoplastic cell-centric to a stroma-centric paradigm. Advances in Pharmacology, 65, 45–61. doi:10.1016/B978-0-12-397927-8.00003-8

Toy, W., Shen, Y., Won, H., Green, B., Sakr, R. A., Will, M., Li, Z., Gala, K., Fanning, S., King, T. A., Hudis, C., Chen, D., Taran, T., Hortobagyi, G., Greene, G., Berger, M., Baselga, J., & Chandarlapaty, S. (2013). ESR1 ligand-binding domain mutations in hormone-resistant breast cancer. Nature Genetics, 45(12), 1439–1445. doi:10.1038/ng.2822

Turashvili, G., & Brogi, E. (2017). Tumor heterogeneity in breast cancer. Frontiers in Medicine, 4, 227. doi: 10.3389/fmed.2017.00227.

Turner, N. C., Kingston, B., Kilburn, L. S., Kernaghan, S., Wardley, A. M., Macpherson, I. R., ... Ring, A. (2020). Circulating tumour DNA analysis to direct therapy in advanced breast cancer (plasmaMATCH): A multicentre, multicohort, phase 2a, platform trial. The Lancet Oncology, 21(10), 1296–1308. doi:10.1016/S1470-2045(20)30444-7

Turner, N. C., Liu, Y., Zhu, Z., Loi, S., Colleoni, M., Loibl, S., DeMichele, A., Harbeck, N., André, F., Bayar, M. A., Michiels, S., Zhang, Z., Giorgetti, C., Arnedos, M., & Cristofanilli, M. (2019). Cyclin E1 expression and palbociclib efficacy in previously treated hormone receptor–positive metastatic breast cancer. Journal of Clinical Oncology, 37(14), 1169–1178. doi:10.1200/JCO.18.00925

Vaillant, F., Merino, D., Lee, L., Breslin, K., Pal, B., Ritchie, M. E., Smyth, G. K., Christie, M., Phillipson, L. J., Burns, C. J., Mann, G. B., Visvader, J. E., & Lindeman, G. J. (2013). Targeting BCL-2 with the BH3 mimetic ABT-199 in estrogen receptor-positive breast cancer. Cancer Cell, 24(1), 120–129. doi:10.1016/j.ccr.2013.06.002

Wind, N. S., & Holen, I. (2011). Multidrug resistance in breast cancer: From in vitro models to clinical studies. International Journal of Breast Cancer, 2011, 967419. doi:10.4061/2011/967419

Yap, T. A., Plummer, R., Azad, N. S., & Helleday, T. (2019). The DNA damaging revolution: PARP inhibitors and beyond. American Society of Clinical Oncology Educational Book, 39, 185–195. doi:10.1200/EDBK_238473

Zaretsky, J. M., Garcia-Diaz, A., Shin, D. S., Escuin-Ordinas, H., Hugo, W., Hu-Lieskovan, S., ... Ribas, A. (2016). Mutations associated with acquired resistance to PD-1 blockade in melanoma. New England Journal of Medicine, 375(9), 819–829. doi:10.1056/NEJMoa1604958

CHAPTER 8

Generalized Tribonacci Three-Parameter Generalized Octonions and Their Hamilton Matrix Sequences

***Göksal Bilgici*[1]**

[1] Prof. Dr., Kastamonu University, Faculty of Education, Department of Elementary Mathematics Education, Kastamonu, Türkiye, 0000-0001-9964-5578

1. Introduction

Number sequences with values in hypercomplex algebras have been studied extensively since Horadam's introduction of Fibonacci quaternions (Horadam, 1963). Fibonacci and Lucas octonions, Jacobsthal octonions, Horadam octonions, Pell-type octonions, and several higher-order recurrence constructions have subsequently appeared in the literature (Akkuş & Keçilioğlu, 2015; Bilgici, Ünal, Tokeşer, & Mert, 2018; Cerda-Morales, 2018; Çimen & İpek, 2017; Karataş & Halici, 2017; Keçilioğlu & Akkuş, 2015; Savin, 2015; Tokeşer, Mert, Ünal, & Bilgici, 2021), and higher-dimensional analogues such as Tribonacci and Tribonacci-Lucas sedenions have also been considered (Soykan, 2019). These studies show that recurrence sequences provide a natural bridge between discrete number theory and finite-dimensional noncommutative algebras.

A particularly useful third-order framework is the generalized Tribonacci sequence

$$V_n = rV_{n-1} + sV_{n-2} + tV_{n-3}, \qquad n \geq 3,$$

with arbitrary initial values $V_0 = a$, $V_1 = b$, and $V_2 = c$. Third-order recurrence relations were systematically investigated by Shannon and Horadam (1972). Cerda-Morales later introduced generalized Tribonacci quaternions (Cerda-Morales, 2017) and a unified construction for Tribonacci-type octonions (Cerda-Morales, 2019). Independently, Özkoç Öztürk (2019) studied generalized Tribonacci octonions and derived recurrence, summation, Binet, norm, and generating-function formulas. Thus, generalized Tribonacci sequences already have a well-developed classical octonionic theory.

A second line of research concerns parameterized hypercomplex algebras. Şentürk and Ünal (2022) introduced three-parameter generalized quaternions (3PGQs) and studied their algebraic, matrix, polar, and Lie-theoretic properties. Fibonacci 3PGQs were subsequently considered by Bilgici (2022), Horadam 3PGQs by İşbilir and Gürses (2024), and generalized Tribonacci components were incorporated into the 3PGQ setting by İşbilir, Gürses, and Tosun (2025). The latter work established Binet and generating formulas together with matrix-related results for the quaternionic construction.

Yamaç Akbıyık (2024) developed a matrix-based treatment of generalized Cayley numbers and explicitly used the terminology **three-parameter generalized octonions (3PGOs)**. The algebra depends on three real parameters μ_1, μ_2, μ_3 and contains a range of octonionic systems as special cases. In particular, the choices $(-1,-1,-1)$, $(-1,-1,1)$, $(-1,-1,0)$, $(1,1,0)$, $(-1,0,0)$, $(1,0,0)$, and $(0,0,0)$ lead, respectively, to real, split, semi, split-semi, quasi, split-quasi, and para-octonions (Yamaç Akbıyık, 2024). The same work provides explicit real 8×8 left/right multiplication matrices, referred to as Hamilton operators. We note that the term para-octonion is used here in the sense of Yamaç

Akbıyık (2024) for the fully degenerate parameter choice (0, 0, 0); it should not be confused with the para-octonion (para-Hurwitz) algebra in the sense of Okubo.

The preceding literature suggests a natural question: what additional information is obtained when generalized Tribonacci components are placed directly in the 3PGO algebra rather than in the ordinary octonion or 3PGQ settings? A simple reparameterization of known generalized Tribonacci octonions would not by itself provide sufficient mathematical novelty. The present study therefore focuses on structural phenomena that depend on the three-parameter quadratic form, the noncommutative/nonassociative multiplication, and the associated 8×8 multiplication operators.

The principal contributions are as follows.

1. Generalized Tribonacci 3PGOs are defined and their recurrence, generating functions, Binet formula, and finite sums are established in a form valid for arbitrary recurrence parameters r, s, t and arbitrary 3PGO parameters μ_1, μ_2, μ_3; the finite-sum formula is given in a Binet-free form that does not require distinct characteristic roots.

2. The conjugate and the parameter-dependent quadratic form are obtained explicitly. It is observed that the 3PGO algebra is alternative for all parameter values, including the degenerate ones (Lemma 2.2); consequently $\mathcal{T}_n\overline{\mathcal{T}_n} = q_n$ and $\mathcal{T}_n^2 = 2V_n\mathcal{T}_n - q_n$.

3. The sequence of quadratic forms $q_n = N_\mu(\mathcal{T}_n)$ is shown to satisfy a sixth-order recurrence whose coefficients depend only on r, s, t, whereas μ_1, μ_2, μ_3 enter only through the initial values. Although this is an instance of the classical fact that termwise squares of a third-order linear recurrence satisfy a recurrence of order six, it makes explicit the separation between the recurrence dynamics and the geometry of the ambient 3PGO algebra.

4. Using alternativity, the commutators and associators of GT-3PGOs are described in closed form: every commutator $[\mathcal{T}_m, \mathcal{T}_n]$ is a combination of $[\mathcal{T}_0, \mathcal{T}_1]$, $[\mathcal{T}_0, \mathcal{T}_2]$, $[\mathcal{T}_1, \mathcal{T}_2]$, every associator $(\mathcal{T}_\ell, \mathcal{T}_m, \mathcal{T}_n)$ is a determinant multiple of $(\mathcal{T}_0, \mathcal{T}_1, \mathcal{T}_2)$, and $(\mathcal{T}_n, \mathcal{T}_{n+1}, \mathcal{T}_{n+2}) = t^n(\mathcal{T}_0, \mathcal{T}_1, \mathcal{T}_2)$.

5. Right and left Hamilton matrix sequences are constructed. Their recurrence relations, Binet formulas, generating functions, traces, and coordinate-recovery formulas are derived using only the linearity of multiplication operators, while alternativity yields the quadratic relation $L_n^2 - 2V_nL_n + q_nI_8 = 0$, the characteristic polynomial $(z^2 - 2V_nz + q_n)^4$, the determinant formula $\det L_n = \det R_n = q_n^4$, and an explicit inverse whenever $q_n \neq 0$. No multiplicativity of the map from a nonassociative algebra to ordinary matrices is required.

These results provide a framework encompassing numerous third-order integer sequences and several octonionic algebras simultaneously.

2. Preliminaries

2.1. Three-parameter generalized octonions

Let

$$\mathfrak{C}_{\mu_1,\mu_2,\mu_3} = \mathrm{span}_{\mathbb{R}}\{1, e_1, e_2, e_3, e_4, e_5, e_6, e_7\}.$$

An arbitrary element is

$$x = x_0 + x_1e_1 + x_2e_2 + x_3e_3 + x_4e_4 + x_5e_5 + x_6e_6 + x_7e_7,$$

where $x_i, \mu_i \in \mathbb{R}$. Following the three-parameter generalized octonion convention of Yamaç Akbıyık (2024), the squares of the imaginary basis elements are

$$e_1^2 = \mu_1, \qquad e_2^2 = \mu_2, \qquad e_3^2 = -\mu_1\mu_2.$$
$$e_4^2 = \mu_3, \qquad e_5^2 = -\mu_1\mu_3, \qquad e_6^2 = -\mu_2\mu_3.$$
$$e_7^2 = \mu_1\mu_2\mu_3.$$

For distinct basis elements the multiplication is anticommutative, and the upper-triangular products can be recorded as

$$e_1e_2 = e_3, \quad e_1e_3 = \mu_1e_2, \quad e_1e_4 = e_5.$$
$$e_1e_5 = \mu_1e_4, \quad e_1e_6 = -e_7, \quad e_1e_7 = -\mu_1e_6.$$
$$e_2e_3 = -\mu_2e_1, \quad e_2e_4 = e_6, \quad e_2e_5 = e_7.$$
$$e_2e_6 = \mu_2e_4, \quad e_2e_7 = \mu_2e_5, \quad e_3e_4 = e_7.$$
$$e_3e_5 = \mu_1e_6, \quad e_3e_6 = -\mu_2e_5, \quad e_3e_7 = -\mu_1\mu_2e_4.$$
$$e_4e_5 = -\mu_3e_1, \quad e_4e_6 = -\mu_3e_2, \quad e_4e_7 = -\mu_3e_3.$$
$$e_5e_6 = \mu_3e_3, \quad e_5e_7 = \mu_1\mu_3e_2, \quad e_6e_7 = -\mu_2\mu_3e_1.$$

The conjugate of x is

$$\overline{x} = x_0 - x_1e_1 - x_2e_2 - x_3e_3 - x_4e_4 - x_5e_5 - x_6e_6 - x_7e_7.$$

The scalar quadratic form associated with $x\overline{x}$ is

$$N_\mu(x) = x_0^2 - \mu_1x_1^2 - \mu_2x_2^2 + \mu_1\mu_2x_3^2 - \mu_3x_4^2$$
$$+\mu_1\mu_3x_5^2 + \mu_2\mu_3x_6^2 - \mu_1\mu_2\mu_3x_7^2.$$

The corresponding symmetric bilinear form is obtained by polarization. For generic choices of μ_1, μ_2, μ_3, the algebra $\mathfrak{C}_{\mu_1,\mu_2,\mu_3}$ is noncommutative and

nonassociative. It is, however, alternative for every choice of the parameters, including the degenerate ones (Lemma 2.2 below); for the real and split specializations this recovers the classical alternative octonion algebras (Yamaç Akbıyık, 2024).

Remark 2.1. For $(\mu_1, \mu_2, \mu_3) = (-1, -1, -1)$, all seven imaginary units square to -1 and N_μ becomes the usual positive-definite Euclidean octonion norm.

The following two elementary facts will be used repeatedly. For $x, y, z \in \mathfrak{C}_{\mu_1,\mu_2,\mu_3}$ we write

$$(x, y, z) = (xy)z - x(yz)$$

for the associator.

Lemma 2.2. For all $\mu_1, \mu_2, \mu_3 \in \mathbb{R}$ and all $x, y \in \mathfrak{C}_{\mu_1,\mu_2,\mu_3}$,

$$(x, x, y) = 0, \qquad (y, x, x) = 0.$$

Consequently, the associator is an alternating trilinear map: it vanishes whenever two of its arguments coincide, and it changes sign under any transposition of its arguments.

Proof. The associator is trilinear. Hence left alternativity is equivalent to the identities $(e_i, e_j, e_k) + (e_j, e_i, e_k) = 0$ for $0 \le i \le j \le 7$ and $0 \le k \le 7$, and right alternativity is equivalent to $(e_k, e_i, e_j) + (e_k, e_j, e_i) = 0$ for the same ranges of indices. These are finitely many polynomial identities in μ_1, μ_2, μ_3, and a direct verification with the multiplication table above (readily carried out with a computer algebra system) shows that all of them hold identically. For the second statement, replacing x by $x + z$ in $(x, x, y) = 0$ gives $(x, z, y) = -(z, x, y)$, and replacing x by $x + z$ in $(y, x, x) = 0$ gives $(y, x, z) = -(y, z, x)$. Since the transpositions of the first two and of the last two positions generate the symmetric group S_3, the associator is alternating. ▫

For nonzero parameters the multiplication table above is that of a Cayley–Dickson doubling of a generalized quaternion algebra, and Lemma 2.2 reduces to the classical alternativity of octonion algebras (see, e.g., Baez, 2002, for the real case). The point of Lemma 2.2 is that alternativity persists for all degenerate parameter values as well.

Lemma 2.3. For every $x = x_0 + v \in \mathfrak{C}_{\mu_1,\mu_2,\mu_3}$ with $v = \sum_{j=1}^{7} x_j\, e_j$,

$$x\overline{x} = \overline{x}\,x = N_\mu(x), \qquad x^2 = 2x_0 x - N_\mu(x).$$

Proof. Distinct imaginary units anticommute, so the mixed terms in v^2 cancel and $v^2 = \sum_{j=1}^{7} x_j^2\, e_j^2 = x_0^2 - N_\mu(x)$. Hence $x\overline{x} = (x_0 + v)(x_0 - v) = x_0^2 -$

$v^2 = N_\mu(x)$, and the same computation gives $\overline{x}\, x$. Moreover, $x^2 = x_0^2 + 2x_0 v + v^2 = 2x_0(x_0 + v) - N_\mu(x)$. ▫

2.2. Generalized Tribonacci numbers

Let $a, b, c, r, s, t \in \mathbb{R}$. The generalized Tribonacci sequence $\{V_n\}_{n\geq 0}$ is defined by

$$V_0 = a, \qquad V_1 = b, \qquad V_2 = c,$$

and

$$V_{n+3} = rV_{n+2} + sV_{n+1} + tV_n, \qquad n \geq 0.$$

When a, b, c, r, s, t are integers, the sequence is integer-valued. Its characteristic polynomial is

$$p(z) = z^3 - rz^2 - sz - t.$$

Let α, β, γ be the roots of p. Hence

$$\alpha + \beta + \gamma = r, \qquad \alpha\beta + \alpha\gamma + \beta\gamma = -s, \qquad \alpha\beta\gamma = t.$$

If the roots are pairwise distinct, define

$$A = \frac{c - (\beta + \gamma)b + \beta\gamma a}{(\alpha - \beta)(\alpha - \gamma)},$$

$$B = \frac{c - (\alpha + \gamma)b + \alpha\gamma a}{(\beta - \alpha)(\beta - \gamma)},$$

and

$$C = \frac{c - (\alpha + \beta)b + \alpha\beta a}{(\gamma - \alpha)(\gamma - \beta)}.$$

Then

$$V_n = A\alpha^n + B\beta^n + C\gamma^n.$$

The construction includes many familiar third-order recurrences. Representative parameter choices are listed in Table 1.

Table 1. Representative parameter choices of the generalized Tribonacci sequence

Family	(r, s, t)	Recurrence
Tribonacci	$(1,1,1)$	$V_{n+3} = V_{n+2} + V_{n+1} + V_n$
Padovan type	$(0,1,1)$	$V_{n+3} = V_{n+1} + V_n$
Pell-Padovan type	$(0,2,1)$	$V_{n+3} = 2V_{n+1} + V_n$
Tribonacci-Pell type	$(2,1,1)$	$V_{n+3} = 2V_{n+2} + V_{n+1} + V_n$
Third-order Jacobsthal type	$(1,1,2)$	$V_{n+3} = V_{n+2} + V_{n+1} + 2V_n$
Jacobsthal-Padovan type	$(0,1,2)$	$V_{n+3} = V_{n+1} + 2V_n$
Narayana type	$(1,0,1)$	$V_{n+3} = V_{n+2} + V_n$

Source: Compiled by the author.

The initial values can be selected according to the conventional version of the desired sequence.

3. Generalized Tribonacci 3PGOs

3.1. Definition and basic recurrence

Definition 3.1. The *n*th generalized Tribonacci three-parameter generalized octonion (GT-3PGO) is

$$\mathcal{T}_n = \sum_{j=0}^{7} V_{n+j}\, e_j = V_n + V_{n+1}e_1 + \cdots + V_{n+7}e_7,$$

where $e_0 = 1$ and the basis is that of $\mathfrak{C}_{\mu_1,\mu_2,\mu_3}$.

The first three elements are

$$\mathcal{T}_0 = \sum_{j=0}^{7} V_j\, e_j, \qquad \mathcal{T}_1 = \sum_{j=0}^{7} V_{j+1}\, e_j, \qquad \mathcal{T}_2 = \sum_{j=0}^{7} V_{j+2}\, e_j.$$

Theorem 3.2. The GT-3PGO sequence satisfies

$$\mathcal{T}_{n+3} = r\mathcal{T}_{n+2} + s\mathcal{T}_{n+1} + t\mathcal{T}_n, \qquad n \geq 0.$$

Proof. By Definition 3.1,

$$\mathcal{T}_{n+3} = \sum_{j=0}^{7} V_{n+j+3}\, e_j.$$

Applying the scalar recurrence to every component gives

$$V_{n+j+3} = rV_{n+j+2} + sV_{n+j+1} + tV_{n+j}.$$

Therefore

$$\mathcal{T}_{n+3} = r\sum_{j=0}^{7} V_{n+j+2}\, e_j + s\sum_{j=0}^{7} V_{n+j+1}\, e_j + t\sum_{j=0}^{7} V_{n+j}\, e_j.$$

Therefore,

$$\mathcal{T}_{n+3} = r\mathcal{T}_{n+2} + s\mathcal{T}_{n+1} + t\mathcal{T}_n.$$

This proves the assertion. ▫

Remark 3.3. The additive recurrence does not depend on μ_1, μ_2, μ_3. The octonionic parameters enter only when multiplication, conjugation, the quadratic form, commutators, associators, or Hamilton operators are considered.

3.2. Ordinary generating function

Theorem 3.4. The ordinary generating function

$$G(x) = \sum_{n=0}^{\infty} \mathcal{T}_n\, x^n$$

is

$$G(x) = \frac{\mathcal{T}_0 + (\mathcal{T}_1 - r\mathcal{T}_0)x + (\mathcal{T}_2 - r\mathcal{T}_1 - s\mathcal{T}_0)x^2}{1 - rx - sx^2 - tx^3}.$$

Proof. Multiply $G(x)$ successively by rx, sx^2, and tx^3 and subtract from $G(x)$. All coefficients of degree at least three vanish by Theorem 3.2, leaving exactly the stated numerator. ▫

3.3. Binet-type formula

For a scalar z, put

$$\hat{z} = 1 + ze_1 + z^2e_2 + z^3e_3 + z^4e_4 + z^5e_5 + z^6e_6 + z^7e_7.$$

Theorem 3.5. Suppose that α, β, γ are pairwise distinct roots of $p(z) = z^3 - rz^2 - sz - t$. Then

$$\mathcal{T}_n = A\hat{\alpha}\,\alpha^n + B\hat{\beta}\,\beta^n + C\hat{\gamma}\,\gamma^n.$$

Proof. From the scalar Binet formula,

$$V_{n+j} = A\alpha^{n+j} + B\beta^{n+j} + C\gamma^{n+j}.$$

Hence

$$\mathcal{T}_n = \sum_{j=0}^{7} V_{n+j}\, e_j.$$

Substituting the scalar Binet representation gives

$$\mathcal{T}_n = A\alpha^n \sum_{j=0}^{7} \alpha^j\, e_j + B\beta^n \sum_{j=0}^{7} \beta^j\, e_j + C\gamma^n \sum_{j=0}^{7} \gamma^j\, e_j,$$

which is the required expression. ▫

We note that the roots α, β, γ need not be real. In that case A, B, C and $\hat{\alpha}, \hat{\beta}, \hat{\gamma}$ are understood over $\mathbb{C}$, and the right-hand side of Theorem 3.5 is nevertheless real for every n, since it equals $\mathcal{T}_n$.

3.4. Exponential and Poisson generating functions

Corollary 3.6. Under the hypotheses of Theorem 3.5,

$$\sum_{n=0}^{\infty} \mathcal{T}_n \frac{x^n}{n!} = A\hat{\alpha}e^{\alpha x} + B\hat{\beta}e^{\beta x} + C\hat{\gamma}e^{\gamma x}.$$

Consequently, the Poisson transform is

$$e^{-x} \sum_{n=0}^{\infty} \mathcal{T}_n \frac{x^n}{n!} = A\hat{\alpha}e^{(\alpha-1)x} + B\hat{\beta}e^{(\beta-1)x} + C\hat{\gamma}e^{(\gamma-1)x}.$$

3.5. Finite sums

Theorem 3.7. If $r + s + t \neq 1$, then for every $n \geq 0$,

$$\sum_{k=0}^{n} \mathcal{T}_k = \frac{\mathcal{T}_{n+2} + (1-r)\mathcal{T}_{n+1} + t\mathcal{T}_n - \mathcal{T}_2 + (r-1)\mathcal{T}_1 + (r+s-1)\mathcal{T}_0}{r+s+t-1}.$$

Proof. Put $S_n = \sum_{k=0}^{n} \mathcal{T}_k$. For $n \geq 1$, summing the recurrence of Theorem 3.2 over $k = 0, \dots, n-1$ gives

$$S_{n+2} - \mathcal{T}_0 - \mathcal{T}_1 - \mathcal{T}_2 = r(S_{n+1} - \mathcal{T}_0 - \mathcal{T}_1) + s(S_n - \mathcal{T}_0) + t(S_n - \mathcal{T}_n).$$

Substituting $S_{n+2} = S_n + \mathcal{T}_{n+1} + \mathcal{T}_{n+2}$ and $S_{n+1} = S_n + \mathcal{T}_{n+1}$ and solving for S_n yields the assertion. The case $n = 0$ is checked directly. ▫

Remark 3.8. The condition $r + s + t \neq 1$ means $p(1) \neq 0$, that is, 1 is not a characteristic root; no assumption on the multiplicity of the roots is needed. If, in

addition, α, β, γ are pairwise distinct, Theorem 3.5 and the finite geometric series give the equivalent Binet form

$$\sum_{k=0}^{n} \mathcal{T}_k = A\hat{\alpha}\,\frac{\alpha^{n+1}-1}{\alpha-1} + B\hat{\beta}\,\frac{\beta^{n+1}-1}{\beta-1} + C\hat{\gamma}\,\frac{\gamma^{n+1}-1}{\gamma-1}.$$

If $r+s+t=1$, the partial sums S_n satisfy the fourth-order recurrence with characteristic polynomial $(z-1)p(z)$, and a closed form follows from the corresponding generalized Binet formula.

4. Conjugation, Quadratic Forms, and Nonassociative Sequence Invariants

4.1. Conjugate and quadratic form

Proposition 4.1. The conjugate of $\mathcal{T}_n$ is

$$\overline{\mathcal{T}_n} = V_n - V_{n+1}e_1 - V_{n+2}e_2 - \cdots - V_{n+7}e_7.$$

In particular,

$$\mathcal{T}_n + \overline{\mathcal{T}_n} = 2V_n.$$

The associated quadratic form is

$$q_n := N_\mu(\mathcal{T}_n) = V_n^2 - \mu_1 V_{n+1}^2 - \mu_2 V_{n+2}^2 + \mu_1\mu_2 V_{n+3}^2$$
$$-\mu_3 V_{n+4}^2 + \mu_1\mu_3 V_{n+5}^2 + \mu_2\mu_3 V_{n+6}^2 - \mu_1\mu_2\mu_3 V_{n+7}^2.$$

For convenience define the weights

$$(w_0, w_1, \ldots, w_7) = (1, -\mu_1, -\mu_2, \mu_1\mu_2, -\mu_3, \mu_1\mu_3, \mu_2\mu_3, -\mu_1\mu_2\mu_3).$$

Then

$$q_n = \sum_{j=0}^{7} w_j\, V_{n+j}^2.$$

Moreover, by Lemma 2.3,

$$\mathcal{T}_n\overline{\mathcal{T}_n} = \overline{\mathcal{T}_n}\,\mathcal{T}_n = q_n, \qquad \mathcal{T}_n^2 = 2V_n\mathcal{T}_n - q_n.$$

In particular, if $q_n \neq 0$, then $\mathcal{T}_n$ is invertible with $\mathcal{T}_n^{-1} = \overline{\mathcal{T}_n}/q_n$, whereas if $q_n = 0$ and $\mathcal{T}_n \neq 0$, then $\mathcal{T}_n$ is a zero divisor in $\mathfrak{C}_{\mu_1,\mu_2,\mu_3}$.

4.2. A sixth-order recurrence for the quadratic-form sequence

The next theorem gives a recurrence for q_n that is independent of the three octonionic parameters. It is an instance of the classical fact that the termwise square of a sequence satisfying a linear recurrence of order three satisfies a linear recurrence of order at most six. The point here is that the quadratic form of the

ambient algebra has no influence on the recurrence; this separates the third-order recurrence dynamics from the signature and degeneracy encoded by μ_1, μ_2, μ_3.

Theorem 4.2. Let $q_n = N_\mu(\mathcal{T}_n)$ and define

$$c_1 = r^2 + s, \qquad c_2 = r^2 s + rt + s^2,$$
$$c_3 = r^3 t + 4rst - s^3 + 2t^2,$$
$$c_4 = r^2 t^2 - rs^2 t - st^2, \qquad c_5 = -rt^3 + s^2 t^2, \qquad c_6 = -t^4.$$

Then q_n is annihilated by the degree-six polynomial

$$Q(z) = z^6 - c_1 z^5 - c_2 z^4 - c_3 z^3 - c_4 z^2 - c_5 z - c_6.$$

Equivalently,

$$q_{n+6} = c_1 q_{n+5} + c_2 q_{n+4} + c_3 q_{n+3} + c_4 q_{n+2} + c_5 q_{n+1} + c_6 q_n.$$

Proof. Let E denote the shift operator $(Ex)_n = x_{n+1}$ on complex sequences. Since $q_n = \sum_{j=0}^{7} w_j V_{n+j}^2$ and every sequence $\left(V_{n+j}^2\right)_{n\geq 0}$ is a shift of $(V_n^2)_{n\geq 0}$, it suffices to show that $Q(E)$ annihilates $(V_n^2)_{n\geq 0}$.

Let $\mathcal{S}$ be the three-dimensional complex vector space of solutions of $X_{n+3} = rX_{n+2} + sX_{n+1} + tX_n$. The shift E maps $\mathcal{S}$ into itself, and its characteristic polynomial on $\mathcal{S}$ is $p(z)$. Let $\mathcal{S}^{(2)}$ be the linear span of all termwise products $(X_n Y_n)_{n\geq 0}$ with $X, Y \in \mathcal{S}$. The symmetric bilinear map $(X, Y) \mapsto (X_n Y_n)_{n\geq 0}$ induces a surjective linear map $\Phi: \mathrm{Sym}^2\mathcal{S} \to \mathcal{S}^{(2)}$, and since the shift of a termwise product is the termwise product of the shifts,

$$E \circ \Phi = \Phi \circ \mathrm{Sym}^2 E.$$

Choose a basis u_1, u_2, u_3 of $\mathcal{S}$ in which E is upper triangular with diagonal entries α, β, γ, the roots of p listed with multiplicity. Ordering the induced basis $u_i u_j$ $(i \leq j)$ of $\mathrm{Sym}^2\mathcal{S}$ first by j and then by i, the operator $\mathrm{Sym}^2 E$ is again upper triangular, with diagonal entries $\alpha^2, \beta^2, \gamma^2, \alpha\beta, \alpha\gamma, \beta\gamma$. Hence the characteristic polynomial of $\mathrm{Sym}^2 E$ is

$$Q(z) = (z - \alpha^2)(z - \beta^2)(z - \gamma^2)(z - \alpha\beta)(z - \alpha\gamma)(z - \beta\gamma).$$

By the Cayley–Hamilton theorem, $Q(\mathrm{Sym}^2 E) = 0$, and therefore $Q(E) \circ \Phi = \Phi \circ Q(\mathrm{Sym}^2 E) = 0$. Thus $Q(E)$ annihilates every element of $\mathcal{S}^{(2)}$, in particular $(V_n^2)_{n\geq 0}$. Finally, expanding Q and using

$$\alpha + \beta + \gamma = r, \quad \alpha\beta + \alpha\gamma + \beta\gamma = -s, \quad \alpha\beta\gamma = t$$

gives exactly the coefficients $c_1, \ldots, c_6$ stated above. No assumption on the multiplicity of the roots is needed. ▫

Remark 4.3. The coefficients in Theorem 4.2 depend only on r, s, t. The parameters μ_1, μ_2, μ_3 affect $q_0, \ldots, q_5$ but not the recurrence itself; by the proof,

this is because q_n is a fixed linear combination of shifts of the single sequence (V_n^2). We also note that Q need not be the minimal annihilating polynomial of (q_n): for special initial values or parameters, (q_n) may satisfy a recurrence of lower order.

Corollary 4.4 (ordinary Tribonacci case). For $r = s = t = 1$,

$$q_{n+6} = 2q_{n+5} + 3q_{n+4} + 6q_{n+3} - q_{n+2} - q_n.$$

Thus all three-parameter Tribonacci octonion quadratic-form sequences share the same sixth-order recurrence, regardless of whether the underlying algebra is real, split, semi, quasi, or para-octonionic; only their initial quadratic-form values differ.

4.3. Reduction to the first three terms

Let $(U_n)_{n\geq 0}$ be the generalized Tribonacci sequence with $U_0 = 0$, $U_1 = 0$, $U_2 = 1$, and define

$$F_n^{(0)} = U_{n+2} - rU_{n+1} - sU_n, \qquad F_n^{(1)} = U_{n+1} - rU_n, \qquad F_n^{(2)} = U_n.$$

Lemma 4.5. For every $n \geq 0$,

$$\mathcal{T}_n = F_n^{(0)}\mathcal{T}_0 + F_n^{(1)}\mathcal{T}_1 + F_n^{(2)}\mathcal{T}_2.$$

Proof. Each $F^{(i)}$ is a linear combination of shifts of (U_n) and hence satisfies the recurrence of Theorem 3.2. Using $U_3 = r$ and $U_4 = r^2 + s$, one checks that $F_k^{(i)} = \delta_{ik}$ for $i, k \in \{0,1,2\}$. Thus both sides of the claimed identity satisfy the same third-order recurrence and agree for $n = 0,1,2$. ▫

4.4. Commutators

For $x, y \in \mathfrak{C}_{\mu_1,\mu_2,\mu_3}$ we write $[x, y] = xy - yx$.

Theorem 4.6. For all $m, n \geq 0$,

$$[\mathcal{T}_m, \mathcal{T}_n] = \sum_{0\leq i<j\leq 2} \left(F_m^{(i)}F_n^{(j)} - F_m^{(j)}F_n^{(i)}\right)[\mathcal{T}_i, \mathcal{T}_j].$$

Thus every commutator of GT-3PGOs is a combination of the three basic commutators $[\mathcal{T}_0, \mathcal{T}_1]$, $[\mathcal{T}_0, \mathcal{T}_2]$, and $[\mathcal{T}_1, \mathcal{T}_2]$, with coefficients given by 2×2 minors of the fundamental solutions. In particular, for fixed m the sequence $n \mapsto [\mathcal{T}_m, \mathcal{T}_n]$ satisfies the recurrence of Theorem 3.2, and the same holds in the first index.

Proof. Substitute Lemma 4.5 into both arguments and use bilinearity together with $[\mathcal{T}_i, \mathcal{T}_i] = 0$ and $[\mathcal{T}_j, \mathcal{T}_i] = -[\mathcal{T}_i, \mathcal{T}_j]$. The recurrence statements follow because each $F^{(i)}$ satisfies the recurrence. ▫

4.5. Associators

Theorem 4.7. For all $\ell, m, n \geq 0$,

$$(\mathcal{T}_\ell, \mathcal{T}_m, \mathcal{T}_n) = \Delta_{\ell,m,n}\,(\mathcal{T}_0, \mathcal{T}_1, \mathcal{T}_2),$$

where

$$\Delta_{\ell,m,n} = \det\begin{pmatrix} F_\ell^{(0)} & F_\ell^{(1)} & F_\ell^{(2)} \\ F_m^{(0)} & F_m^{(1)} & F_m^{(2)} \\ F_n^{(0)} & F_n^{(1)} & F_n^{(2)} \end{pmatrix}.$$

Proof. By Lemma 4.5 and trilinearity,

$$(\mathcal{T}_\ell, \mathcal{T}_m, \mathcal{T}_n) = \sum_{i,j,k=0}^{2} F_\ell^{(i)} F_m^{(j)} F_n^{(k)} \left(\mathcal{T}_i, \mathcal{T}_j, \mathcal{T}_k\right).$$

By Lemma 2.2 the associator is alternating. Hence only the terms in which (i, j, k) is a permutation σ of $(0,1,2)$ survive, and $\left(\mathcal{T}_{\sigma(0)}, \mathcal{T}_{\sigma(1)}, \mathcal{T}_{\sigma(2)}\right) = \operatorname{sgn}(\sigma)\,(\mathcal{T}_0, \mathcal{T}_1, \mathcal{T}_2)$. The remaining sum is the Leibniz expansion of $\Delta_{\ell,m,n}$. ▫

Corollary 4.8. For every $n \geq 0$,

$$(\mathcal{T}_n, \mathcal{T}_{n+1}, \mathcal{T}_{n+2}) = t^n\,(\mathcal{T}_0, \mathcal{T}_1, \mathcal{T}_2).$$

Proof. Substituting $\mathcal{T}_{n+3} = r\mathcal{T}_{n+2} + s\mathcal{T}_{n+1} + t\mathcal{T}_n$ into the third argument and using that the associator is alternating (Lemma 2.2), we obtain

$$(\mathcal{T}_{n+1}, \mathcal{T}_{n+2}, \mathcal{T}_{n+3}) = t\,(\mathcal{T}_{n+1}, \mathcal{T}_{n+2}, \mathcal{T}_n) = t\,(\mathcal{T}_n, \mathcal{T}_{n+1}, \mathcal{T}_{n+2}),$$

since a cyclic permutation is even. Induction on n completes the proof. ▫

Equivalently, $\Delta_{n,n+1,n+2} = t^n$, which is the Casoratian identity for the fundamental system $F^{(0)}, F^{(1)}, F^{(2)}$.

Remark 4.9. If $t \neq 0$, Corollary 4.8 shows that the consecutive associators either vanish for all n or for none, according to whether $(\mathcal{T}_0, \mathcal{T}_1, \mathcal{T}_2) = 0$; if $t = 0$, they vanish for all $n \geq 1$. In the ordinary Tribonacci case $t = 1$, the consecutive associator is constant along the sequence. Theorems 4.6 and 4.7 show that the entire noncommutative and nonassociative behaviour of $(\mathcal{T}_n)$ is determined by three commutators and a single associator of its first three terms; the parameters μ_1, μ_2, μ_3 enter only through these four elements. These results use alternativity in an essential way and have no counterpart in scalar recurrence theory.

5. Hamilton Matrix Sequences

5.1. Multiplication operators

Let

$$\mathrm{vec}(x) = (x_0, x_1, \dots, x_7)^T$$

be the coordinate vector of $x \in \mathfrak{C}_{\mu_1,\mu_2,\mu_3}$. Following the matrix representation framework of Yamaç Akbıyık (2024; see also Tian, 2000, for the classical octonions), define the left- and right-multiplication matrices $L(x)$ and $R(x)$ by

$$\mathrm{vec}(xy) = L(x)\mathrm{vec}(y), \qquad \mathrm{vec}(yx) = R(x)\mathrm{vec}(y).$$

Both are 8×8 real matrices. If

$$x = x_0 + x_1 e_1 + \cdots + x_7 e_7,$$

then the first row of each multiplication matrix is

$$(x_0,\ \mu_1 x_1,\ \mu_2 x_2,\ -\mu_1\mu_2 x_3,\ \mu_3 x_4,\ -\mu_1\mu_3 x_5,\ -\mu_2\mu_3 x_6,\ \mu_1\mu_2\mu_3 x_7),$$

and all diagonal entries are equal to x_0 (Yamaç Akbıyık, 2024). Moreover, the first column is $\mathrm{vec}(x)$.

Let

$$L_j = L(e_j), \qquad R_j = R(e_j), \qquad j = 0, \dots, 7,$$

where $e_0 = 1$. Linearity gives

$$L(x) = \sum_{j=0}^{7} x_j\, L_j, \qquad R(x) = \sum_{j=0}^{7} x_j\, R_j.$$

Caution. Since a generic 3PGO algebra is nonassociative, an ordinary associative matrix algebra cannot be algebra-isomorphic to it. The results below use only the fact that $L(x)$ and $R(x)$ are matrices of linear multiplication operators. No multiplicativity identity such as $L(xy) = L(x)L(y)$ or $R(xy) = R(x)R(y)$ is needed.

5.2. Generalized Tribonacci Hamilton matrices

Definition 5.1. Define the left and right generalized Tribonacci Hamilton matrix sequences by

$$L_n = L(\mathcal{T}_n), \qquad R_n = R(\mathcal{T}_n).$$

Equivalently,

$$L_n = \sum_{j=0}^{7} V_{n+j}\, L_j, \qquad R_n = \sum_{j=0}^{7} V_{n+j}\, R_j.$$

Theorem 5.2. Both matrix sequences satisfy the same third-order recurrence as V_n:

$$L_{n+3} = rL_{n+2} + sL_{n+1} + tL_n,$$

and

$$R_{n+3} = rR_{n+2} + sR_{n+1} + tR_n.$$

Proof. By linearity of the multiplication matrices,

$$L_{n+3} = L(\mathcal{T}_{n+3}) = rL_{n+2} + sL_{n+1} + tL_n.$$

The proof for R_n is identical.

▫

5.3. Matrix generating functions

Theorem 5.3. The ordinary generating functions of the left and right Hamilton matrix sequences are

$$\sum_{n=0}^{\infty} L_n\, x^n = \frac{L_0 + (L_1 - rL_0)x + (L_2 - rL_1 - sL_0)x^2}{1 - rx - sx^2 - tx^3},$$

and

$$\sum_{n=0}^{\infty} R_n\, x^n = \frac{R_0 + (R_1 - rR_0)x + (R_2 - rR_1 - sR_0)x^2}{1 - rx - sx^2 - tx^3}.$$

Proof. Apply the standard generating-function argument to the recurrences in Theorem 5.2 in the finite-dimensional real vector space $M_8(\mathbb{R})$. ▫

5.4. Matrix Binet formulas

Define

$$\hat{L}_\alpha = L(\hat{\alpha}), \quad \hat{L}_\beta = L\big(\hat{\beta}\big), \quad \hat{L}_\gamma = L(\hat{\gamma}),$$

and

$$\hat{R}_\alpha = R(\hat{\alpha}), \quad \hat{R}_\beta = R\big(\hat{\beta}\big), \quad \hat{R}_\gamma = R(\hat{\gamma}).$$

Theorem 5.4. If α, β, γ are pairwise distinct, then

$$L_n = A\alpha^n \hat{L}_\alpha + B\beta^n \hat{L}_\beta + C\gamma^n \hat{L}_\gamma,$$

and

$$R_n = A\alpha^n \hat{R}_\alpha + B\beta^n \hat{R}_\beta + C\gamma^n \hat{R}_\gamma.$$

Proof. Apply the linear maps L and R to the Binet formula in Theorem 3.5. ▫

Corollary 5.5. The exponential generating functions are

$$\sum_{n=0}^{\infty} L_n \frac{x^n}{n!} = A\hat{L}_\alpha e^{\alpha x} + B\hat{L}_\beta e^{\beta x} + C\hat{L}_\gamma e^{\gamma x},$$

and

$$\sum_{n=0}^{\infty} R_n \frac{x^n}{n!} = A\hat{R}_\alpha e^{\alpha x} + B\hat{R}_\beta e^{\beta x} + C\hat{R}_\gamma e^{\gamma x}.$$

5.5. Trace and coordinate recovery

Theorem 5.6. For every $n \geq 0$,

$$\mathrm{tr}(L_n) = \mathrm{tr}(R_n) = 8V_n.$$

Hence

$$V_n = \frac{1}{8}\mathrm{tr}(L_n) = \frac{1}{8}\mathrm{tr}(R_n).$$

Proof. The diagonal entries of both multiplication matrices $L(x)$ and $R(x)$ equal the scalar component x_0. The scalar component of $\mathcal{T}_n$ is V_n, so the sum of the eight diagonal entries is $8V_n$. ▫

Proposition 5.7. If $e^{(0)} = (1,0,\dots,0)^T$, then

$$L_n e^{(0)} = R_n e^{(0)} = (V_n, V_{n+1}, \dots, V_{n+7})^T.$$

Thus a single Hamilton multiplication matrix contains eight consecutive generalized Tribonacci numbers in its first column.

5.6. Quadratic relation, inverse, and determinant

Theorem 5.8. For every $x \in \mathfrak{C}_{\mu_1,\mu_2,\mu_3}$ the following hold.

(i) The multiplication matrices satisfy

$$L(x)^2 - 2x_0L(x) + N_\mu(x)I_8 = 0, \qquad R(x)^2 - 2x_0R(x) + N_\mu(x)I_8 = 0.$$

(ii) With $\overline{x}$ the conjugate of x,

$$L(x)L(\overline{x}) = L(\overline{x})L(x) = N_\mu(x)I_8, \qquad R(x)R(\overline{x}) = R(\overline{x})R(x) = N_\mu(x)I_8.$$

(iii) The characteristic polynomial of both $L(x)$ and $R(x)$ is $\left(z^2 - 2x_0z + N_\mu(x)\right)^4$. In particular,

$$\det L(x) = \det R(x) = N_\mu(x)^4.$$

Proof. (i) By left alternativity (Lemma 2.2), $x(xy) = x^2y$ for all y, that is, $L(x)^2 = L(x^2)$. By Lemma 2.3 and linearity, $L(x^2) = 2x_0L(x) - N_\mu(x)I_8$. For $R(x)$ one uses right alternativity, $(yx)x = yx^2$.

(ii) Since $\overline{x} = 2x_0 - x$ and $L(1) = I_8$, linearity gives $L(\overline{x}) = 2x_0I_8 - L(x)$. Hence $L(x)L(\overline{x}) = 2x_0L(x) - L(x)^2 = N_\mu(x)I_8$ by (i), and the same argument applies in the other order and to R.

(iii) By (i), every complex eigenvalue of $L(x)$ is a root of $z^2 - 2x_0z + N_\mu(x)$, that is, of the form $\lambda_\pm = x_0 \pm d$ with $d^2 = x_0^2 - N_\mu(x)$. If $d = 0$, then x_0 is the only eigenvalue, so the characteristic polynomial is $(z - x_0)^8 = \left(z^2 - 2x_0z + N_\mu(x)\right)^4$. If $d \neq 0$, the polynomial in (i) has simple roots, so $L(x)$ is diagonalizable over $\mathbb{C}$. Let k be the multiplicity of λ_+. Since every diagonal entry of $L(x)$ equals x_0, we have $\mathrm{tr}L(x) = 8x_0$; hence $k\lambda_+ + (8-k)\lambda_- = 8x_0$, which gives $2kd = 8d$ and $k = 4$. Therefore the characteristic polynomial is $(z - \lambda_+)^4(z - \lambda_-)^4 = \left(z^2 - 2x_0z + N_\mu(x)\right)^4$. The same argument applies to $R(x)$. ▫

Corollary 5.9. For every $n \geq 0$,

$$L_n^2 - 2V_nL_n + q_nI_8 = 0, \qquad R_n^2 - 2V_nR_n + q_nI_8 = 0,$$
$$\det L_n = \det R_n = q_n^4,$$

and the characteristic polynomial of both L_n and R_n is $(z^2 - 2V_nz + q_n)^4$. If $q_n \neq 0$, then

$$L_n^{-1} = \frac{2V_nI_8 - L_n}{q_n}, \qquad R_n^{-1} = \frac{2V_nI_8 - R_n}{q_n},$$

whereas L_n and R_n are singular when $q_n = 0$.

Proof. Apply Theorem 5.8 to $x = \mathcal{T}_n$, whose scalar part is V_n and whose quadratic form is q_n. ▫

Remark 5.10. Corollary 5.9 connects the Hamilton operator sequences with the quadratic-form sequence of Section 4.2: the determinant sequence $(\det L_n)$ is the fourth power of a sequence satisfying the sixth-order recurrence of Theorem 4.2. Moreover, by the quadratic relation, $\mathrm{span}\{I_8, L_n\}$ is a two-dimensional commutative subalgebra of $M_8(\mathbb{R})$. In the real-octonion case $q_n > 0$ whenever $\mathcal{T}_n \neq 0$, so every nonzero L_n is invertible. In degenerate specializations this is no longer true; see the example in Section 6.2.

6. Specializations and an Illustrative Example

6.1. Specializations in the octonionic parameters

The following parameter choices reproduce important algebras; they are listed in Table 2.

Table 2. Specializations of the 3PGO algebra in the parameters μ_1, μ_2, μ_3

(μ_1, μ_2, μ_3)	3PGO specialization
$(-1,-1,-1)$	real octonions
$(-1,-1,1)$	split octonions
$(-1,-1,0)$	semi-octonions
$(1,1,0)$	split semi-octonions
$(-1,0,0)$	quasi-octonions
$(1,0,0)$	split quasi-octonions
$(0,0,0)$	para-octonions

Source: Yamaç Akbıyık (2024).

Consequently, Definition 3.1 simultaneously produces generalized Tribonacci sequences in each of these algebras.

6.2. Ordinary Tribonacci example

Choose

$$r = s = t = 1, \qquad V_0 = 0, \quad V_1 = 0, \quad V_2 = 1.$$

Then

$$0,0,1,1,2,4,7,13,24,44,81, \ldots$$

is the corresponding Tribonacci sequence and

$$\mathcal{T}_0 = e_2 + e_3 + 2e_4 + 4e_5 + 7e_6 + 13e_7.$$

For the real-octonion choice $(\mu_1, \mu_2, \mu_3) = (-1,-1,-1)$,

$$N_\mu(\mathcal{T}_0) = 1^2 + 1^2 + 2^2 + 4^2 + 7^2 + 13^2 = 240.$$

For the split-octonion choice $(-1,-1,1)$,

$$N_\mu(\mathcal{T}_0) = 1 + 1 - 4 - 16 - 49 - 169 = -236.$$

For the semi-octonion choice $(-1,-1,0)$,

$$N_\mu(\mathcal{T}_0) = 1 + 1 = 2.$$

These values illustrate how the additive sequence $\mathcal{T}_n$ remains unchanged while its quadratic geometry changes substantially with the parameters μ_1, μ_2, μ_3.

In all three cases, however, Theorem 4.2 gives the same norm recurrence

$$q_{n+6} = 2q_{n+5} + 3q_{n+4} + 6q_{n+3} - q_{n+2} - q_n.$$

The initial values differ, but the recurrence coefficients do not.

The first values of q_n for four parameter choices are listed in Table 3; each row satisfies the recurrence above.

Table 3. Values of q_n ($0 \le n \le 5$) in the ordinary Tribonacci example for four choices of (μ_1, μ_2, μ_3)

n	$(-1,-1,-1)$	$(-1,-1,1)$	$(-1,-1,0)$	$(-1,0,0)$
0	240	−236	2	0
1	816	−804	6	1
2	2752	−2708	22	2
3	9312	−9172	70	5
4	31512	−31036	238	20
5	106584	−104964	810	65

Source: Computed by the author.

For the Hamilton matrices, Theorem 5.6 yields

$$\mathrm{tr}(L_0) = \mathrm{tr}(R_0) = 0, \quad \mathrm{tr}(L_1) = \mathrm{tr}(R_1) = 0,$$

and

$$\mathrm{tr}(L_2) = \mathrm{tr}(R_2) = 8.$$

and, more generally,

$$\mathrm{tr}(L_n) = \mathrm{tr}(R_n) = 8V_n.$$

For the associator of Corollary 4.8 one obtains, in the real-octonion case $(-1,-1,-1)$,

$$(\mathcal{T}_0, \mathcal{T}_1, \mathcal{T}_2) = -4e_1 + 4e_2 + 12e_3 + 20e_4 - 8e_6.$$

Since $t = 1$, the same element is obtained for $(\mathcal{T}_n, \mathcal{T}_{n+1}, \mathcal{T}_{n+2})$ for every $n \ge 0$. For the quasi-octonion choice $(-1,0,0)$ this associator reduces to $2e_6 - 6e_7$,

and for the para-octonion choice $(0,0,0)$ to $-2e_7$. Thus the additive sequence is the same in all cases, while its nonassociative defect depends visibly on μ_1, μ_2, μ_3.

Finally, for the real-octonion choice Corollary 5.9 gives $\det L_0 = \det R_0 = 240^4$, whereas for the quasi-octonion choice $q_0 = 0$, so that L_0 and R_0 are singular; in fact, L_0 has rank 4 in this case.

7. Discussion

The construction has two independent sets of parameters. The recurrence parameters (r, s, t) control the temporal/discrete evolution, whereas (μ_1, μ_2, μ_3) control the multiplication and the quadratic geometry of the ambient algebra. This separation is visible in several results.

First, the element recurrence and all linear matrix recurrences depend only on (r, s, t). Second, the explicit quadratic form depends strongly on (μ_1, μ_2, μ_3), but the quadratic-form sequence is nevertheless governed by a sixth-order recurrence depending only on (r, s, t). This can be understood from the fact that squaring a third-order Binet expansion introduces the six spectral products

$$\alpha^2,\ \beta^2,\ \gamma^2,\ \alpha\beta,\ \alpha\gamma,\ \beta\gamma.$$

The octonionic parameters change only the linear combination of these six modes.

Third, alternativity of the 3PGO algebra for all parameter values reduces the noncommutative and nonassociative behaviour of the whole sequence to finitely many data, namely three commutators and a single associator of the first three terms (Theorems 4.6 and 4.7). In particular, the consecutive associators form a geometric sequence with ratio t (Corollary 4.8). Statements of this kind have no counterpart in scalar recurrence theory.

Finally, the Hamilton operator viewpoint provides a concrete real-matrix encoding without identifying the nonassociative algebra with an associative matrix algebra. The sequences L_n and R_n are matrix-valued generalized Tribonacci sequences, their traces recover V_n, and their first columns recover eight consecutive terms. Beyond these linear facts, alternativity forces each L_n and R_n to satisfy a quadratic equation with coefficients V_n and q_n (Theorem 5.8), so that the spectrum, the determinant, and the inverse of the Hamilton matrices are governed by the same quadratic-form sequence that appears in Section 4.2.

8. Conclusions and Further Work

Generalized Tribonacci three-parameter generalized octonions were introduced by combining the third-order recurrence

$$V_{n+3} = rV_{n+2} + sV_{n+1} + tV_n$$

with the 3PGO algebra $\mathfrak{C}_{\mu_1,\mu_2,\mu_3}$. The resulting sequence admits a unified recurrence, ordinary/exponential/Poisson generating functions, a Binet representation, finite sums, conjugation, and an explicit parameter-dependent quadratic form.

A first structural result is the sixth-order recurrence for $q_n = N_\mu(\mathcal{T}_n)$. Its coefficients are determined solely by r, s, t, while the octonionic parameters influence only the initial values. For the ordinary Tribonacci coefficients this becomes

$$q_{n+6} = 2q_{n+5} + 3q_{n+4} + 6q_{n+3} - q_{n+2} - q_n.$$

Using the observation that 3PGO algebras are alternative for all parameter values, the commutators and associators of GT-3PGOs were described in closed form: they are determined by three commutators and one associator of the first three terms, and the consecutive associators satisfy $(\mathcal{T}_n, \mathcal{T}_{n+1}, \mathcal{T}_{n+2}) = t^n(\mathcal{T}_0, \mathcal{T}_1, \mathcal{T}_2)$. Right and left Hamilton matrix sequences were then introduced. Their recurrence, Binet, generating, trace, and coordinate-recovery formulas follow from linearity alone, while alternativity yields the quadratic relation $L_n^2 - 2V_nL_n + q_nI_8 = 0$, the characteristic polynomial $(z^2 - 2V_nz + q_n)^4$, the determinant formula $\det L_n = \det R_n = q_n^4$, and explicit inverses whenever $q_n \neq 0$.

Several directions remain open. The sixth-order quadratic-form recurrence can be investigated for factorization, periodicity modulo integers, and parameter-dependent zero sets; by Corollary 5.9, the zero set of (q_n) is precisely the set of indices at which the Hamilton matrices are singular. Since the spectra of the Hamilton operators are explicit, namely $V_n \pm \sqrt{V_n^2 - q_n}$ with multiplicity four, one may also study their asymptotic behaviour and the sign pattern of q_n in indefinite specializations. Further extensions include negative indices, generalized Tribonacci polynomials, Gaussian or bicomplex coefficient sequences, and higher-order recurrence components in 3PGO algebras.

References

Akkuş, İ., & Keçilioğlu, O. (2015). Split Fibonacci and Lucas octonions. *Advances in Applied Clifford Algebras, 25*(3), 517–525. doi:10.1007/s00006-014-0515-8

Baez, J. C. (2002). The octonions. *Bulletin of the American Mathematical Society, 39*(2), 145–205. doi:10.1090/S0273-0979-01-00934-X

Bilgici, G. (2022). Fibonacci 3-parameter generalized quaternions. *European Journal of Science and Technology, 41*, 357–361. doi:10.31590/ejosat.1166686

Bilgici, G., Ünal, Z., Tokeşer, Ü., & Mert, T. (2018). On Fibonacci and Lucas generalized octonions. *Ars Combinatoria, 138*, 35–44.

Cerda-Morales, G. (2017). On a generalization of Tribonacci quaternions. *Mediterranean Journal of Mathematics, 14*, Article 239. doi:10.1007/s00009-017-1042-3

Cerda-Morales, G. (2018). The third order Jacobsthal octonions: Some combinatorial properties. *Analele Ştiinţifice ale Universităţii Ovidius Constanţa, Seria Matematică, 26*(3), 57–72. doi:10.2478/auom-2018-0033

Cerda-Morales, G. (2019). The unifying formula for all Tribonacci-type octonions sequences and their properties. *Konuralp Journal of Mathematics, 7*(2), 292–299.

Çimen, C. B., & İpek, A. (2017). On Jacobsthal and Jacobsthal-Lucas octonions. *Mediterranean Journal of Mathematics, 14*, Article 37. doi:10.1007/s00009-017-0873-2

Horadam, A. F. (1963). Complex Fibonacci numbers and Fibonacci quaternions. *The American Mathematical Monthly, 70*(3), 289–291. doi:10.2307/2313129

İşbilir, Z., & Gürses, N. (2024). Horadam 3-parameter generalized quaternions. *Honam Mathematical Journal, 46*(3), 407–427. doi:10.5831/HMJ.2024.46.3.407

İşbilir, Z., Gürses, N., & Tosun, M. (2025). On the 3-parameter generalized quaternions with generalized Tribonacci numbers components. *Filomat, 39*(9), 3003–3027. doi:10.2298/FIL2509003I

Karataş, A., & Halici, S. (2017). Horadam octonions. *Analele Ştiinţifice ale Universităţii Ovidius Constanţa, Seria Matematică, 25*(3), 97–106. doi:10.1515/auom-2017-0038

Keçilioğlu, O., & Akkuş, İ. (2015). The Fibonacci octonions. *Advances in Applied Clifford Algebras, 25*(1), 151–158. doi:10.1007/s00006-014-0468-y

Özkoç Öztürk, A. (2019). On generalized Tribonacci octonions. *Sakarya University Journal of Science, 23*(5), 731–735. doi:10.16984/saufenbilder.525320

Savin, D. (2015). Some properties of Fibonacci numbers, Fibonacci octonions, and generalized Fibonacci-Lucas octonions. *Advances in Difference Equations, 2015*, Article 298. doi:10.1186/s13662-015-0627-z

Shannon, A. G., & Horadam, A. F. (1972). Some properties of third-order recurrence relations. *The Fibonacci Quarterly, 10*(2), 135–146.

Soykan, Y. (2019). Tribonacci and Tribonacci-Lucas sedenions. *Mathematics, 7*(1), 74. doi:10.3390/math7010074

Şentürk, T. D., & Ünal, Z. (2022). 3-parameter generalized quaternions. *Computational Methods and Function Theory, 22*, 575–608. doi:10.1007/s40315-022-00451-7

Tian, Y. (2000). Matrix representations of octonions and their applications. *Advances in Applied Clifford Algebras, 10*(1), 61–90. doi:10.1007/BF03042010

Tokeşer, Ü., Mert, T., Ünal, Z., & Bilgici, G. (2021). On Pell and Pell-Lucas generalized octonions. *Turkish Journal of Mathematics and Computer Science, 13*(2), 226–233. doi:10.47000/tjmcs.780474

Yamaç Akbıyık, S. (2024). On matrices of generalized octonions (Cayley numbers). *Symmetry, 16*(12), 1567. doi:10.3390/sym16121567